Electrochemistry in the mimicry of oxidative drug metabolism

Nouri-Nigjeh, Eslam

Electrochemistry in the Mimicry of Oxidative Drug Metabolism

Eslam Nouri-Nigjeh

2011

The research presented in this thesis was financially supported by Dutch Technology Foundation, STW (Grant 07047).

Paranimfen: Julien Roeser

Niels Alting

ISBN printed version: 978-94-6191-032-5

ISBN electronic version: 978-94-6191-032-5

Cover design: Eslam Nouri-Nigjeh

Printing: Ipskamp

RIJKSUNIVERSITEIT GRONINGEN

Electrochemistry in the Mimicry of Oxidative Drug Metabolism

Proefschrift

ter verkrijging van het doctoraat in de
Wiskunde en Natuurwetenschappen
aan de Rijksuniversiteit Groningen
op gezag van de
Rector Magnificus, dr. E. Sterken,
in het openbaar te verdedigen op
maandag 24 oktober 2011
om 14.30 uur

door

Eslam Nouri Nigjeh

geboren op 21 september 1980
te Mianeh, Iran

Promotor:	Prof. dr. R. P. H. Bischoff
Copromotors:	Dr. A. P. Bruins Dr. H. P. Permentier
Beoordelingscommissie:	Prof. Dr. U. Karst Prof. Dr. L. Nyholm Prof. Dr. E. M. J. Verpoorte

Table of contents:

Scope and outline of this thesis:

The present thesis is aimed at exploring and extending the application of electrochemistry in combination with mass spectrometry (MS) as an analytical technique in the fast and accurate assessment of oxidative drug metabolism by Cytochrome P450s (CYP) during the early stages of drug discovery and development. Likewise, the results of this study could be used as a new way for small-scale synthesis of drug metabolites which is of importance in the development of new pharmaceutical products.

Chapter 1 provides a general introduction about different electrochemical techniques that have been developed so far for oxidative drug metabolism, including direct electrochemical oxidation (in combination with mass spectrometry), electrochemically generated reactive oxygen species (ROS), and modified surfaces by metalloporphyrines and enzymes. The limitations and advantages of different electrochemical techniques are discussed in the context of *in vivo* oxidative drug metabolism. This part also presents my work on the immobilization of metalloporphyrines via self-assembled monolayers (SAM) of alkanethiols, and their analysis using Surface Enhanced Resonance Raman Spectroscopy (SERRS).

Chapter 2 presents a new approach in the generation of ROS by electrochemical reduction of molecular oxygen and further radical reactions through the Haber-Weiss reaction. Construction of a two-compartment electrochemical cell opens the possibility of separating anodic and cathodic reactions and reaction products. In addition, the effect of different ionization techniques in product identification by mass spectrometry is discussed.

Chapter 3 explores the use of square-wave potential pulses in the high-yield and selective generation of metabolites of lidocaine. Here, I introduce cycle time as a new parameter to tune oxidation yield and selectivity. Electrochemical techniques and stable isotope labeling combined with liquid chromatography (LC)-MS analysis are utilized to elucidate the reaction mechanism.

Chapter 4 uses square-wave potential pulses in the O-dealkylation of phenacetin to acetaminophen, a reaction that is not possible by direct electrochemical oxidation. Oxidation intermediates have been stabilized and characterized by LC-MS(/MS) analysis to reveal the oxidation mechanism and the relevance of pulse time.

Chapter 5 presents a novel approach in the imitation of oxidative drug metabolism based on the electrocatalytic activation of hydrogen peroxide on a platinum electrode. I hypothesize that generation of reactive platinum-oxo species promotes oxygen insertion reactions in analogy to the oxo-ferryl radical cations in CYP. The reaction mechanism is studied by using a competitive substrate in order to gain more insight into the nature of the short-lived reactive intermediates.

Chapter 6 summarises my results and provides a perspective for this research in the context of oxidative drug metabolism and small-scale synthesis of drug metabolites.

Chapter 1
General Introduction*

Prediction of oxidative drug metabolism at the early stages of drug discovery and development requires fast and accurate analytical techniques to mimic the in vivo oxidation reactions by Cytochrome P450s (CYP). Direct electrochemical oxidation combined with mass spectrometry, although limited to the oxidation reactions initiated by charge transfer, has shown promise in the mimicry of certain CYP-mediated metabolic reactions. The electrochemical approach may further be utilized in an automated manner in microfluidics devices facilitating fast screening of oxidative drug metabolism. A wide range of in vivo oxidation reactions, particularly those initiated by hydrogen atom transfer, can be imitated through the electrochemically-assisted Fenton reaction. This reaction is based on homolytic activation of hydrogen peroxide and autoxidation by hydroxyl radicals, wherein electrochemistry is used for the reduction of molecular oxygen to hydrogen peroxide, as well as the reduction of Fe^{3+} to Fe^{2+}. Metalloporphyrins, as surrogates for the prosthetic group in CYP, utilizing metallo-oxo reactive species, can also be used in combination with electrochemistry. Electrochemical reduction of metalloporphyrins in solution or immobilized on the electrode surface activates molecular oxygen in an analogous manner as the catalytical cycle of CYP and different metalloporphyrins can mimic selective oxidation reactions. Chemoselective, stereoselective, and regioselective oxidation reactions may be mimicked using electrodes that have been modified with immobilized enzymes, especially CYP itself. This review summarizes the recent attempts in utilizing electrochemistry as a versatile analytical and preparative technique in the mimicry of oxidative drug metabolism by CYP.

* Published as: Nouri-Nigjeh, E.; Bischoff, R.; Bruins, A.P.; Permentier, H.P. Electrochemistry in the mimicry of oxidative drug metabolism by Cytochrome P450s, Current drug metabolism, Special issue: Analytical techniques in Drug metabolism, Vol. 12, 2011, 359-371.

1.1 Introduction

Drug compounds may be converted in the body to therapeutically active or toxic metabolites. Study of oxidative drug metabolism is conventionally performed in animal models (*in vivo*) or perfused organs (*in vitro*). However, the increasing number of drug candidates and the critical role of metabolism in drug evaluation have raised the interest in the study of drug metabolism in the earlier stages of new drug developments. Therefore, there is a tangible need for the development of new analytical techniques capable of fast assessment and mimicry of oxidative drug metabolism [1].

1.1.1 Cytochrome P450s (CYP)

The firmly held view that oxygen in drug metabolism is derived from water, was discarded when the early isotope studies by Hayaishi in the 1950s pointed out that the oxygen source in *in vivo* oxidation is molecular oxygen [2, 3]. Since the triplet electronic structure of molecular oxygen prevents its direct reaction with mainly singlet organic compounds, the *in vivo* oxidation requires catalytic activation of molecular oxygen [4]. The main enzyme responsible for this activation reaction was first isolated from liver microsomes, and has a characteristic UV-visible spectroscopic signature at 450 nm when its reduced form is exposed to carbon monoxide. Therefore, it was named Cytochrome P450 (abbreviated as CYP) [5]. The most widely studied CYP, i.e. CYP101 or P450cam (a bacterial CYP), named for its camphor monooxygenation reaction, was the first CYP isolated in sufficient quantities for characterization by high resolution X-ray crystallography [6]. The CYP101 structure shown in **Figure 1** has a prosthetic group – iron protoporphyrin (heme) – that is anchored through coordination with the sulfur atom of the cysteine-357 residue. The prosthetic heme group is bracketed between two protein helices and lies close to the enzyme surface, although no part of it is directly exposed to bulk solvent. The substrate (e.g. a drug molecule) interacts with the hydrophobic active-site pocket, and the release of an active-site water molecule provides the thermodynamic driving force for substrate binding. The substrate-protein interactions aid in controlling stereospecificity of the oxidation reaction. Detailed reviews on the functional structure of CYPs can be found in the literature [2, 6, 7].

Our current knowledge about the catalytic activation of molecular oxygen by CYPs and about the consequent drug metabolism is mainly derived from direct observation of the intermediates through various spectroscopic techniques [8-10], the use of diagnostic substrates with mechanistically revealing rearrangements including radical clocks [11], and synthetic metalloporphyrins [12]. Advanced computational methods based on hybrid QM/MM (quantum mechanical/molecular

mechanical) models, that simulate heme by QM and protein by MM models, have enabled the study of active species in their native protein environmnent [13].

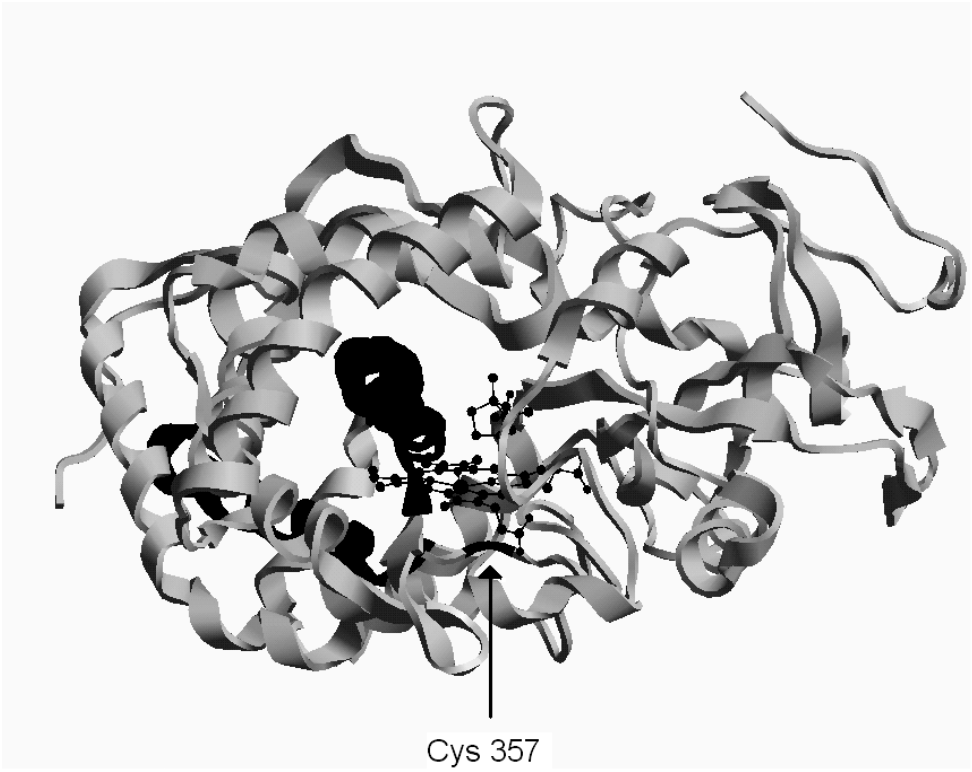

Figure 1. A schematic representation of CYP101 (P450 Camphor, PDB entry 2CPP). The prosthetic group iron protoporphyrin (heme) is bracketed between the helices I and L (dark). The heme is anchored through coordination with sulfur in the cysteine-357 residue (arrow). The subtrate, camphor, is shown in black above the heme [6].

CYPs activate molecular oxygen and transfer a single oxygen atom to a substrate while the other oxygen atom ends up in water [14]. These oxygen transfer reactions include: aromatic/aliphatic hydroxylations, olefin epoxidation, and heteroatom oxidations (nitrogen and sulfur) [15]. In addition, CYPs can promote other forms of oxidative transformations, for instance heteroatom-dealkylation, dehalogenation, and dehydrogenation. The widely accepted catalytic activation mechanism of molecular oxygen by CYPs is shown in **Figure 2** [13]. The hexa-coordinated Fe^{III}-porphyrin complex (**1**) in the resting state has the distal ligand

position occupied by water. Binding of a substrate molecule to the hydrophobic active-site pocket initiates the reaction by displacement of the water ligand leaving a penta-coordinated Fe^{III}-porphyrin (**2**). This complex is a slightly better electron acceptor than the resting state form and is reduced by the CYP reductase protein (CPR) to Fe^{II}-porphyrin (**3**). Coordination with molecular oxygen then generates oxy-Fe^{II}-porphyrin (**4**) which is a good electron acceptor. A subsequent reduction by CPR results in the Fe^{II}-peroxo species (**5**), which is a good base and is protonated easily to form an Fe^{II}-hydroperoxo species (**6**), also known as Compound 0. The second protonation on the proximal oxygen atom activates the O-O bond, and the splitting-off of a water molecule generates the high-valent Fe^{IV}-oxo radical cation species (**7**), known as Compound I, that can transfer an oxygen atom to the substrate. After oxidation, the substrate usually becomes more hydrophilic and leaves the hydrophobic pocket, water molecules re-enter and the resting state is restored. The details of the selective oxygen transfer reaction have, however, remained elusive. The large k_H/k_D kinetic isotope effect indicates a hydrogen abstraction reaction, and the large rearrangement of the fast radical clocks suggests the formation of a radical-in-cage at the active site [16]. The reactive species that are involved in CYP-mediated oxidations are presumably not limited to Compound I, and the nucleophilic and/or electrophilic reactions by Fe^{II}-(hydro)peroxo species (**5** and **6** in Figure 2) should also be considered [17, 18]. For detailed information about CYP-mediated oxidations in drug metabolism the reader is referred to the review articles by Guengerich [19, 20].

1.1.2 Instrumentation

In direct electrochemical oxidations, the electrode behaves as an oxidant which can be tuned by the applied potential in order to perform charge transfer reactions. An overview of the electrochemical reactions within the realm of organic chemistry can be found in the book Organic Electrochemistry [21]. In addition, there is a recent special issue of Chemical Reviews reviewing different aspects of electrochemistry in molecular and biomolecular reactions [22].

The first record of electrochemistry (EC) coupled with mass spectrometry (MS) was a study by Bruckenstein and Gadde on the detection of volatile intermediates generated during reactions on a porous platinum electrode of which one side contacted the solution while the other side contacted the vacuum inlet in the mass spectrometer [23]. Later, the development of thermospray ionization (TSP) allowed the direct introduction of oxidized samples whereby the solvent was forced by pressure from the working electrode into the heated capillary tube of the thermospray source [24, 25]. However, after the development of electrospray ionization (ESI), this became the ionization method of choice for analyzing nonvolatile, polar, and thermally labile compounds [26]. ESI-MS was used for the study of on-line linear sweep voltammetry [27]. A more practically suitable thin-layer, flow-through three-electrode cell was developed by Van Berkel and colleagues, with an Ag/AgCl reference electrode, and the working and counter electrodes separated by a spacing gasket [28, 29]. The same group demonstrated

the study of oxidation reactions by controlling the intrinsic electrochemistry of the electrospray ion source [30]. Electrochemistry can be coupled to MS through other ionization techniques, including atmospheric pressure chemical ionization (APCI), fast-atom bombardment (FAB), and particle-beam ionization (PB) [31].

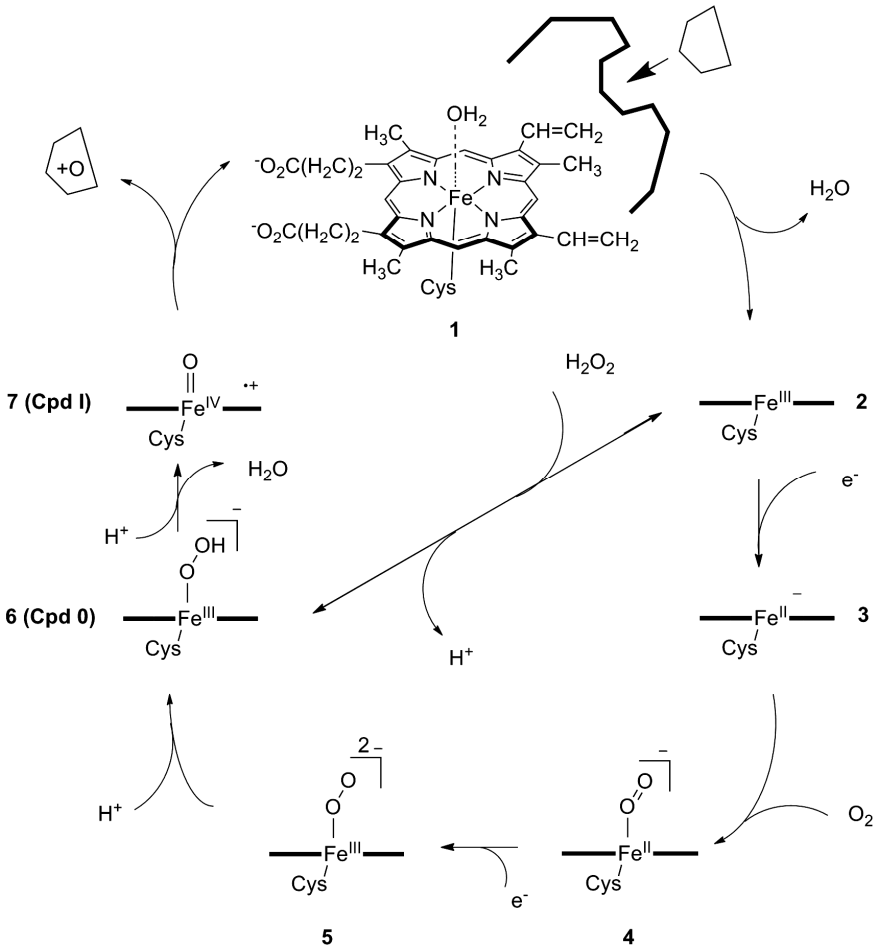

Figure 2. Schematic representation of the catalytic cycle of Cytochrome P450. The heme is depicted by two bold horizontal lines, and the cysteinate proximal ligand is abbreviated as Cys. The oxidation state of the iron center and the overall number of charges are shown by roman and arabic numbering, respectively [13]. The substrate shown here is a general cartoon presentation of a substrate.

The technical aspects of drug metabolism simulation in off-line EC batch reactors and on-line EC/(LC)/MS systems with different ionization techniques have been recently reviewed by Lohmann and Karst [32]. The various electrochemical cells used in online EC/(LC)/MS, including coulometric, amperometric, and in-source electrochemical cells, have been reviewed separately by Baumann and Karst [33]. Electrochemical cells that can be used for direct coupling to MS are commercially available from several companies, Thin-layer electrochemical cells with exchangeable working electrodes of different materials, including platinum, gold, silver, glassy carbon, and boron-doped diamond (BDD), are available from ESA-Dionex (Chelmsford, MA USA), Antec Leyden (Zoeterwoude, The Netherlands), and BASi (West Lafayette, Indiana, USA). In general, direct electrochemical oxidation applications (see section 2) are performed with these electrodes, but BDD can also be used to generate hydroxyl radicals which may produce additional oxidative drug metabolites (see section 3). Coulometric porous flow-through cells of glassy carbon and platinum (available from ESA-Dionex) provide a much large surface area, hence higher conversion rates, than thin-layer cells. The disadvantage is that the porous cells cannot be disassembled and cleaned thoroughly by surface polishing. The reference electrode in the described electrochemical cells is usually a palladium pseudoreference electrode, but in some types an Ag/AgCl reference electrode is used which offers more reliable potential measurements.

The important role of CYPs in phase-I drug metabolism has raised much interest in the development of fast and accurate analytical techniques to study their action during the early stages of drug discovery and development. Previously, we have reviewed the use of direct electrochemical oxidation in the mimicry of oxidative drug metabolism as well as proteomics [34]. The present review provides an overview of recent developments in the utilization of various electrochemical approaches (some combined with mass spectrometry) in the generation and analysis of oxidative drug metabolites, including direct electrochemistry, electrochemical generation of reactive oxygen species, Gif-chemistry, and metalloporphyrins and enzymes immobilized on electrodes.

1.2 Direct electrochemical oxidation

Direct electrochemical oxidation is the most straightforward method to imitate drug metabolism. In 1981 Shone *et al*. were the first to utilize direct electrochemical oxidation successfully in the imitation of biotransformation and preparation of drug metabolites, for the N-dealkylated metabolites of lisuride, diazepam, methysergide, and imipramine [35]. In a systematic study by Bruins and colleagues, reactions such as the N-dealkylation of lidocaine were readily performed electrochemically, whereas some reactions failed, for example the O-dealkylation of 7-ethoxycoumarin [36]. They eventually concluded that direct electrochemical oxidation provides oxidative drug metabolites only when initiated by one or more one-electron oxidations, and only if they do not require potentials higher than the

oxidation potential of the solvent (usually water) [37]. In addition to N-dealkylation, biotransformations that could be imitated by direct electrochemical oxidation included S-oxidation, P-oxidation, alcohol oxidation and dehydrogenation [37]. In contrast, oxidative metabolites resulting from hydrogen atom abstraction, such as O-dealkylation and hydroxylation of the nonactivated aromatic rings, cannot be imitated by direct electrochemistry [37]. Although direct electrochemical oxidation is limited to the oxidation reactions initiated by single electron transfer, it has received considerable attention due to its simplicity and the potential for preparative synthesis of drug metabolites for further structural analysis, for instance by NMR [38]. Furthermore, interest in EC-MS has increased due to the possibility of using direct electrochemical oxidation in miniaturized devices such as microfluidics chips [39, 40], and its ability to detect unstable, reactive, and volatile intermediates of the oxidation products by direct coupling with mass spectrometry [41]. In the next sections we specifically discuss the mechanisms of different classes of CYP oxidation reactions in relation to analogous reactions performed with direct electrochemistry.

1.2.1 Aromatic and aliphatic hydroxylation

One of the outstanding oxidative capabilities of CYP is the hydroxylation of saturated aliphatic hydrocarbons. This kind of oxidation in synthetic chemistry can only be done under vigorous oxidative conditions. As illustrated in **Figure 3-a**, there are two mechanisms that have been proposed to explain aliphatic hydroxylation by Compound I, namely a radical-in-cage mechanism (oxygen rebound) and a concerted mechanism (oxygen insertion). According to the first mechanism the reaction occurs through an initial hydrogen atom abstraction followed by oxygen rebound that proceeds through a radical-in-cage intermediate, while the oxygen insertion mechanism does not postulate a radical intermediate [42]. Early studies found retention of stereochemistry and therefore favoured the oxygen insertion mechanism. In contrast, the loss of stereochemistry observed during the oxidation of fast radical clocks suggested the generation of radical intermediates. The large D/H kinetic isotope effect also suggested a reaction involving hydrogen atom abstraction. Compound I might not be the only electrophilic oxidant in aliphatic hydroxylation reactions, since some studies have found evidence for involvement of iron-hydroperoxo species [17, 43]. Since the C-H bond in aromatic compounds is stronger than in aliphatic ones, *in vivo* aromatic hydroxylation does not necessarily obey the same mechanism as aliphatic hydroxylation. The widely accepted mechanism for aromatic hydroxylation is an oxygen insertion mechanism, the so-called NIH (National Institutes of Health) mechanism, that proceeds through an arene oxide intermediate **(Figure 3-b)**. The small D/H kinetic isotope effect supports the NIH mechanism for aromatic hydroxylation. The shifted-deuterium effect observed for aromatic hydroxylation could also be explained by a nonconcerted addition of Compound I, that does not involve an arene intermediate, as shown in **Figure 3-b** [15].

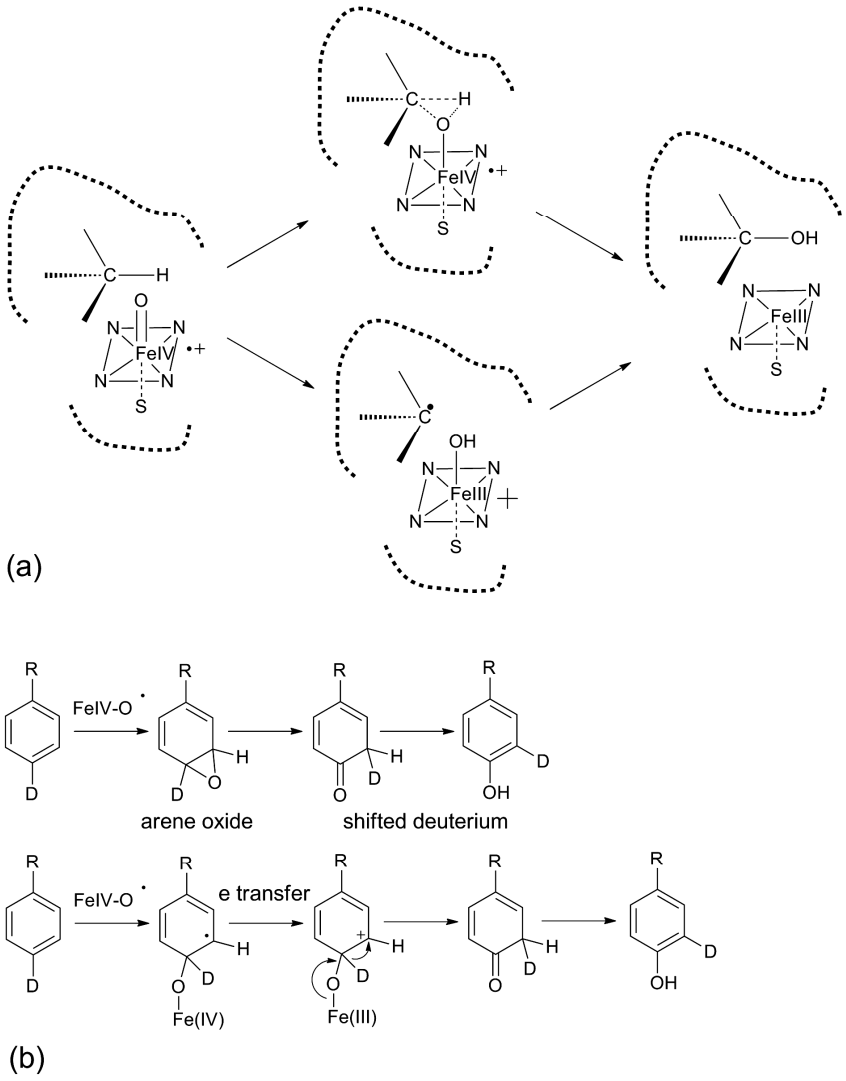

Figure 3. (a) Aliphatic hydroxylation by CYP through oxygen rebound and oxygen insertion mechanisms; (b) Aromatic hydroxylation through the NIH mechanism (top), and through the nonconcerted oxygen addition mechanism (bottom), adapted from Meunier *et al* [15].

Direct electrochemical oxidation has been used widely to perform hydroxylation of organic compounds. At positive electrochemical potentials it is possible, in principle, to abstract electrons from any chemical bond, but electron transfer from

saturated aliphatic hydrocarbons requires such a high positive potential that any solvent would usually be oxidized. For instance, Jurva *et al*. showed that the CYP4A11-catalyzed 12-hydroxylation of lauric acid could not be imitated electrochemically at positive potentials of up to 1.5 V versus Pd/H_2 in aqueous acetonitrile with acetic acid [37]. However, n-alkane oxidation in water-free acetonitrile with Et_4NBF_4 as electrolyte can be achieved at a peak potential of 3.5 V versus Ag/Ag^+ [21].

Electrochemical oxidation of aromatic rings is initiated by electron abstraction. This electron transfer requires a lower positive potential than for aliphatic hydrocarbons due to resonance stabilization of the aromatic radical cations. The electron transfer potential from an aromatic ring that is activated by electron-donating substituents is even less positive. For instance, the oxidation potential for benzene compounds with one to six methyl substituents decreased from 1.93 to 1.20 V versus Ag/Ag^+ [44]. The presence of electron-donating groups on the aromatic ring stabilizes a positive charge or a radical electron localized in the ortho and para positions. In a comparative study by Johansson *et al.* [45] aromatic hydroxylation of the dopamine agonist N-0437 was observed with direct electrochemical oxidation as it has a strong electron-donating group in the aromatic ring. In contrast, aromatic hydroxylation of mephenytoin was only achieved by an EC-Fenton reaction (see section 3.2) and metalloporphyrin in solution (see part 4.1). The absence of a strong electron-donating group in mephenytoin prevents aromatic hyrdoxylation using direct electrochemical oxidation. Hydroxylation requires the presence of water or hydroxyl anions to allow the anodic substitution reaction [46]. Since the oxidation products may be oxidized further at lower potentials than the starting compound, overoxidation is unavoidable. For the dopamine agonist N-0923, oxidation started at potentials as low as 200 mV versus Pd/H_2. The phenol moiety is oxidized readily to a catechol or p-hydroquinone, but these are oxidized further to quinone, as shown in **Figure 4** [36]. Therefore, despite some mechanistic resemblance of electrochemical oxidation to CYP-mediated reactions, the radical intermediate generated after initial oxidation will react further in various ways as determined by the ring substituents [37]. In another example, aromatic hydroxylation of clozapine at 400 mV versus Pd/H_2 was observed to be followed by substitution reactions [47]. A complicated mechanism of oxidation of tetrazepam has been shown to proceed through consecutive hydroxylation and dehydration steps that result in a wide range of allylic and aromatic hydroxylations products [48]. Solvent conditions, such as proton donor availability, also affect hydroxylation reactions. Benzylic hydoxylation imitated by direct electrochemistry was shown for metoprolol at a higher yield in acidic than basic conditions [45].

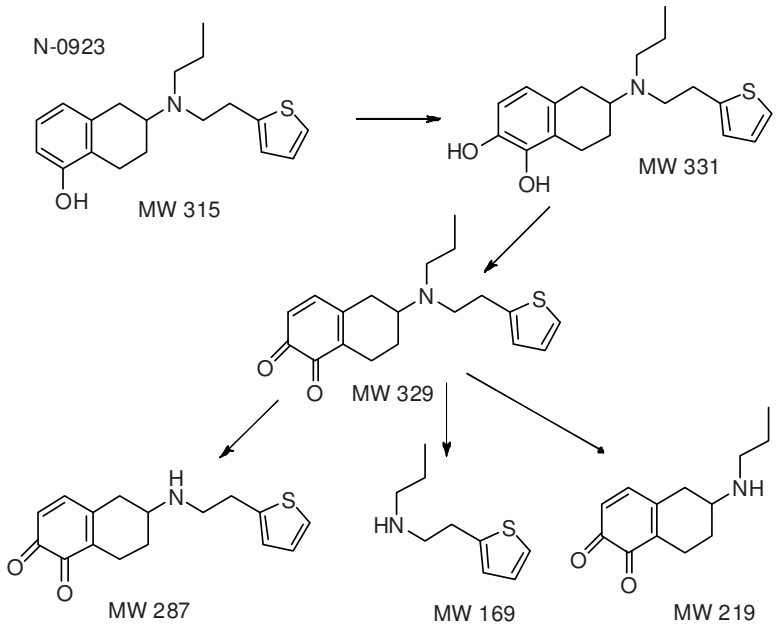

Figure 4. Proposed electrochemical oxidation pathway of the dopamine agonist N-0923 [36].

A great advantage of direct electrochemical oxidation compared with oxidation by enzymes, namely the ability to separate and isolate reactions in different on-line compartments, has been highlighted in work of the Karst group. Coupling of a second electrochemical cell under reductive conditions has been used in the imitation and generation of metabolites from the oxidative metabolism, particularly for hydroxylation and dehydrogenation reactions (sections 2.3). Post EC cell addition of reagents such as glutathione produce the same covalent adducts as formed *in vivo* by phase II drug metabolism (conjugation reactions), in an integrated on-line system [49-52].

Polycyclic aromatic compounds such as naphthalene and anthracene can be oxidized electrochemically, due to the low oxidation potential of polycyclic compounds, they are converted to the corresponding radical cations, which may react further with solvent components to generate hydroxylation products. These hydroxylation products can be detected by using negative-ion mode APCI, as they can be deprotonated efficiently [53].

1.2.2 Heteroatom dealkylation and oxidation

For *in vivo* N-dealkylation by CYP two competing mechanisms are proposed, one initiated by the hydroxylation of the alpha-carbon (hydrogen atom transfer, HAT), and the other by a one-electron oxidation of the heteroatom itself (single electron transfer, SET), as depicted in **Figure 5-a**. The HAT mechanism is initiated by transfer of the alpha-carbon hydrogen to Compound I, and proceeds by oxygen rebound to a carbinol intermediate that after intramolecular rearrangement results in N-dealkylation. The SET mechanism is initiated by electron transfer from the heteroatom to Compound I which generates a radical cation intermediate that, after a second electron transfer and deprotonation reactions leads to an iminium intermediate (**Figure 5-a**). Reaction with hydroperoxo-iron gives the carbinol intermediate, which then follows the same reaction as for the HAT mechanism [15]. The SET mechanism is more widely accepted, since it is supported by the observation of a small D/H kinetic isotope effect which suggests the absence of a hydrogen transfer reaction in the kinetically rate determining step [15]. In contrast, O-dealkylation is considered to proceed via the HAT mechanism and hydroxylation on the alpha-carbon [15]. *In vivo* N-oxidation may either occur via the concerted oxygen atom transfer from Compound I to the amine, or it could be initiated by electron transfer and N-O bond formation, as shown in **Figure 5-b** [15]. S-oxidation is also considered to be a result of concerted oxygen atom transfer from Compound I [54].

Electrochemistry has been used extensively in the imitation of the N-dealkylation metabolism of aliphatic amines, tertiary amides and cyclic tertiary allylamines by CYP [55-57]. The electrochemical reaction of the tertiary amine group of lidocaine [36], shown in **Figure 6**, proceeds through one-electron transfer to generate an imine intermediate that, after hydrolysis and intramolecular rearrangement, gives the N-dealkylation product [58]. The electrochemical mechanism resembles to a large extent the SET mechanism by CYP. Electrochemical N-demethylation of N,N-dimethylamides has shown small D/H kinetic isotope effects indicating the same direct electron transfer mechanism for aliphatic amines and amides [55]. N-dealkylation of other drug compounds with tertiary amine groups such as zotepine [59], and clozapine [47] as well as secondary amines such as metoprolol [45] has been performed successfully.

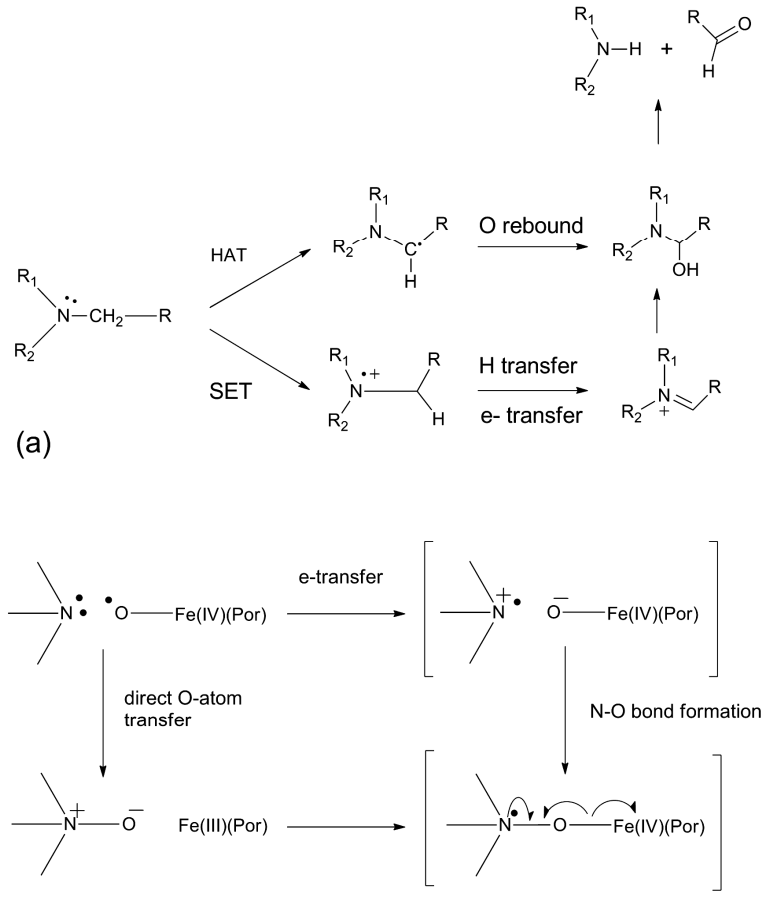

Figure 5. (a) Proposed *in vivo* N-dealkylation mechanism by CYP proceeding via two pathways intiated by hydrogen atom transfer (HAT) and single electron transfer (SET), respectively; (b) Proposed *in vivo* N-oxidation mechanism by CYP resulting from direct oxygen transfer, or via initial electron transfer, followed by N-O bond formation [15]. Por indicates heme porphyrin.

Competition between different oxidation reactions are often an issue, for instance for clozapine and N-0923, where the application of higher positive potentials diverts the major oxidation reaction pathway from ring hydroxylation to N-dealkylation [36, 53]. In a recent study by Jurva and colleagues, the addition of KCN during electrochemical oxidation completely blocked the N-dealkylation of haloperidol, whereas in liver microsomes experiment the reaction was not

impaired. This suggests that an exocyclic iminium intermediate (which is reactive toward KCN) may not be formed in the CYP-catalyzed reactions, again highlighting a different mechanism for electrochemistry and CYP reactions, in this case for N-dealkylation [60].

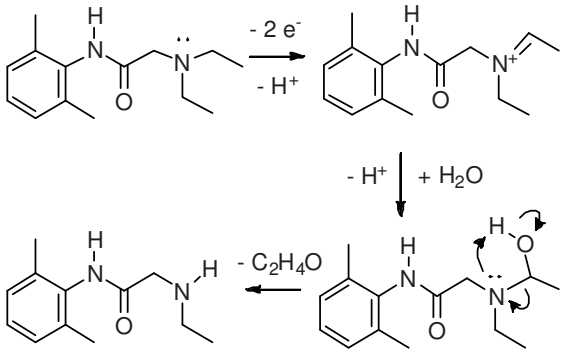

Figure 6. Proposed electrochemical N-dealkylation mechanism for lidocaine [58].

Direct electrochemistry is not generally capable of imitation of O-dealkylation reactions, as mentioned earlier, and it also does not generate N-oxides, but S-oxidation of sulfides to sulfoxides has been reported to occur readily [37, 59]. O-dealkylation of metoprolol under acidic conditions has been shown with a very low yield. S-oxidation of S-methylthiopurine was shown under neutral conditions [45]. Nozaki et al. showed both N-dealkylation and S-oxidation, but not O-dealkylation, of zotepine by direct electrochemistry [59].

1.2.3 Dehydrogenation and epoxidation

The dehydrogenation reaction is a special feature of CYP in which it actually behaves as an oxidase-dehydrogenase, and converts molecular oxygen to water. A HAT mechanism for the dehydrogenation of valproic acid (VPA) has been suggested, since the D/H kinetic isotope effect on the C-4 position was the same for 4-ene-VPA and 4-hydroxy-VPA [61]. Epoxidation of olefins occurs with the retention of stereochemistry, which suggests a concerted oxygen insertion mechanism by Compound I [15].

Electrochemical dehydrogenation has been observed for few drug compounds. Paracetamol is oxidized by several CYP isoforms through dehydrogenation to its toxic metabolite N-acetyl-p-benzoquinoneimine (NAPQI). The same dehydrogenation product can be obtained electrochemically, but this reaction is proposed to proceed through two successive electron/proton transfer reactions [49,

62]. Since the *in vivo* dehydrogenation mechanism is HAT-initiated, its mimicry would presumably be difficult by electrochemistry. Simulation of the *in vivo* phase II detoxification mechanism of the NAPQI metabolite by adduct formation with glutathione was shown in an on-line EC/LC/MS system [49]. In a similar study by Madsen *et al.,* the stability of NAPQI was studied, and its reaction kinetics with glutathione and other nucleophiles was determined using electrochemical measurements [63]. Electrochemical oxidation is useful for electrophilic metabolites of which the chemical reactivity is so high, that it prevents their detection *in vivo*. Electrochemical oxidation in the absence of nucleophiles could help isolate and detect the reactive intermediates, for example the quinoneimine intermediate metabolite of amodiaquine [63, 64].

Electrochemical studies can aid in the better understanding of charge/proton transfers in dehydrogenation and other oxidative pathways. Oliveira-Brett *et al.* have studied the oxidation of drugs including metolazone, apomorphine, and thalidomide at glassy carbon electrodes using cyclic, differential pulse, and square-wave voltammetry [65-67]. Two oxidation processes were observed, a reversible diffusion-controlled oxidation with two-electron and two-proton transfer reactions, and an irreversible diffusion-controlled oxidation at more positive potentials with one-electron and one-proton transfer reactions. The first reaction caused the dehydrogenation of the sulfonamide moiety of metolazone, and the latter an aromatic hydroxylation reaction [65-67].

Jurva *et al*. showed that the 4,5-epoxidation of benzo[*a*]pyrene could not be imitated electrochemically as it resulted instead in benzo[*a*]pyrene quinones [37]. Jeftic and Adams have proposed that this oxidation is initiated by a one-electron transfer process to the radical cation, which can either undergo a polymerization reaction, or, after several hydrolysis and oxidation steps, ends as benzo[*a*]pyrene quinones [68]. Xu *et al*. later studied the same reactions using an on-line EC/ESI-MS method [69]. Ultimately, electrochemical oxidation of benzo[*a*]pyrene resulted in several quinones, instead of the desired epoxidation metabolite.

1.3 Indirect electrochemical oxidation by reactive oxygen species (ROS)

Direct electrochemical oxidation is limited to the generation of oxidative drug metabolites initiated by electron transfer reactions which do not exceed the oxidation potential of the solvent. On the other hand, electrochemistry can be used to generate reactive oxygen species (ROS), which may mediate the production of other oxidative drug metabolites, including HAT-initiated reaction products.

Electrochemical reduction of molecular oxygen initiates activation of molecular oxygen toward reaction with organic compounds. This activation through successive electrochemical reduction and protonation steps will be discussed first, and then extended to the catalytic activation using iron cations (Fenton reaction

and Gif chemistry), which are more reminiscent of the *in vivo* catalytic cycle of CYP.

1.3.1 Electrochemically generated reactive oxygen species

Electrochemical reduction of molecular oxygen in aprotic solvents, such as acetonitrile, results in superoxide anion production (**reaction 1**). The superoxide anion is sufficiently stable in the absence of proton donors, and can be further reduced at higher negative potentials to peroxide anions (**reaction 2**) [70]**.** Electrochemically generated superoxide anions can promote different reactions including proton transfer, hydrogen atom transfer (e.g. from reduced flavins), and one-electron reduction [71]. Superoxide anions can undergo dismutation and form perhydroxyl anions in the presence of residual water or weak acids (**reaction 3**) [72, 73]. However, in the presence of stronger acids, molecular oxygen is reduced directly to perhydroxyl radicals, which can be chemisorbed to the electrode surface and disproportionate to hydrogen peroxide and molecular oxygen [74]. Perhydroxyl radicals are readily reduced to peroxide anions, directly on the electrode or by superoxide anions, but since the recombination of radicals has a very small activation energy barrier, two perhydroxyl radicals may combine to generate hydrogen peroxide and molecular oxygen (**reaction 4**) [70].

$O_2 + e^- \rightarrow O_2^{-\bullet}$ $E^0 = -0.75$ V vs SCE (1)

$O_2^{-\bullet} + e^- \rightarrow O_2^{2-}$ $E^0 = -2.05$ V vs SCE (2)

$O_2^{-\bullet} + H_2O \rightarrow HO_2^{\bullet} + OH^-$ (3)

$HO_2^{\bullet} + HO_2^{\bullet} \rightarrow H_2O_2 + O_2$ (4)

Perhydroxyl radicals are relatively strong oxidizing species in HAT reactions, and are capable of abstracting hydrogen from allylic positions, but they are unlikely to play a major role in oxidation reactions of organic substrates, since they are highly susceptible to recombination and the generation of hydrogen peroxide. A study by Lorenzola *et al.* showed that the final product of oxygen reduction on Pt and Au electrodes in acetonitrile in the presence of residual water is hydrogen peroxide [75], even though surface studies showed the reaction of the intermediate electrogenerated reactive oxygen species with the metallic surface [76]. Reduction of hydrogen peroxide by superoxide anions, known as the Haber-Weiss reaction (**reaction 5**), generates hydroxyl radicals capable of autoxidation and the promotion of HAT reactions [77, 78].

$H_2O_2 + O_2^{-\bullet} \rightarrow OH^{\bullet} + OH^- + O_2$ (5)

A recent study showed that the reduction of molecular oxygen in acetonitrile containing 1% water resulted in hydrogen peroxide, which reacted with lidocaine leading to N-oxidation, but not hydroxylation, suggesting that the amount of hydroxyl radicals was very small [58]. The N-oxide, presumably generated through adduct formation of the tertiary amine and hydrogen peroxide ($R_3N{\cdot}O_2H_2$) and subsequent decomposition [79], which could not be produced by direct electrochemical oxidation (section 2). On the other hand, direct electrochemical oxidation occurs on the counter electrode while reduction is performed at the working electrode, resulting in N-dealkylation in case of lidocaine. A combination of direct and indirect electrochemical oxidation by ROS thus provides access to a wider range of drug metabolites in a single electrochemical experiment [58].

Oxidation of water on the various electrode materials may generate reactive oxygen intermediates, mainly hydroxyl radicals. On the electrode surfaces with a low molecular oxygen evolution overpotential, such as platinum and carbon, the main product of water oxidation is molecular oxygen. A very small fraction of reactive species generated on the surface may be capable of promoting specific oxidation reactions at low yields. In general, these electrode materials have higher oxidation states available so that chemisorbed hydroxyl radicals may interact with the electrode to generate higher oxide species [80]. Boron-doped diamond (BDD), which has a high oxygen evolution overpotential and is a poor catalyst for oxygen evolution, can produce hydroxyl radicals upon water oxidation, as verified by using spin trap, and NMR studies [80]. The electrochemistry of water oxidation on BDD electrodes has been studied by differential-pulse voltammetry, showing that water oxidation to hydroxyl radicals at pH values lower than 9 proceeds through a concerted transfer of one electron, and one proton [81]. Interestingly, anodic and cathodic pretreatments result in different surface terminations of BDD, significantly influencing the surface resistance and capacitance, as shown by electrochemical impedance spectroscopy, and cyclic voltammetry [82]. The electrochemical oxidation of hydroquinone, resorcinol and catechol, which has been shown using a BDD electrode, probably proceeds through reaction with hydroxyl radicals, rather than through direct electrochemical oxidation of the substrate [83].

1.3.2 Electrochemically-assisted Fenton reaction

Electrochemical reduction of molecular oxygen in acetonitrile containing small amounts of water only results in generation of hydrogen peroxide as the final ROS product [58, 75]. The kinetics of hydroxyl radical generation through the Haber-Weiss reaction (0.13 $M^{-1}s^{-1}$, measured by radiolysis) is very slow compared with catalytic reactions (63 $M^{-1}s^{-1}$ for the Fenton reaction, described below) [84, 85]. As a consequence, in order to generate hydroxyl radicals in sufficient amounts to initiate oxidation through hydrogen atom transfer, it is necessary to catalyze formation in the presence of metallic cations.

The homolytic activation of hydrogen peroxide using Fe^{2+} cations is known as the Fenton reaction. It is considered to be a free-diffusing reaction and its selectivity depends on the choice of metallic cations, their relative concentration, the dissolved gas and pH [86, 87]. The general theme is that lower-valence metallic cations, such as Fe^{2+} cations, reduce hydrogen peroxide to a hydroxyl radical and a hydroxyl anion (**reaction 6**) [85]. A catalytic amount of Fe^{2+} cations is sufficient to initiate the reaction since they can be regenerated through **reaction 7**. Sawyer and coworkers have proposed a different oxidation pathway for this reaction, where there is a large excess of hydrogen peroxide to Fe^{2+} and whereby the generation of free radicals is excluded [88, 89]. Although this hypothesis was criticized later [90], the exact mechanism of the Fenton reaction remains elusive.

$$H_2O_2 + Fe^{2+} \rightarrow OH^{\bullet} + OH^{-} + Fe^{3+} \quad (6)$$

$$H_2O_2 + Fe^{3+} \rightarrow HO_2^{\bullet} + H^{+} + Fe^{2+} \quad (7)$$

Aliphatic hydroxylation by hydroxyl radicals proceeds through hydrogen atom transfer and radical recombination. Aromatic hydroxylation of benzoic acid to mono- and polyhydroxylated products by hydroxyl radicals generated by concurrent electrochemical reduction of molecular oxygen and Fe^{3+} cations allowed the measurement of the kinetics of each hydroxylation step [84]. The rate of hydroxylation shows a clear tendency to increase with the number of hydroxyl groups already present in the aromatic ring. The reaction is initiated with a very fast nucleophilic addition of hydroxyl radicals to the aromatic ring, and the resulting radical then undergoes different reactions depending on the medium, including dimerization, dismutation, oxidation, water elimination, or reaction with dissolved molecular oxygen to generate hydroxylation products through a peroxy intermediate (Dorfman mechanism) [84].

Electrochemistry can be used both in the generation of hydrogen peroxide through the reduction of molecular oxygen (section 3.1), and the reduction of Fe^{3+} cations to trigger the Fenton reaction. **Figure 7** illustrates the different stages of the electrochemically-assisted Fenton reaction and the reactions leading to aliphatic and aromatic hydroxylations, due to hydrogen atom abstraction and nucleophilic addition by hydroxyl radicals, respectively. Jurva *et al*. used the radical scavenger 5,5-dimethyl-1-pyrroline-N-oxide (DMPO) to trap the generated radicals [91]. Although non-hydroxyl radicals resulting from autoxidation reactions were also detected, the Fenton reaction proved useful for oxygen atom insertion into organic molecules in case direct electrochemistry methods fail [91]. Successful imitation of the enzymatic oxidation of metoprolol to benzylic and aromatic hydroxylation as well as O- and N-dealkylation products was shown. In addition, a systematic study using different drug compounds proved that aliphatic, benzylic and aromatic hydroxylation as well as N- and O-dealkylation, N- and S-oxidation, and

dehydrogenation reactions are possible [45]. The electrochemically-assisted Fenton reaction has also been used successfully for the various oxidation reactions (mainly hydroxylations) of the antimicrobials triclosan and triclocarbon [92], the β-blocker atenolol [93], and for clofibic acid [94].

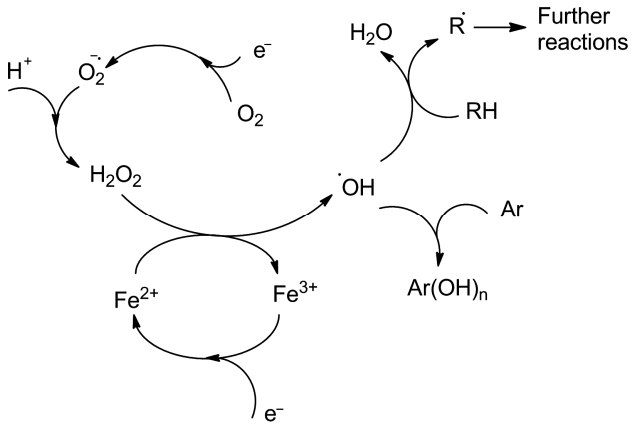

Figure 7. Schematic illustration of generation of hydroxyl radicals through the electrochemically-assisted Fenton reaction, and their subsequent reactions with aliphatic and aromatic compounds [84].

The electro-Fenton reaction is not the only method for the electrochemical generation of hydroxyl radicals. As shown earlier, water oxidation on BDD electrodes also produces hydroxyl radicals. It was found that by operating electrochemical cells at a high current, within the water oxidation potential, reactive hydroxyl radicals adsorbed on the BDD electrode were formed that promoted aromatic and aliphatic hydroxylations [85]. The kinetics of oxidation of paracetamol on the BDD electrode was high compared with that on platinum or glassy carbon electrodes [95], suggesting that BDD is an attractive electrode material for drug oxidation studies.

1.3.3 Electrochemically assisted Gif chemistry

Whereas the Fenton reaction proceeds through homolytic activation of the O-O bond and the generation of freely diffusing radicals, the activation of hydrogen peroxide by CYP (hydrogen peroxide shunt pathway, **Figure 2**) proceeds through heterolytic activation of the O-O bond and generation of Compound I. A model system (named GoAgg^{II}) resembling Compound I was first developed by Barton, who used Fe^{2+} cations in the presence of hydrogen peroxide in a pyridine/acetic

acid solution to promote a non-radical oxidation pathway [96]. Later, he showed that the addition of catalytic amounts of picolinic acid decreases the reaction half-time from 4-6 h to 5-10 min (model system named GoAgg^{III}) [97]. The main difference between CYP and the GoAgg models (collectively called Gif chemistry) is the absence of a porphyrin ligand that binds the iron to transfer electrons and to reduce Fe^{V} to Fe^{IV}. Barton suggested that the carbon-centered radicals do not play a role in Gif chemistry because they would be quenched by hydrogen atom transfer from the S-H bond in hydrogen sulfide that used to be added in the early Gif reactions. In addition, a radical reaction was excluded because the kinetics of oxidation of primary to tertiary hydrocarbons with Gif chemistry did not follow the pattern of their bond energies. A comparative study showed a different product distribution for alkanes obtained with Gif chemistry compared with halogen radical reaction [98]. Newcomb and co-workers suggested the presence of free alkyl radicals in Gif chemistry by using hypersensitive cyclopropane-based radical clocks (with very fast rearrangement kinetics) [99]. Clearly, mechanistic studies of Gif reactions should be interpreted carefully, as most current results are consistent with a free oxygen-centered radical mechanism rather than one involving high-valency iron-oxo species [100]. A review by Gozzo discusses different possible mechanisms involved in Gif chemistry [101].

Gif chemistry can be induced electrochemically by reducing molecular oxygen to an active form, which is probably the superoxide anion. The electrochemically-assisted Gif chemistry (so-called GO) promotes aliphatic hydroxylation as well as ketone formation reactions of test compounds [102]. A constant potential of -0.6 to -0.7 V vs. SCE with tetraethylammonium salt as electrolyte permits the reduction of molecular oxygen in pyridine/acetic acid solution without direct reduction of the pyridinium ion. Acetic acid can be replaced by α-picolinic or trifluoroacetic acid which protonate pyridine sufficiently to avoid the need for additional electrolytes.

1.4 Electrochemically assisted oxidation by metalloporphyrins as biomimetic models of CYP

Free hydroxyl radicals generated during the Fenton reaction promote a variety of oxidation reactions, which, however, lack selectivity. Metalloporphyrins can be used to generate metallo-oxo species, similar to Compound I, and to act as biomimetic models in the oxidative drug metabolism toward oxygen transfer reactions [103]. Unsubstituted metalloporphyrins were used as early biomimetic models, but since they are easily degraded, they were replaced by sterically hindered metalloporphyrins such as meso-tetraphenyl porphyrins (TPP). Metalloporphyrins with iron and manganese as metallic centers are the most widely used porphyrins in oxygen transfer reactions. Halide-substitution of the phenyl groups of TPP activates its metallic center and makes it a stronger oxidant [1]. The oxygen source in most of these biomimetic models is not molecular oxygen, but a single oxygen atom donor, such as iodosyl benzene (PhIO), and meta-chloro

perbenzoic acid (*m*-CPBA). These reactions are mainly performed in organic solvents, in which a basic nitrogen atom is required as proximal ligand to increase reactivity. They have benefits over reactions with freely diffusing radicals since a wide range of chemoselective [1], enantioselective [104], and regioselective [105] oxidation reactions can be achieved by proper selection of porphyrins with different metallic centers and substituents, solvent, and proximal ligand. In a review by Balogh and Keseru, differently substituted metalloporphyrins were used in the mimicry of oxidative drug metabolism. Oxidation products were collected and were found to be comparable to the *in vivo* metabolites, demonstrating the usefulness of metalloporphyrin-based chemical models in metabolic studies [106]. In a systematic study by Johansson *et al*. aliphatic and aromatic hydroxylation (even for non-activated aromatic rings), heteroatom dealkylation and oxidation, and dehydrogenation were shown to be mimicked successfully using different substituted iron and manganese meso-tetraphenyl porphyrins (FeTPP and MnTPP) activating hydrogen peroxide [45]. The chemical biomimetic models and their extension to drug metabolism have been reviewed in detail by Karst *et al.* [32]. In a recent review by Nam, different non-heme systems are presented in comparison with heme-based reactive species in the promotion of various oxidation reactions [107].

1.4.1 Metalloporphyrins in solution

Electrochemistry can assist metalloporphyrin models in a catalytic cycle identical to CYP in the activation of molecular oxygen. The oxygen source is molecular oxygen, and the reaction requires electrochemical reduction for the activation of the molecular oxygen bond.

Metalloporphyrins in solution have been used for the electrocatalytic activation of molecular oxygen. An early study suggested that the catalytic cycle could be initiated by the reduction of the metal center followed by coordination with molecular oxygen, and further reduction and protonation which would ultimately lead to the generation of metallo-oxo species [108]. There is also a need for an axial coordinator, such as 1-methyl imidazole. To sustain the catalytic cycle, and in case protic solvents are used, protons are required for the O-O bond activation, whereas in aprotic solvents this can be achieved with acid anhydrides [109]. Epoxidation of olefins has been shown to occur upon electrocatalytic activation of molecular oxygen by metalloporphyrins in solution [108]. Simándi has reviewed reactions of various metal complexes, including metalloporphyrins, in the catalytic activation of molecular oxygen in the oxidation of saturated and unsaturated hydrocarbons, and of aromatic compounds [110].

1.4.2 Metalloporphyrins immobilized on the electrode surface

Metalloporphyrins immobilized on the electrode surface suffer less from degradation. In addition, electron transfer from the surface facilitates the electrocatalytic activation of molecular oxygen. Different methods for immobilization of metalloporphyrins on a surface have been reviewed by Meunier and Brule *et al*., which include coordinative binding, encapsulation (within zeolites, silica or clay), electrostatic adsorption, covalent anchorage and polymerization [111, 112]. The catalytic behavior of metalloporphyrin complexes in molecular sieves, in the epoxidation of cyclohexene was reported by Rani *et al.* [113]. Parton and colleagues proved that the zeolite-encaged iron complexes in a polymer membrane activated by peroxides resembles CYP in the oxidation of tertiary hydrocarbons [114]. Electropolymerized manganese porphyrin films have also been shown to be a versatile model system for the electrocatalytic activation of molecular oxygen and the oxidation of various small organic compounds and drug molecules [115]. Direct reduction of electropolymerized metalloporphyrins followed by coordination of molecular oxygen (the identical catalytic cycle as for CYP) has been proposed for the generation of metallo-oxo species [116]. On the other hand, Collman and coworkers suggested that in thick electropolymerized metalloporphyrin films, the direct reduction of molecular oxygen on the electrode surface to hydrogen peroxide, and its subsequent activation by metalloporphyrins through the peroxide shunt would generate high-valent metallo-oxo species capable of epoxidation of olefins [117].

Immobilized metalloporphyrins on the electrode surface may allow selective oxidation and generation of a wider range of drug metabolites compared with direct electrochemical oxidation which is merely capable of initiating charge transfer oxidations. Functionalized electrodes with metalloporphyrins could be used in combination with mass spectrometry for fast assessment of oxidative drug metabolism. For this purpose, metalloporphyrins were bound to an electrode via axial ligation to a self-assembled monolayers (SAM) [118]. Specifically, a 4-pyridinethiol SAM on a gold electrode was generated through thiol linkage and used to anchor metalloporphyrins by axial coordination [119]. The presence of metalloporphyrins anchored on the electrode surface was verified by the characteristic surface enhanced Raman spectroscopy (SERS) peaks.

Heme, the prosthetic group of CYP, has been shown to be useful as the electrocatalyst for the activation of molecular oxygen in alkene epoxidation reactions [120]. In an ongoing study in our group, a SAM of 4-pyridinethiol on gold and roughened silver electrodes was used to anchor heme, as shown in **Figure 8-a**. The generation of the SAM from a diluted solution of 4-pyridinethiol in ethanol on silver was studied by surface enhanced resonance Raman spectroscopy (SERRS). The presence of the SAM on the surface was verified by characteristic SERRS peaks. Following exposure of the modified surface to heme in dimethyl sulfoxide (DMSO) for ten hours, extra peaks were observed between 1200-1500 cm^{-1} in the SERRS spectrum (**Figure 8-b**) which can be attributed to the axial coordination of

heme via the SAM. An *in situ* SERRS study with electrochemistry was used to study the physical state of the iron center during the electrocatalytic activation of molecular oxygen in an acetonitrile solution. Similar spectra have been shown for the reduction of the iron center in Cytochrome c adsorbed on SAMs of 4-pyridinethiol on a silver electrode [121]. No spectral change was observed after the application of reductive potentials which may be explained by the generation of stable iron-oxygen species on the electrode surface in the absence of strong proton donors.

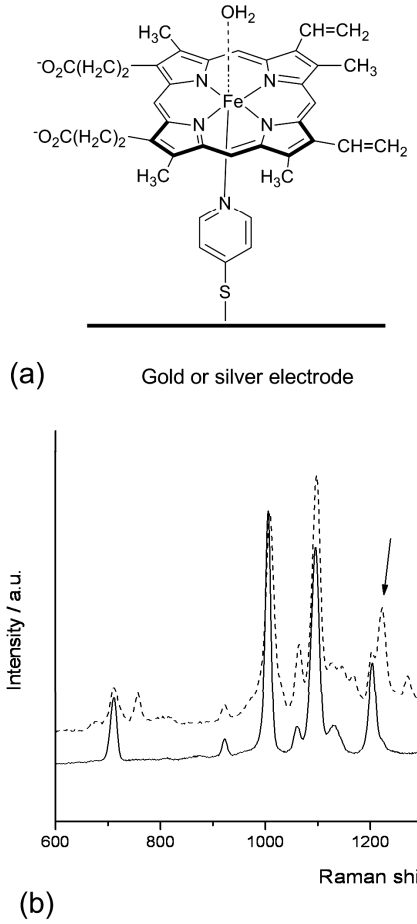

Figure 8. (a) Schematic representation of heme anchored through coordination via a self-assembled monolayer (SAM) of 4-pyridinethiol on a gold electrode, and (b) the experimental surface enhanced resonance Raman spectrum of the electrode surface before (lower trace) and after (upper trace) heme coordination [136].

1.5 Enzyme-modified electrodes

The final electrochemical mimicry method that we discuss employs enzymes anchored to the electrode surface. Peroxidases containing a heme prosthetic group anchored via histidine to the protein backbone have been used as biomimetic models. In peroxidases, unlike CYP, the catalytic cycle is triggered by the replacement of water from the distal ligand by hydrogen peroxide and the subsequent splitting off of one water molecule results in Compound I (similar to the CYP hydrogen peroxide shunt). Peroxidases are the catalysts of choice for sulfoxidation, hydroxylation and epoxidation on account of their high activity and enantioselectivity [122]. Immobilized peroxidases on poly-(γ-methyl-L-glutamate) catalyze the hydroxylation of benzene and exhibit an even higher activity than peroxidases in solution [123]. Peroxidases in solution or immobilized on a surface for the activation of hydrogen peroxide do not require a reduction step. A study by Sheldon and coworkers showed that peroxidases promote selective oxidation reactions with molecular oxygen in the presence of a chemical reductant [124].

Synthetic heme peptides, containing a heme group bound either covalently or by coordination to (helical) peptides, have been shown to reproduce the catalytic activity of heme oxidases and to provide an environment for heme which is similar to the native enzyme as shown in **Figure 1** [125]. Synthetic heme peptides were immobilized on a gold electrode via hydrophobic interactions on a surface coated with a SAM of decane-1-thiol. The electrochemical response of reduction of the metallic center, and its role in the catalytic activation of molecular oxygen, were verified using electrochemical techniques [126].

Although isolated CYPs suffer from low stability, and need an additional reductase cofactor to regenerate the enzyme, purified CYPs on electrode surfaces have been succesfully used at high turn-over rates [127]. A study by the group of Rusling showed that it is possible to oxidize styrene and cis-β-methylstyrene by using CYP101 and myoglobin embedded in thin films of polyion and surfactant. Myoglobin and CYP101 mediate the electrochemical reduction of molecular oxygen to hydrogen peroxide, which is used further through the peroxide shunt [128]. The same group later showed the possible direct charge transfer to CYP from the electrode by reduced redox partners on a polycation-coated electrode, and accordingly they observed electrocatalytic oxidation of styrene [129]. Mie *et al*. advanced this study by using different hydrophobic coating materials and showed that CYP and CYP-reductase on a simple hydrophobic electrode surface can promote drug metabolism reactions [130].

In order to eliminate the need for a reductase, Gilardi and colleagues utilized a protein engineering strategy to obtain sufficient interaction of CYP with the electrode surface by assembling a redox module and the enzyme domain to generate an enzyme-reductase fusion protein [131]. They used covalent bonding of the mutated CYP to the electrode surface via self-assembled monolayers [132].

Direct immobilization of human flavin-containing monooxygenase on a glassy carbon electrode derivatized with the cationic surfactant didodecylammonium bromide (DDAB) was shown to be efficient in the mimicry of N-oxide formation of tamoxifen, when a potential of -600 mV versus Ag/AgCl was applied for 30 min in the aerated cell [133]. Oriented immobilization of human CYP 2E1 was achieved by engineering two multisite mutants of P450 2E1, where all the exposed cysteines were modified into serines, except for one cysteine which was used to link the protein covalently to the gold electrode. As shown in **Figure 9**, the enzyme and its mutants were immobilized on a dithio-bismaleimidoethane SAM, and the transformation of p-nitrophenol to p-nitrocatechol was used as a test reaction. Activation at -500 mV for 30 min showed higher levels of products for the mutants that could be ascribed to the controlled immobilization on the gold electrode. Presumably, in the mutated CYPs the proximal side involved in electron transfer is linked to the electrode surface, while the distal side is exposed to the bulk solution [134]. Gilardi and co-workers recently showed that the CYP 3A4 fused with the electron transfer module flavodoxin (FLD), immobilized covalently on a SAM of 6-hexanethiol and 7-mercaptoheptanoic acid, could be integrated in a microfluidic platform [135]. In the microfluidic system, cyclic voltammometry was used to study the reduction and oxidation of the fused enzyme. The platform was also used to identify the specific kinetic parameters of oxidation of different drug compounds.

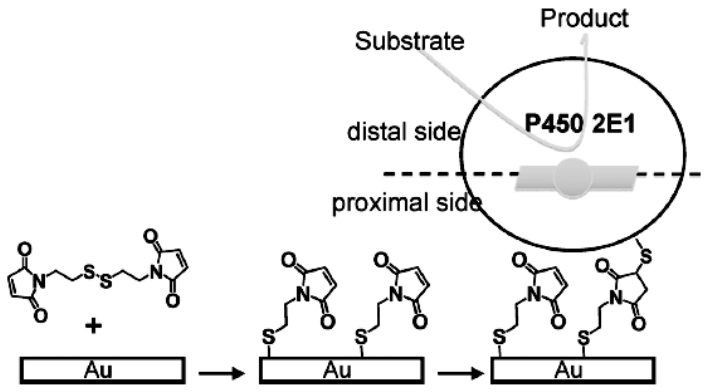

Figure 9. Surface immobilization of CYP 2E1, through covalent linkage to a dithio-bismaleimidoethane (DTME) SAM on a gold electrode surface [134].

1.6 Perspective

Direct electrochemical oxidation is a versatile analytical technique in the fast assessment of oxidative drug metabolism (particularly in combination with mass spectrometry), but it is limited to the oxidation reactions initiated by charge transfer. There is a continuing trend toward utilization of new electrochemical techniques to more effectively and selectively mimic oxidative drug metabolism. Indirect electrochemical oxidation mediated by reactive oxygen species generated through electrochemical oxygen reduction, and through the (electrochemically mediated) Fenton reaction and Gif chemistry helps in the generation of metabolites that cannot be obtained by direct electrochemical oxidation. Metalloporphyrins with different substituents and different metallic centers are useful as more specific biomimetic models in selective oxidation. The ongoing research to anchor metalloporphyrins on electrode surfaces to activate molecular oxygen could provide new possibilities for studying oxidative drug metabolism, and would allow the benefit of on-line coupling of functionalized electrodes with mass spectrometry or other analytical techniques. Mutated CYP enzymes that are anchored on the electrode and receive electrons directly from the surface are the closest mimicry model to *in vivo* CYP. Finally, the method of choice for electrochemical mimicry depends on the purpose of the study. For preparative synthesis of metabolites, direct electrochemical oxidation is a good option, though limited to the metabolites generated with electron transfer reactions (see section 2). For the metabolites not obtainable from this technique, the two other mimicry techniques should be tried, i.e. electrochemically generated reactive oxygen species (section 3), and metalloporphyrines (section 4). For the prediction of oxidative drug metabolism, the electrodes modified with enzymes (section 5), a field which is expanding fast, would be the method of choice.

1.7 References

[1] Bernadou, J.; Meunier, B. Biomimetic chemical catalysts in the oxidative activation of drugs. *Adv. Synth. Catal.* **2004**, *346*, 171-184.

[2] Oritz de Montellano, P. R. *Cytochrome P450: Structure, Mechanism, and Biochemistry*, 3rd ed.; Kluwer Academic/Plenum Publishers: New York, **2005**.

[3] Hayaishi, O.; Katagiri, M.; Rothberg, S. Mechanism of the pyrocatechase reaction. *J. Am. Chem. Soc.* **1955**, *77*, 5450-5451.

[4] Sawyer, D. T. *Oxygen Chemistry*; Oxford University Press, **1991**.

[5] Omura, T.; Sato, R. A new Cytochrome in liver microsomes. *J. Biol. Chem.* **1962**, *237*, 1375-1376.

[6] Poulos, T. L.; Finzel, B. C.; Howard, A. J. High-resolution crystal structure of cytochrome P450cam. *J. Mol. Biol.* **1987**, *195*, 687-700.

[7] Ravichandran, K. G.; Boddupalli, S. S.; Hasermann, C. A.; Peterson, J. A.; Deisenhofer, J. Crystal structure of hemoprotein domain of P450BM-3, a prototype for microsomal P450's. *Science* **1993**, *261*, 731-736.

[8] Davydov, R.; Makris, T. M.; Kofman, V.; Werst, D. E.; Sligar, S. G.; Hoffman, B. M. Hydroxylation of Camphor by Reduced Oxy-Cytochrome P450cam: Mechanistic Implications of EPR and ENDOR Studies of Catalytic Intermediates in Native and Mutant Enzymes. *J. Am. Chem. Soc.* **2001**, *123*, 1403-1415.

[9] Bonifacio, A.; Millo, D.; Keizers, P.; Boegschoten, R.; Commandeur, J.; Vermeulen, N.; Gooijer, C.; van der Zwan, G. Active-site structure, binding and redox activity of the heme–thiolate enzyme CYP2D6 immobilized on coated Ag electrodes: a surface-enhanced resonance Raman scattering study. *J. Biol. Inorg. Chem.* **2008**, *13*, 85-96.

[10] Bortolini, O.; Conte, V. Mass spectrometric characterization of high-valent metal-oxo, -peroxo and -peroxy intermediates of relevance in oxidation processes. *Mass Spectrom. Rev.* **2006**, *25*, 724-740.

[11] Liu, K. E.; Johnson, C. C.; Newcomb, M.; Lippard, S. J. Radical clock substrate probes and kinetic isotope effect studies of the hydroxylation of hydrocarbons by methane monooxygenase. *J. Am. Chem. Soc.* **1993**, *115*, 939-947.

[12] Bell, S. R.; Groves, J. T. A Highly Reactive P450 Model Compound I. *J. Am. Chem. Soc.* **2009**, *131*, 9640-9641.

[13] Shaik, S.; Cohen, S.; Wang, Y.; Chen, H.; Kumar, D.; Thiel, W. P450 Enzymes: Their Structure, Reactivity, and Selectivity-Modeled by QM/MM Calculations. *Chem. Rev.* **2010**, *110*, 949-1017.

[14] Shaik, S.; Kumar, D.; de Visser, S. I. P.; Altun, A.; Thiel, W. Theoretical Perspective on the Structure and Mechanism of Cytochrome P450 Enzymes. *Chem. Rev.* **2005**, *105*, 2279-2328.

[15] Meunier, B.; de Visser, S. I. P.; Shaik, S. Mechanism of Oxidation Reactions Catalyzed by Cytochrome P450 Enzymes. *Chem. Rev.* **2004**, *104*, 3947-3980.

[16] Groves, J. T. High-valent iron in chemical and biological oxidations. *J. Inorg. Biochem.* **2006**, *100*, 434-447.

[17] Newcomb, M.; Hollenberg, P. F.; Coon, M. J. Multiple mechanisms and multiple oxidants in P450-catalyzed hydroxylations. *Arch. Biochem. Biophys.* **2003**, *409*, 72-79.

[18] Hlavica, P. Models and mechanisms of O-O bond activation by cytochrome P450: A critical assessment of the potential role of multiple active intermediates in oxidative catalysis. *Eur. J. Biochem.* **2004**, *271*, 4335-4360.

[19] Guengerich, F. P. Common and Uncommon Cytochrome P450 Reactions Related to Metabolism and Chemical Toxicity. *Chem. Res. Toxicol.* **2001**, *14*, 611-650.

[20] Guengerich, F. P. Cytochrome P450 and Chemical Toxicology. *Chem. Res. Toxicol.* **2001**, *14*, 611-650.

[21] Lund, H.; Hammerich, O. *Organic Electrochemistry*, 4th ed.; Marcel Dekker, INC., **2001**.

[22] Special issue in Molecular and Biomolecular Electrochemistry. *Chem. Rev.* **2008**, *108.*

[23] Bruckenstein, S.; Gadde, R. R. Use of a porous electrode for in situ mass spectrometric determination of volatile electrode reaction products. *J. Am. Chem. Soc.* **1971**, *93*, 793-794.

[24] Hambitzer, G.; Heitbaum, J. Electrochemical Thermospray Mass Spectrometry Instrumentation for Coupling Electrochemistry to Mass Spectrometry. *Anal. Chem.* **1986**, *58*, 1067-1070.

[25] Volk, K. J.; Lee, M. S.; Yost, R. A.; Brajter-Toth, A. Electrochemistry/thermospray/tandem mass spectrometry in the study of biooxidation of purines. *Anal. Chem.* **1988**, *60*, 720-722.

[26] Zhou, F.; Van Berkel, G. J. Electrochemistry Combined Online with Electrospray Mass Spectrometry. *Anal. Chem.* **1995**, *67*, 3643-3649.

[27] Lu, W.; Xu, X.; Cole, R. B. On-Line Linear Sweep Voltammetry Electrospray Mass Spectrometry. *Anal. Chem.* **1997**, *69*, 2478-2484.

[28] Deng, H.; Van Berkel, G. J. A Thin-Layer Electrochemical Flow Cell Coupled On-Line with Electrospray-Mass Spectrometry for the Study of Biological Redox Reactions. *Electroanalysis* **1999**, *11*, 857-865.

[29] Van Berkel, G. J.; Asano, K. G.; Kertesz, V. Enhanced Study and Control of Analyte Oxidation in Electrospray Using a Thin-Channel, Planar Electrode Emitter. *Anal. Chem.* **2002**, *74*, 5047-5056.

[30] Kertesz, Van Berkel, G. J. Using the Electrochemistry of the Electrospray Ion Source. *Anal. Chem.* **2007**, *79*, 5510-5520.

[31] Diehl, G.; Karst, U. On-line electrochemistry - MS and related techniques. *Anal. Bioanal. Chem.* **2002**, *373*, 390-398.

[32] Lohmann, W.; Karst, U. Biomimetic modeling of oxidative drug metabolism : Strategies, advantages and limitations. *Anal. Bioanal. Chem.* **2008**, *391*, 79-96.

[33] Baumann, A.; Karst, U. Online electrochemistry/mass spectrometry in drug metabolism studies: principles and applications. *Expert Opin. Drug Metab. Toxicol.* **2010**, *6*, 715-731.

[34] Permentier, H. P.; Bruins, A. P.; Bischoff, R. Electrochemistry-mass spectrometry in drug metabolism and protein research. *Mini Rev. Med. Chem.* **2008**, 8, 46-56.

[35] Shono, T.; Toda, T.; Oshino, N. Preparation of N-dealkylated drug metabolites by electrochemical simulation of biotransformation. *Drug Metab. Dispos.* **1981**, *9*, 481-482.

[36] Jurva, U.; Wikström, H. V.; Bruins, A. P. In vitro mimicry of metabolic oxidation reactions by electrochemistry/mass spectrometry. *Rapid Commun. Mass Spectrom.* **2000**, *14*, 529-533.

[37] Jurva, U.; Wikström, H. V.; Weidolf, L.; Bruins, A. P. Comparison between electrochemistry/mass spectrometry and cytochrome P450 catalyzed oxidation reactions. *Rapid Commun. Mass Spectrom.* **2003**, *17*, 800-810.

[38] Johansson, T.; Jurva, U.; Grönberg, G.; Weidolf, L.; Masimirembwa, C. Novel Metabolites of Amodiaquine Formed by CYP1A1 and CYP1B1: Structure Elucidation Using Electrochemistry, Mass Spectrometry, and NMR. *Drug Metab. Dispos.* **2009**, *37*, 571-579.

[39] Odijk, M.; Baumann, A.; Lohmann, W.; van den Brink, F. T. G.; Olthuis, W.; Karst, U.; van den Berg, A. A microfluidic chip for electrochemical conversions in drug metabolism studies. *Lab Chip* **2009**, *9*, 1687-1693.

[40] Odijk, M.; Baumann, A.; Olthuis, W.; van den Berg, A.; Karst, U. Electrochemistry-on-chip for on-line conversions in drug metabolism studies. *Biosens. Bioelectron.*, **2010**, *26*,1521-1527.

[41] Karst, U. Electrochemistry/Mass Spectrometry (EC/MS)—A New Tool To Study Drug Metabolism and Reaction Mechanisms. *Angew. Chem. Int. Ed. Engl.* **2004**, *43*, 2476-2478.

[42] Meunier, B.; de Visser, S. P.; Shaik, S. Mechanism of oxidation reactions catalyzed by cytochrome P450 enzymes. *Chem. Rev.* **2004**, *104*, 3947-3980.

[43] Chandrasena, R. E. P.; Vatsis, K. P.; Coon, M. J.; Hollenberg, P. F.; Newcomb, M. Hydroxylation by the Hydroperoxy-Iron Species in Cytochrome P450 Enzymes. *J. Am. Chem. Soc.* **2003**, *126*, 115-126.

[44] Schlesener, C. J.; Amatore, C.; Kochi, J. K. Marcus theory in organic chemistry. Mechanisms of electron and proton transfers from aromatics and their cation radicals. *J. Phys. Chem.* **1986**, *90*, 3747-3756.

[45] Johansson, T.; Weidolf, L.; Jurva, U. Mimicry of phase I drug metabolism - Novel methods for metabolite characterization and synthesis. *Rapid Commun. Mass Spectrom.* **2007**, *21*, 2323-2331.

[46] Eberson, L.; Nyberg K. Anodic Aromatic substitution. *Acc. Chem. Res.* **1973**, *3*, 106-112.

[47] van Leeuwen, S. M.; Blankert, B.; Kauffmann, J. M.; Karst, U. Prediction of clozapine metabolism by on-line electrochemistry/liquid chromatography/mass spectrometry. *Anal. Bioanal. Chem.* **2005**, *382*, 742-750-750.

[48] Baumann, A.; Lohmann, W.; Schubert, B.; Oberacher, H.; Karst, U. Metabolic studies of tetrazepam based on electrochemical simulation in comparison to in vivo and in vitro methods. *J. Chromatogr. A* **2009**, *1216*, 3192-3198.

[49] Lohmann, W.; Karst, U. Simulation of the detoxification of paracetamol using on-line electrochemistry/liquid chromatography/mass spectrometry. *Anal. Bioanal. Chem.* **2006**, *386*, 1701-1708.

[50] Lohmann, W.; Karst, U. Generation and Identification of Reactive Metabolites by Electrochemistry and Immobilized Enzymes Coupled On-line to Liquid Chromatography/Mass Spectrometry. *Anal. Chem.* **2007**, *79*, 6831-6839.

[51] Lohmann, W.; Dötzer, R.; Gütter, G.; Van Leeuwen S. M.; Karst, U. On-Line Electrochemistry/Liquid Chromatography/Mass Spectrometry for the Simulation of Pesticide Metabolism. *J. Am. Soc. Mass Spectrom.* **2009**, *20*, 138-145.

[52] Baumann, A.; Lohmann, W.; Rose, K.; Ahn, K. C.; Hammock, B. D.; Karst, U.; Schebb, N. H. Electrochemistry-Mass Spectrometry Unveils the Formation of Reactive Triclocarbon Metabolites. *Drug Metab. Dispos.* **2010**, *38*, 2130-2138.

[53]van Leeuwen, S.; Hayen, H.; Karst, U. Liquid chromatography–electrochemistry–mass spectrometry of polycyclic aromatic hydrocarbons. *Anal. Bioanal. Chem.* **2004**, *378*, 917-925-925.

[54] Sharma, P. K.; de Visser, S. l. P.; Shaik, S. Can a Single Oxidant with Two Spin States Masquerade as Two Different Oxidants? A Study of the Sulfoxidation Mechanism by Cytochrome P450. *J. Am. Chem. Soc.* **2003**, *125*, 8698-8699.

[55] Hall, L. R.; Iwamoto, R. T.; Hanzlik, R. P. Electrochemical models for cytochrome P-450. N-Demethylation of tertiary amides by anodic oxidation. *J. Org. Chem.* **1989**, *54*, 2446-2451.

[56] Smith, P. J.; Mann, C. K. Electrochemical dealkylation of aliphatic amines. *J. Org. Chem.* **1969**, *34*, 1821-1826.

[57] Jurva, U.; Bissel, P.; Isin, E. M.; Igarashi, K.; Kuttab, S.; Castagnoli, Jr. N. Model electrochemical-mass spectrometric studies of the cytochrome P450-catalyzed oxidations of cyclic tertiary allylamines. *J. Am. Chem. Soc.* **2005**, *127*, 12368-12377.

[58] Nouri-Nigjeh, E.; Permentier, H. P.; Bischoff, R.; Bruins, A. P. Lidocaine Oxidation by Electrogenerated Reactive Oxygen Species in the Light of Oxidative Drug Metabolism. *Anal. Chem.* **2010**, *82*, 7625–7633.

[59] Nozaki, K.; Kitagawa, H.; Kimura, S.; Kagayama, A.; Arakawa, R. Investigation of the electrochemical oxidation products of zotepine and their fragmentation using on-line electrochemistry/electrospray ionization mass spectrometry. *J. Mass Spectrom.* **2006**, *41*, 606-612.

[60] Johansson, T.; Weidolf, L.; Castagnoli, Jr. N.; Jurva, U. P450-catalyzed vs. electrochemical oxidation of haloperidol studies by ultra-performance liquid chromatography/electrospray ionization mass spectrometry. *Rapid Commun. Mass Spectrom.* **2010**, *24*, 1231-1240.

[61] Rettie, A. E.; Boberg, M.; Rettenmeier, A. W.; Baillie, T. A. Cytochrome P-450-catalyzed desaturation of valproic acid in vitro. Species differences, induction effects, and mechanistic studies. *J. Biol. Chem.* **1988**, *263*, 13733-13738.

[62] Koymans, L.; Donnè-Op Den Kelder, G. M.; Te Koppele, J. M.; Vermeulen, N. P. E. Generalized cytochrome P450-mediated oxidation and oxygenation reactions in aromatic substrates with activated N-H, O-H, C-H, or S-H substituents. *Xenobiotica* **1993**, *23*, 633-648.

[63] Madsen, K. G.; Olsen, J.; Skonberg, C.; Hansen, S. H.; Jurva, U. Development and Evaluation of an Electrochemical Method for Studying Reactive Phase-I Metabolites: Correlation to *in vivo* Drug Metabolism. **2007**, *20*, 821-831.

[64] Jurva, U.; Holmèn, A.; Grönberg, G.; Masimirembwa, C.; Weidolf, L. Electrochemical Generation of Electrophilic Drug Metabolites: Characterization of Amodiaquine Quinoneimine and Cysteinyl Conjugates by MS, IR, and NMR. *Chem. Res. Toxicol.* **2008**, *21*, 928-935.

[65] Pontinha, A. D. R.; Oliveira, S. C. B.; Oliveira-Brett A. M. Electrochemical Oxidation of Metolazone at a Glassy Carbon Electrode. *Electroanalysis* **2008**, *23*, 2531-2536.

[66] Garrido, J. M. P. J.; Delerue-Matos, C.; Borges, F.; Macedo, T. R. A.; Oliveira-Brett A. M. New insights into the oxidation pathways of apomorphine. *J. Chem. Soc., Perkin Trans.* **2002**, *2*, 1713-1717.

[67] Oliveira, S. C. B.; Vivan, M.; Oliveira-Brett A. M. Electrochemical Behavior of Thalidomide at a Glassy Carbon Electrode. *Electroanalysis* **2008**, *22*, 2429-2434.

[68] Jeftic, L.; Adams, R. N. Electrochemical oxidation pathways of benzo[a]pyrene. *J. Am. Chem. Soc.* **1970**, *92*, 1332-1337.

[69] Xu, X.; Lu, W.; Cole, R. B. On-Line Probe for Fast Electrochemistry/Electrospray Mass Spectrometry Investigation of Polycyclic Aromatic Hydrocarbons. *Anal. Chem.* **1996**, *68*, 4244-4253.

[70] Sawyer, D. T.; Seo, E. T. One-electron mechanism for the electrochemical reduction of molecular oxygen. *Inorg. Chem.* **1977**, *16*, 499-501.

[71] Sawyer, D. T.; Valentine, J. S. How super is superoxide? *Acc. Chem. Res.* **1981**, *14*, 393-400.

[72] Singh, P. S.; Evans, D. H. Study of the Electrochemical Reduction of Dioxygen in Acetonitrile in the Presence of Weak Acids. *J. Phys. Chem. B* **2006**, *110*, 637-644.

[73] Che, Y.; Tsushima, M.; Matsumoto, F.; Okajima, T.; Tokuda, K.; Ohsaka, T. Water-Induced Disproportionation of Superoxide Ion in Aprotic Solvents. *J. Phys. Chem.* **1996**, *100*, 20134-20137.

[74] Cofre, P.; Sawyer, D. T. Electrochemical reduction of dioxygen to perhydroxyl (HO2.cntdot.) in aprotic solvents that contain Broensted acids. *Anal. Chem.* **1986**, *58*, 1057-1062.

[75] Lorenzola, T. A.; Lopez, B. A.; Giordano, M. C. Molecular Oxygen Electroreduction at Pt and Au Electrodes in Acetonitrile Solutions. *J. Electrochem. Soc.* **1983**, *130*, 1359-1365.

[76] Sawyer, D. T.; Chiericato, G.; Angelis, C. T.; Nanni, E. J.; Tsuchiya, T. Effects of media and electrode materials on the electrochemical reduction of dioxygen. *Anal. Chem.* **1982**, *54*, 1720-1724.

[77] Kolthoff, I. M.; Jordan, J. Oxygen Induced Electroreduction of Hydrogen Peroxide and Reduction of Oxygen at the Rotated Gold Wire Electrode. *J. Am. Chem. Soc.* **1952**, *74*, 4801-4805.

[78] Ozawa, T.; Hanaki, A. Reactions of superoxide with water and with hydrogen peroxide. *Chem. Pharm. Bull.* **1981**, *29*, 926-928.

[79] Oswald, A. A.; Guertin, D. L. Organic Nitrogen Compounds. I. Peroxide Intermediates of Tertiary Alkylamine Oxidation by Hydrogen Peroxide. *J. Org. Chem.* **1963**, *28*, 651-657.

[80] Panizza, M.; Cerisola, G. Direct and Mediated Anodic Oxidation of Organic Pollutants. *Chem. Rev.* **2009**, *109*, 6541-6569.

[81] Enache, T. A.; Chiorcea-Paquim, A.; fatibello-Filho, O.; Oliveira-Brett, A. M. Hydroxyl radicals electrochemically generated *in situ* on a boron-doped diamond electrode. *Electrochem. Commun.* **2009**, *11*, 1342-1345.

[82] Oliveira, S. C. B.; Oliveira-Brett A. M. Voltammetric and electrochemical impedance spectroscopy characterization of a cathodic and anodic pre-treated boron doped diamond electrode. *Electrochimica Acta* **2010**, *55*, 4599-4605.

[83] Bensalah, N.; Abdellatif, G.; Caňzares, P.; Săez, C.; Lobato, J.; Rodrigo, M. A. Electrochemical Oxidation of Hydroquinone, Resorcinol, and Catechol on Boron-Doped Diamond Anodes. *Environ. Sci. Technol.* **2005**, *39*, 7234-7239.

[84] Oturan, M. A.; Pinson, J. Hydroxylation by Electrochemically Generated OH.bul. Radicals. Mono- and Polyhydroxylation of Benzoic Acid: Products and Isomer Distribution. *J. Phys. Chem.* **1995**, *99*, 13948-13954.

[85] Brillas, E.; Sirès, I.; Oturan, M. A. Electro-Fenton Process and Related Electrochemical Technologies Based on Fenton Reaction Chemistry. *Chem. Rev.* **2009**, *109*, 6570-6631.

[86] Walling, C. Fenton's reagent revisited. *Acc. Chem. Res.* **1975**, *8*, 125-131.

[87] Anipsitakis, G. P.; Dionysiou, D. D. Radical Generation by the Interaction of Transition Metals with Common Oxidants. *Environ. Sci. Technol.* **2004**, *38*, 3705-3712.

[88] Sawyer, D. T.; Sobkowiak, A.; Matsushita, T. Metal [MLx; M = Fe, Cu, Co, Mn]/Hydroperoxide-Induced Activation of Dioxygen for the Oxygenation of Hydrocarbons: Oxygenated Fenton Chemistry. *Acc. Chem. Res.* **1996**, *29*, 409-416.

[89] Hage, J. P.; Llobet, A.; Sawyer, D. T. Aromatic hydroxylation by fenton reagents {Reactive intermediate[Lx+FeIIIOOH(BH+)], not free hydroxyl radical (HO·)}. *Bioorg. Med. Chem.* **1995**, *3*, 1383-1388.

[90] Walling, C. Intermediates in the Reactions of Fenton Type Reagents. *Acc. Chem. Res.* **1998**, *31*, 155-157.

[91] Jurva, U.; Wikström, H. V.; Bruins, A. P. Electrochemically assisted Fenton reaction: reaction of hydroxyl radicals with xenobiotics followed by on-line analysis with high-performance liquid chromatography/tandem mass spectrometry. *Rapid Commun. Mass Spectrom.* **2002**, *16*, 1934-1940.

[92] Sirés, I.; Oturan, N.; Oturan, M. A.; Rodríguez, R. M.; Garrido, J. A.; Brillas, E. Electro-Fenton degradation of antimicrobials triclosan and triclocarban. *Electrochim. Acta* **2007**, *52*, 5493-5503.

[93] Isarain-Chávez, E.; Arias, C.; Cabot, P. L.; Centellas, F.; Rodríguez, R. M.; Garrido, J. A.; Brillas, E. Mineralization of the drug [beta]-blocker atenolol by electro-Fenton and photoelectro-Fenton using an air-diffusion cathode for H2O2 electrogeneration combined with a carbon-felt cathode for Fe2+ regeneration. *Appl. Catal. B* **2010**, *96*, 361-369.

[94] Sirés, I.; Arias, C.; Cabot, P. L.; Centellas, F.; Garrido, J. A.; Rodríguez, R. M.; Brillas, E. Degradation of clofibric acid in acidic aqueous medium by electro-Fenton and photoelectro-Fenton. *Chemosphere* **2007**, *66*, 1660-1669.

[95] Brillas, E.; Sirés, I.; Arias, C.; Cabot, P. L.; Centellas, F.; Rodríguez, R. M.; Garrido, J. A. Mineralization of paracetamol in aqueous medium by anodic oxidation with a boron-doped diamond electrode. *Chemosphere* **2005**, *58*, 399-406.

[96] Barton, D. H. R.; Doller, D. The selective functionalization of saturated hydrocarbons: Gif chemistry. *Acc. Chem. Res.* **1992**, *25*, 504-512.

[97] About-Jaudet, E.; Barton, D. H. R.; Csuhai, E.; Ozbalik, N. Effect of ligand variation on the rate of cyclododecane oxidation under modified Go AggII conditions. *Tetrahedron Lett.* **1990**, *31*, 1657-1660.

[98] Barton, D. H. R.; Csuhai, E.; Doller, D.; Ozbalik, N.; Senglet, N. Comparison of gif-type reactivity towards alkanes with standard radical reaction selectivity. Gif oxidation of n-butane and propane. *Tetrahedron Lett.* **1990**, *31*, 3097-3100.

[99] Newcomb, M.; Simakov, P. A.; Park, S.-U. Hypersensitive radical probe studies of Gif oxidations. *Tetrahedron Lett.* **1996**, *37*, 819-822.

[100] Stavropoulos, P.; Çelenligil-çetin, R.; Tapper, A. E. The Gif Paradox. *Acc. Chem. Res.* **2001**, *34*, 745-752.

[101] Gozzo, F. Radical and non-radical chemistry of the Fenton-like systems in the presence of organic substrates. *J. Mol. Catal. A Chem.* **2001**, *171*, 1-22.

[102] Balavoine, G.; Barton, D. H. R.; Boivin, J.; Gref, A.; Ozbalik, N.; Rivière, H. Selective oxidation of saturated hydrocarbons using an electrochemical modification of the gif system. *Tetrahedron Lett.* **1986**, *27*, 2849-2852.

[103] Chorghade, M. S.; Hill, D. R.; Lee, E. C.; Pariza, R. J.; Dolphin, D. H.; Hino, F.; Zhang, L. Y. Metalloporphyrins as chemical mimics of cytochrome P-450 systems. *Pure Appl. Chem.* **1996**, *68*, 753-756.

[104] Gross, Z.; Ini, S. Remarkable Effects of Metal, Solvent, and Oxidant on Metalloporphyrin-Catalyzed Enantioselective Epoxidation of Olefins. *J. Org. Chem.* **1997**, *62*, 5514-5521.

[105] Groves, J. T.; Neumann, R. Regioselective oxidation catalysis in synthetic phospholipid vesicles. Membrane-spanning steroidal metalloporphyrins. *J. Am. Chem. Soc.* **1989**, *111*, 2900-2909.

[106] Balogh, G. T.; Keseru, G. M. Metalloporphyrin mediated biomimetic oxidations. A useful tool for the investigation of cytochrome P450 catalyzed oxidative metabolism. *Arkivoc* **2004**, *2004*, 124-139.

[107] Nam, W. High-Valent Iron[IV] Oxo Complexes of Heme and Non-Heme Ligands in Oxygenation Reactions. *Acc. Chem. Res.* **2007**, *40*, 522-531.

[108] Creager, S. E.; Raybuck, S. A.; Murray, R. W. An efficient electrocatalytic model cytochrome P-450 epoxidation cycle. *J. Am. Chem. Soc.* **1986**, *108*, 4225-4227.

[109] Creager, S. E.; Murray, R. W. Electrochemical reactivity of manganese(II) porphyrins. Effects of dioxygen, benzoic anhydride, and axial ligands. *Inorg. Chem.* **1987**, *26*, 2612-2618.

[110] Simandi, L. I. *Catalytic activation of dioxygen by metal complexes*; Kluwer Academic Publishers, Dorderecht, The Netherlands, **1992**.

[111] Meunier, B. Metalloporphyrins as versatile catalysts for oxidation reactions and oxidative DNA cleavage. *Chem. Rev.* **1992**, *92*, 1411-1456.

[112] Brule, E.; de Miguel, Y. R. Supported metalloporphyrin catalysts for alkene epoxidation. *Org. Biomol. Chem.* **2006**, *4*, 599-609.

[113] Radha Rani, V.; Radha Kishan, M.; Kulkarni, S. J.; Raghavan, K. V. Immobilization of metalloporphyrin complexes in molecular sieves and their catalytic activity. *Catal. Commun.* **2005**, *6*, 531-538.

[114] Parton, R. F.; Vankelecom, I. F. J.; Casselman, M. J. A.; Bezoukhanova, C. P.; Uytterhoeven, J. B.; Jacobs, P. A. An efficient mimic of cytochrome P-450 from a zeolite-encaged iron complex in a polymer membrane. *Nature* **1994**, *370*, 541-544.

[115] Bedioui, F.; Devynck, J.; Bied-Charreton, C. Electropolymerized manganese porphyrin films as catalytic electrode materials for biomimetic oxidations with molecular oxygen. *J. Mol. Catal. A Chem.* **1996**, *113*, 3-11.

[116] Bedioui, F.; Devynck, J.; Bied-Charreton, C. Immobilization of metalloporphyrins in electropolymerized films: design and applications. *Acc. Chem. Res.* **1995**, *28*, 30-36.

[117] Nishihara, H.; Pressprich, K.; Murray, R. W.; Collman, J. P. Electrochemical olefin epoxidation with manganese meso-tetraphenylporphyrin catalyst and hydrogen peroxide generation at polymer-coated electrodes. *Inorg. Chem.* **1990**, *29*, 1000-1006.

[118] Offord, D. A.; Sachs, S. B.; Ennis, M. S.; Eberspacher, T. A.; Griffin, J. H.; Chidsey, C. E. D.; Collman, J. P. Synthesis and Properties of Metalloporphyrin Monolayers and Stacked Multilayers Bound to an Electrode via Site Specific Axial Ligation to a Self-Assembled Monolayer. *J. Am. Chem. Soc.* **1998**, *120*, 4478-4487.

[119] Zhang, Z.; Hou, S.; Zhu, Z.; Liu, Z. Preparation and Characterization of a Porphyrin Self-Assembled Monolayer with a Controlled Orientation on Gold. *Langmuir* **1999**, *16*, 537-540.

[120] Traylor, T. G.; Nakano, T.; Dunlap, B. E.; Traylor, P. S.; Dolphin, D. Mechanisms of hemin-catalyzed alkene epoxidation. The effect of catalyst on the regiochemistry of epoxidation. *J. Am. Chem. Soc.* **1986**, *108*, 2782-2784.

[121] Millo, D.; Bonifacio, A.; Ranieri, A.; Borsari, M.; Gooijer, C.; van der Zwan, G. Voltammetric and Surface-Enhanced Resonance Raman Spectroscopic Characterization of Cytochrome c Adsorbed on a 4-Mercaptopyridine Monolayer on Silver Electrodes. *Langmuir* **2007**, *23*, 4340-4345.

[122] van Rantwijk, F.; Sheldon, R. A. Selective oxygen transfer catalysed by heme peroxidases: synthetic and mechanistic aspects. *Curr. Opin. Biotechnol.* **2000**, *11*, 554-564.

[123] Akasaka, R.; Mashino, T.; Hirobe, M. Hydroxylation of benzene by horseradish peroxidase and immobilized horseradish peroxidase in an organic solvent. *Bioorg. Med. Chem. Lett.* **1995**, *5*, 1861-1864.

[124] van de Velde, F.; van Rantwijk, F.; Sheldon, R. A. Selective oxidations with molecular oxygen, catalyzed by chloroperoxidase in the presence of a reductant. *J. Mol. Catal., B Enzym.* **1999**, *6*, 453-461.

[125] Lombardi, A.; Nastri. F.; Pavone, V. Peptide-Based Heme-Protein Models. *Chem. Rev.* **2001**, *101*, 3165-3189.

[126] Raineri, A.; Monari, S.; Sola, M.; Borsari, M.; Battistuzzi, G.; Ringhieri, P.; Nastri, F.; Pavone, V.; Lombardi, A. Redox and Electrocatalytic Properties of Microchrome VI, a synthetic Heme Peptide Adsorbed on Gold. *Langmuir* **2010**, *26*, 17831-17835.

[127] Shumyantseva, V. V.; Bulko, T. V.; Rudakov, Y. O.; Kuznetsova, G. P.; Samenkova, N. F.; Lisitsa, A. V.; Karuzina, I. I.; Archakov, A. I. Electrochemical properties of cytochrome P450 using nanostructured electrodes: Direct electron transfer and electro catalysis. *J. Inorg. Biochem.* **2007**, *101*, 859-865.

[128] Zu, X.; Lu, Z.; Zhang, Z.; Schenkman, J. B.; Rusling, J. F. Electroenzyme-Catalyzed Oxidation of Styrene and cis-Methylstyrene Using Thin Films of Cytochrome P450cam and Myoglobin. *Langmuir* **1999**, *15*, 7372-7377.

[129] Sultana, N.; Schenkman, J. B.; Rusling, J. F. Protein Film Electrochemistry of Microsomes Genetically Enriched in Human Cytochrome P450 Monooxygenases. *J. Am. Chem. Soc.* **2005**, *127*, 13460-13461.

[130] Mie, Y.; Suzuki, M.; Komatsu, Y. Electrochemically Driven Drug Metabolism by Membranes Containing Human Cytochrome P450. *J. Am. Chem. Soc.* **2009**, *131*, 6646-6647.

[131] Gilardi, G.; Meharenna, Y. T.; Tsotsou, G. E.; Sadeghi, S. J.; Fairhead, M.; Giannini, S. Molecular Lego: design of molecular assemblies of P450 enzymes for nanobiotechnology. *Biosens. Bioelectron.* **2002**, *17*, 133-145.

[132] Fantuzzi, A.; Meharenna, Y. T.; Briscoe, P. B.; Sassone, C.; Borgia, B.; Gilardi, G. Improving catalytic properties of P450 BM3 haem domain electrodes by molecular Lego. *Chem. Commun.* **2006**, 1289-1291.

[133] Sadeghi, S. J.; Meirinhos, R.; Catucci, G.; Dodhia, V. R.; Nardo, G. D.; Gilardi, G. Direct Electrochemistry of Drug Metabolizing Human Flavin-Containing Monooxygenase: Electrochemical Turnover of Benzydamine and Tamoxifen. *J. Am. Chem. Soc.* **2010**, *132*, 458-459.

[134] Mak, L. H.; Sadeghi, S. J.; Fantuzzi, A.; Gilardi, G. Control of Human Cytochrome P450 2E1 Electrocatalytic Response as a Result of Unique Orientation on Gold Electrodes. *Anal. Chem.* **2010**, *82*, 5357-5362.

[135] Fantuzzi, A.; Capria, E.; Mak, L. H.; Dodhia, V. R.; Sadeghi, S. J.; Collins, S.; Somers, G.; Huq, E.; Gilardi, G. An Electrochemical Microfluidic Platform for Human P450 Drug Metabolism Profiling. *Anal. Chem.* **2010**, *82*, 10222-10227.

[136] Nouri-Nigjeh, E.; Permentier, H. P.; Bischoff, R.; Bruins, A. P. Electrodes modified with immobilized hemin via SAMs to mimic difficult oxidation pathways mediated by Cytochrome P450 in EC/MS. **Poster Presentation** in Annual Meeting NWO/CW Studiegroep Analytische Scheikunde, Lunteren, The Netherlands, November 5-6, **2007**.

Chapter 2
Lidocaine oxidation by electrogenerated reactive oxygen species in the light of oxidative drug metabolism*

The study of oxidative drug metabolism by Cytochrome P450s (CYP) is important in the earlier stages of drug development. For this purpose, automated analytical techniques are needed for fast and accurate estimation of oxidative drug metabolism. Previous studies have shown that electrochemistry in combination with mass spectrometry is a versatile analytical technique to generate drug metabolites that result from direct electron transfer. Here we show that electrochemical generation of reactive oxygen species (ROS), a process reminiscent of the catalytic cycle of CYP, extends the applicability of electrochemistry in drug metabolism research. Oxidation products of lidocaine from one and two-compartment electrochemical cells, operated under various conditions were analyzed by LC-MS and metabolite structures were elucidated by collision-induced (LC-MS/MS), and thermally-induced (APCI) fragmentation. Direct oxidation of lidocaine at the anode resulted in N-dealkylation while reaction with H_2O_2, generated at the cathode, produced the N-oxide, both known in vivo lidocaine metabolites. Catalytic activation of hydrogen peroxide, using the Fenton reaction, resulted in benzylic and aromatic hydroxylations thus covering all of the known in vivo phase-I metabolites of lidocaine. This study extends the applicability of electrochemistry combined with mass spectrometry as a valuable technique in assessing oxidative drug metabolism related to CYP.

* Published as: Nouri-Nigjeh, E.; Permentier, H.P.; Bischoff, R.; Bruins, A.P. Lidocaine oxidation by electrogenerated reactive oxygen species in the light of oxidative drug metabolism, Analytical Chemistry, Vol. 82, 2010, 7625-7633.

2.1 Introduction

Evaluation of oxidative drug metabolism is important in the earlier stages of drug development and requires fast, and accurate analytical techniques. This aspect of drug stability is presently studied through enzymatic reactions with Cytochrome P450s (CYP), either in pure, recombinant form or as part of liver microsomes [1, 2]. Electrochemistry coupled with mass spectrometry has been shown to be a fast technique that provides oxidation products generated by direct electron transfer [3-7]. Electrochemistry can also be used to generate reactive oxygen species (ROS), in analogy to the catalytic activation of molecular oxygen by CYP [8]. Lidocaine, a common local-anesthetic drug, is a convenient test compound, whose *in vivo* oxidative metabolism leads to N-dealkylation, N-oxidation, aromatic hydroxylation and benzylic hydroxylation products [4, 9]. The reactions involve a putative oxo-ferryl radical cation intermediate (a reactive electrophile) as part of the heme prosthetic group of CYP [10].

N-dealkylation of lidocaine by CYP is proposed to be initiated by two mechanisms: hydrogen atom transfer (HAT) from the carbon atom adjacent to the nitrogen, and single electron transfer (SET) from nitrogen to CYP (**Scheme 1-a**) [10]. The available experimental evidence supports the SET mechanism [10]. N-oxidation could proceed via initial charge transfer to the oxo-ferryl group, resulting in a radical cation, followed by homolysis of the iron-oxygen bond to generate the new N-O bond. Alternatively, this reaction may proceed through a concerted oxygen insertion process [10]. While the HAT mechanism may explain benzylic hydroxylation, it is not applicable for the hydroxylation of aromatic substrates, because of the energy that is required for the homolytic cleavage of the aromatic C-H bond [10]. In this case, it is proposed that the oxo-ferryl radical cation attacks the aromatic ring to generate an intermediate which reacts to the hydroxylation product through a hydrogen shift (NIH (National Institute of Health) mechanism, **Scheme 1-b**) [10]. New studies provide evidence for the presence of other electrophilic oxidants, e.g. perhydroxo-iron or iron-complexed hydrogen peroxide, in the catalytic cycle of CYP which may generate protonated alcohols (alternative electrophilic oxidants, **Scheme 1-b**) [11].

The majority of organic compounds is not readily oxidized by molecular oxygen, because the triplet electronic structure of molecular oxygen prevents its direct reaction with (mostly singlet) organic compounds. In the catalytic cycle of CYP, molecular oxygen gets activated through a sequence of reductions and protonations. Similarly, electrochemical reduction of molecular oxygen in organic solutions has been shown to lead to the oxidation of various organic substrates [8,

12]. In aprotic solutions, molecular oxygen is reduced to the superoxide anion via a one-electron process (**reaction 1**), and reduced further at more negative potentials to singlet peroxide anions (**reaction 2**). The electrode material could affect the reduction of molecualr oxygen. It has been shown that metallic electrodes, especially in acetonitrile, show a broader reduction peak due to interactions between electrogenerated superoxide anions and a metallic surface [13].

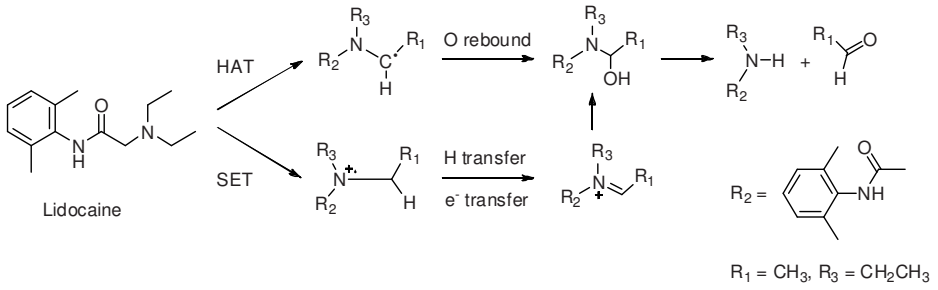

(a) N-dealkylation

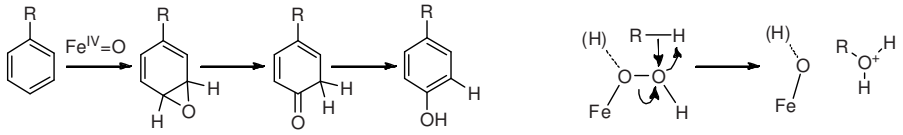

(b) Aromatic hydroxylation

Scheme 1. Proposed CYP-catalyzed reaction mechanisms for (a) the N-dealkylation of lidocaine initiated by single electron transfer (SET) and hydrogen atom transfer (HAT), and (b) the aromatic hydroxylation of lidocaine via the NIH shift or the alternative electrophilic oxidants [10].

$O_2 + e^- \rightarrow O_2^{-\bullet}$ $E^0 = -0.75$ V vs SCE (1)

$O_2^{-\bullet} + e^- \rightarrow O_2^{2-}$ $E^0 = -2.05$ V vs SCE (2)

In the presence of residual water electrogenerated superoxide anions undergo dismutation, leading to the generation of perhydroxyl radicals (**reaction 3**), which are strong oxidizers capable of rapidly abstracting an electron from the electrode or

the electrogenerated superoxide anion to form perhydroxyl anions (**reactions 4 and 5**) [8]. Perhydroxyl radicals are unstable, and decompose spontaneously to hydrogen peroxide and molecular oxygen (**reaction 6**) [8]. In addition, disproportionation of the electrogenerated superoxide anions with water produces perhydroxyl anions and molecular oxygen (**reaction 7**) [8]. The formation of hydrogen peroxide by protonation of the perhydroxyl anion generated in **reactions 4, 5, and 7** has been proven spectroscopically [14]. Generation of hydroxyl radicals through reduction of hydrogen peroxide by superoxide anions (**reaction 8**), has also been reported [15, 16].

$$O_2^{-\bullet} + H_2O \rightarrow HO_2^{\bullet} + OH^- \quad (3)$$

$$HO_2^{\bullet} + e^- \rightarrow HO_2^- \quad (4)$$

$$HO_2^{\bullet} + O_2^{-\bullet} \rightarrow HO_2^- + O_2 \quad (5)$$

$$HO_2^{\bullet} + HO_2^{\bullet} \rightarrow H_2O_2 + O_2 \quad (6)$$

$$2\ O_2^{-\bullet} + H_2O \rightarrow HO_2^- + O_2 + OH^- \quad (7)$$

$$H_2O_2 + O_2^{-\bullet} \rightarrow OH^{\bullet} + OH^- + O_2 \quad (8)$$

In the present study, we produce electrogenerated ROS in the presence of lidocaine, to examine their applicability in the generation of metabolites by CYP. We utilize cyclic voltammetry to follow the reactions, and LC-MS(/MS) to identify reaction products.

2.2 Experimental Procedures

Reagents. Tetrabutylammonium perchlorate (TBAP, 86893), iron chloride ($FeCl_3$, 157740), ethylenediaminetetraacetic acid (EDTA, 431788), ascorbic acid (A5960), m-chloroperbenzoic acid (m-CPBA, 273031), sodium carbonate (204420), hydrogen peroxide 30 vol % (31642) and lidocaine (L7757) were purchased from Sigma-Aldrich. Water was purified by a Maxima Ultrapure water system (ELGA, High Wycombe, Bucks, UK). Ultra-pure HPLC grade acetonitrile (ACN) was purchased from Merck. 3-Hydroxylidocaine (CAS Nr. 34604-55-2) was purchased from Toronto Research Chemicals Inc.

Electrode preparation. The surface of a gold disk electrode with 1.6 mm diameter (MF-2014, Bioanalytical Systems (BASi), West Lafayette, IN, USA) was polished with a lapping sheet (Micromesh grade 3200) prior to each experiment. After mechanical polishing the surface was washed with ethanol and air-dried.

Electrochemical measurements. Electrochemical experiments were performed with a home-made potentiostat controlled by a MacLab system (ADInstruments, Castle Hill, NSW, Australia) and EChem v.1.52 software (eDAQ, Denistone East,

NSW, Australia). The electrochemical cell was a conventional three electrode cell in which the working electrode was a gold disk and the auxiliary electrode a platinum wire (MW-4130, BASi). Potentials were measured against a silver wire pseudo-reference electrode (MF-2017, BASi), instead of conventional reference electrodes, to eliminate the possibility of chloride contamination of the working solution during prolonged electrolysis. For the calibration of the silver reference electrode, the half-peak redox potentials of Fe^{2+}/Fe^{3+} against the silver electrode and a Ag/AgCl 3 M reference electrode (MF-2052, BASi) in an aqueous 0.1 M NaCl solution with 10 mM potassium hexacyanoferrate were measured at 0.2 and 0.6 V, respectively. The potential shift of 0.4 V was also measured for the reduction of molecular oxygen from 0.1 M TBAP dissolved in ACN/H_2O 99/1 (v/v) (**Figure 1**). All experiments were performed at ambient temperature. For deaeration and aeration, argon and synthetic air, respectively, were bubbled at 25 mL/min via a sparge tube (MW-4145, BASi) through the 1 mL solution for 10 minutes prior to each experiment. Cyclic voltammetry measurements were started at 0 V, swept toward negative potentials, and the steady state scans were selected for analysis. A two-compartment electrochemical cell was constructed by using a porous Vycor tip with Teflon heat shrink (MF-2064, BASi) to separate working and auxiliary half-cells. The atmosphere in the both compartments was controlled by sparging with argon or synthetic air. The reference electrode was placed in the working compartment.

Solutions containing 10 mM lidocaine and 0.1 M TBAP dissolved in ACN or ACN/H_2O 99/1 (v/v) (0.1 M TBAP used as electrolyte to provide sufficient conductivity for electrochemical experiments) were subjected to constant potentials ranging from 0 to -2.4 V vs. Ag, in 0.2 V steps, with continuous gas flow, for 10 minutes prior to LC-MS and LC-MS/MS analysis. Electrochemical control experiments were done under argon atmosphere. Reaction with 1 vol % hydrogen peroxide (no electrochemistry) was done for one hour. Samples were collected and diluted 100 times in water containing 10 µM acetaminophen, as an internal standard for LC-MS signal normalization, immediately after the batch oxidations and stored at room temperature until LC-MS analysis. Oxidation mixtures from the two-compartment cell were collected separately. Stability of the oxidation products during storage was examined by analyzing the solution immediately after oxidation and again after storage for two days at room temperature. No changes were observed in the 100 times diluted samples. Three independent batch potentiostatic oxidation experiments were performed, each of which was analyzed twice by LC-MS.

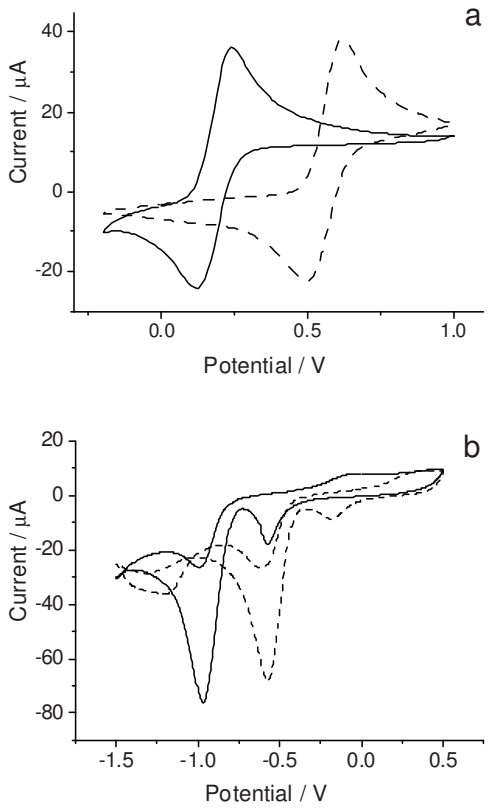

Figure 1. (a) Redox couple of Fe^{2+}/Fe^{3+} recorded in an aqueous 0.1 M NaCl solution with 10 mM potassium hexa-cyanoferrate and (b) reduction of molecular oxygen from ACN/H_2O 99/1 (v/v) solution with 0.1 M TBAP, versus silver wire (solid line) and versus a Ag/AgCl 3 M KCl reference electrode (dashed line). Scan rate 100 mV/s.

Fenton reaction. In a glass vial, 0.1 mL of 10 mM $FeCl_3$, and 10 mM EDTA in ACN/H_2O 50/50 (v/v) was added to 0.8 mL ascorbic acid (6 mM) in ACN/H_2O 50/50 (v/v). Subsequently, 2 µL H_2O_2 (30 % in water) was added, followed by 0.1 mL of 100 mM lidocaine to give a final lidocaine concentration of 10 mM. The mixture was kept for ten hours at 50 °C prior to analysis.

N-oxide synthesis. 3.44 mg of m-chloroperbenzoic acid was added to a 1 mL solution of 10 mM lidocaine in dichloromethane and the mixture was stirred for 1 h at room temperature. Saturated Na_2CO_3 solution (1 mL) was added and the

mixture was stirred for an additional hour [17]. For the LC-MS(/MS) analysis, the sample was taken from the dichloromethane layer.

LC-MS analysis. LC-MS experiments on 100-times diluted samples were carried out on an LC-Packings Ultimate HPLC system (LC-Packings, Amsterdam, the Netherlands) coupled to an API 365 triple quadrupole mass spectrometer (MDS Sciex, Concord, ON, Canada) with electrospray ionization in the positive mode. The original API 365 was used for experiments shown in Figure 3. All other LC-MS(/MS) experiments were performed on an API 365 triple quadrupole upgraded to EP10+ (Ionics, Bolton, ON, Canada). The MS parameters, for the API 365, were as follows: ion spray voltage 5200 V, orifice (OR) voltage 5 V, and ring (RNG) voltage 50 V, with scans between *m/z* 150-300 (step size 1.0 amu, dwell time 2 ms). The MS parameters, for the EP 10+, were as follows: ion spray voltage 4800 V, OR 40 V, and RNG 120 V, with scans between *m/z* 50-600 (step size 1.0 amu, dwell time 1 ms). MS/MS parameters, for EP 10+, were as follows: ion spray voltage 5000 V, OR 40 V, RNG 170 V, and collision energy 20 eV, with product ion scans between *m/z* 50-300 (step size 1.0 amu, dwell time 1 ms). Heated turbo gas (nitrogen) with a flow rate of 1.0 L/min was used at 450 °C for LC-MS and LC-MS/MS experiments. Atmospheric Pressure Chemical Ionization (APCI) experiments were done with OR 5 V, and RNG 40 V, with scans between *m/z* 50-600 (step size 1.0 amu, dwell time 1 ms); the discharge current of the APCI source was 3 µA, and the heated nebulizer temperature was 450 °C.

A C_{18} reversed-phase column (GraceSmart RP 18 5µm, 2.1×150 mm; Grace Davison, Lokeren, Belgium) was used at a flow rate of 200 µL/min. Solvent A: H_2O/ACN 95/5 (v/v) with 0.1 % formic acid; Solvent B: ACN/H_2O 95/5 (v/v) with 0.1 % formic acid. 50 µL of a diluted oxidation product mixture was injected and a linear gradient of 5-50 % B in 20 minutes was used for elution. For APCI experiments, a 5 µL injection was used. Peak heights were normalized with respect to the peak height of the acetaminophen internal reference compound.

2.3 Results and discussion

2.3.1 Electrochemistry of molecular oxygen in the presence and absence of water

Cyclic voltammetry (CV) was used to follow the electrochemical reduction of molecular oxygen in an acetonitrile/tetrabutylammonium perchlorate (TBAP) solution in the absence and presence of water, as shown in **Figure 2**. In the absence of water, CV shows the reduction of molecular oxygen to superoxide anions and the oxidation of the generated superoxide anions back to molecular oxygen in the potential region between -0.5 and -1.5 V (**Figure 2, solid line**). The difference between the reduction and oxidation half-peak potentials is diagnostic for a quasi-reversible reaction [18], and this difference is probably due to the adsorption of the electrogenerated superoxide anions on the electrode surface [19]. At more negative potentials (below -2.0 V), a totally irreversible reduction was observed, which corresponds to the generation of peroxide anions. These reductions have been previously described according to reactions 1 and 2 in dimethyl sulfoxide on a gold electrode [20]. The reduction potentials in dimethyl sulfoxide differ from those observed here, due to the different solvent [21].

CV experiments performed in the presence of 0.2 and 1 vol % water (**Figure 2, dashed** and **dotted lines**) showed that increasing the water content shifts the cathodic peak toward less negative potentials with a two times higher current. The suppression of the corresponding anodic peak indicates the instability of the electrogenerated superoxide anions in the presence of water. Presumably, superoxide anions undergo dismutation through protonation by water (reaction 3), leading to the generation of perhydroxyl radicals ($HO_2^{\bullet}$) [22-24], which react further to hydrogen peroxide or its conjugated base according to reactions 4 to 6. The higher current in the presence of water is attributed to the reactions 4 to 6. An ECE (Electrochemical-Chemical-Electrochemical) mechanism for the reduction of molecular oxygen in the presence of water has been proposed previously [25].

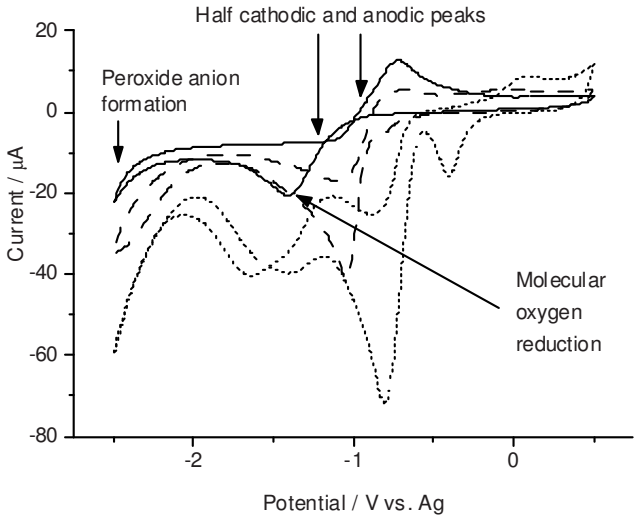

Figure 2. Cyclic voltammetry of molecular oxygen reduction on a gold electrode in 0.1 M tetrabutylammonium perchlorate in acetonitrile (solid line), after addition of 0.2 (dashed line), and 1 vol % water (dotted line), under air atmosphere (scan rate 100 mV/s).

2.3.2 Electrochemistry of lidocaine in the presence and absence of molecular oxygen

The electrochemical behavior of a solution of lidocaine in acetonitrile/TBAP was studied by CV in the presence or absence of dissolved molecular oxygen (**Figure 3**). An intense oxidation peak observed at the potentials above 1.0 V in the absence of molecular oxygen (**Figure 3-a**) is due to the direct oxidation of lidocaine, leading to radical cations, as has been reported for tertiary amines [6]. Direct oxidation of lidocaine on a porous graphite electrode at potentials above 800 mV vs Pd/H_2 has been shown by Jurva et al [5].

In the presence of dissolved molecular oxygen, several additional oxidation peaks of lidocaine were observed (**Figure 3-a, solid line**), which were subsequently studied by CV over various potential windows (**Figure 3-b and c**). Between -0.8 and 1.5 V (**Figure 3-b, dashed line**), an oxidation peak (Ox_1) and an associated reduction peak (Red_1) were observed at peak potentials of -0.5 and 1.0 V, respectively. Ox_1 is due to the direct oxidation of lidocaine and Red_1 is its subsequent reduction in the presence of dissolved molecular oxygen. In the potential window between -1.5 and 0.5 V (**Figure 3-c, solid line**). Another redox

couple was observed (Ox_2 and Red_2) in the same potential region as for the superoxide anion and molecular oxygen redox couple (**Figure 2, solid line**). This indicates that the generation of superoxide anions and their subsequent reoxidation proceeds also in the presence of lidocaine. When extending the scan range to -2.5 V to 0.5 V (**Figure 3-c, dashed line**), another reduction peak was observed at potentials more negative than -2.0 V (Red_3), indicating the generation of peroxide anions (**Figure 2, solid line**). The reaction of peroxide anions with lidocaine leads apparently to a product that can be reoxidized at 0.25 V (Ox_3), since Ox_3 was not observed in the absence of lidocaine.

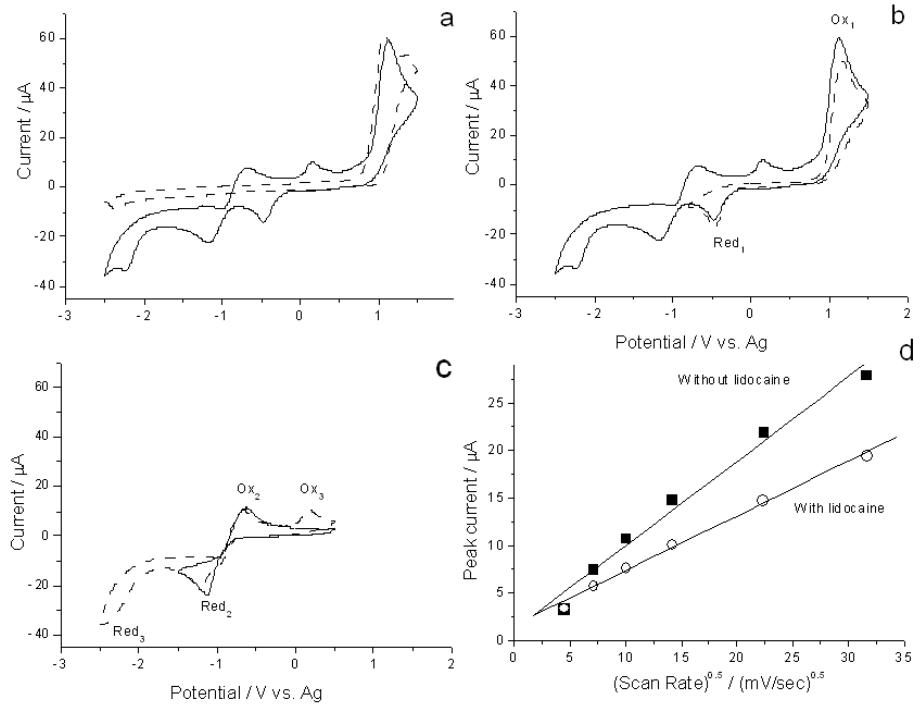

Figure 3. Cyclic voltammetry on a gold electrode with 10 mM lidocaine (a) in 0.1 M tetrabutylammonium perchlorate in acetonitrile under aerated (solid line) and deaerated (dashed line) atmosphere. Cyclic voltammetry of the same solution under aerated atmosphere across different potential windows: (b) -2.5 and 1.5 V (solid line), -0.8 and 1.5 V (dashed), and (c) -1.5 and 0.5 V (solid), -2.5 and 0.5 V (dashed); Scan rate 100 mV/s. (d) Peak current versus the square root of scan rate (I_p-$u^{1/2}$) representations for reoxidation of superoxide anions (Ox_2) in the absence (top line, squares) and presence of 10 mM lidocaine (bottom line, open circles)

The chemical reaction between superoxide anions and lidocaine was studied by determining the peak current of the Ox_2 region, which corresponds to the number of reoxidized superoxide anions (see **Figure 3-b**) at different scan rates in the presence and absence of lidocaine. I_p-$\upsilon^{1/2}$ (peak current vs. the square root of the scan rate) curves (I_p data taken from **Figure 4**) showed that the presence of lidocaine decreased the number of reoxidized superoxide anions, indicating reaction with lidocaine (**Figure 3-d**). The nature of the lidocaine reaction products that are formed in the presence of molecular oxygen was determined by collection of samples at different potentials and their analysis by LC-ESI/MS.

2.3.3 Oxidation of lidocaine: analysis of the reaction products by LC-ESI/MS

LC-ESI/MS of lidocaine after reaction at constant potential of -1.0 V in the presence of molecular oxygen showed one major reaction product at *m/z* 251 and a minor reaction product at *m/z* 207. The product at *m/z* 207 results from the N-dealkylation of lidocaine, as previously reported by Jurva et al. [5], whereas the component at *m/z* 251 is a product with one additional oxygen atom (+16 Da) compared to lidocaine (*m/z* 235). A more detailed product assignment is given in the following section.

The relative amount of both products was studied as a function of potential, in the presence or absence of molecular oxygen (**Figure 5**). In acetonitrile solution, the presence of dissolved molecular oxygen is required for formation of *m/z* 251 (**Figure 5-a**), but there is a large variation in the *m/z* 251 signal in three separate experiments. The reason could be that, although dry acetonitrile was used, absorption of trace amounts of water is difficult to avoid, resulting in varying water content across experiments. To control this, a known concentration of water (1 vol %) was added showing that the presence of both oxygen and water is essential for a reproducible production of both reaction products (**Figure 5-c and d**). The highest amount of the *m/z* 251 reaction product is observed at -1.0 V, which corresponds to the peak potential for superoxide anion formation (**Figure 2**). These conditions were used for further studies.

Since the *m/z* 207 N-dealkylation product is known to be the major product upon direct electrochemical oxidation of lidocaine, and since CV at positive potentials (**Figure 3-a**) suggested direct oxidation of lidocaine, we investigated the possibility whether a reaction takes place at the auxiliary electrode when applying a negative potential to the working electrode. Potential measurements on the auxiliary electrode showed indeed a sufficiently positive potential (+1.1 V), when a potential of -1.0 V was applied to the working electrode.

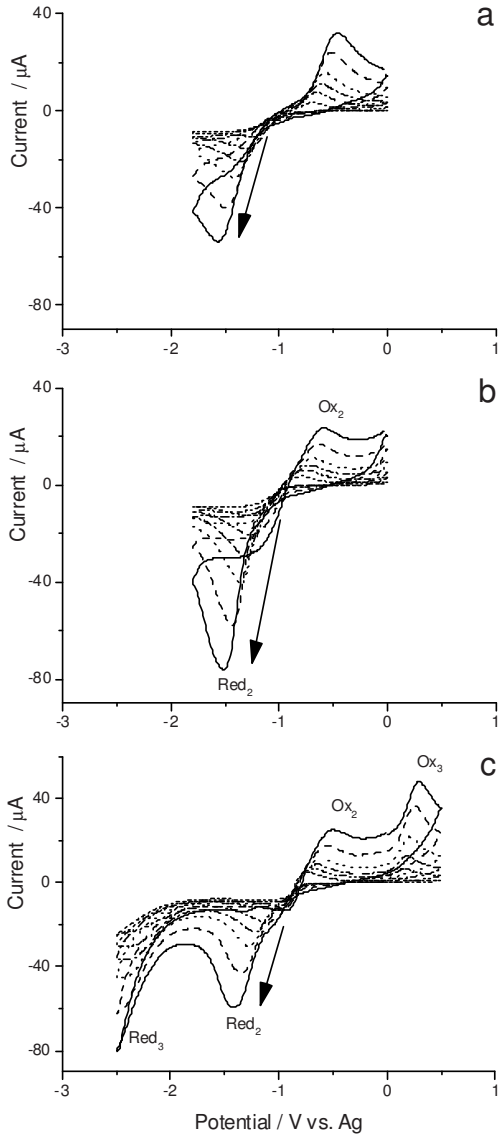

Figure 4. Cyclic voltammetry in 0.1 M tetrabutylammonium perchlorate in acetonitrile under air atmosphere (a) in the absence of lidocaine and (b) in the presence of 10 mM lidocaine across different potential windows: -1.8 to 0.0 V, and (c) -2.5 to 0.5 V. Scan rates were 20, 50, 100, 200, 500, and 1000 mV/s (the arrow indicates the direction of increasing scan rate.

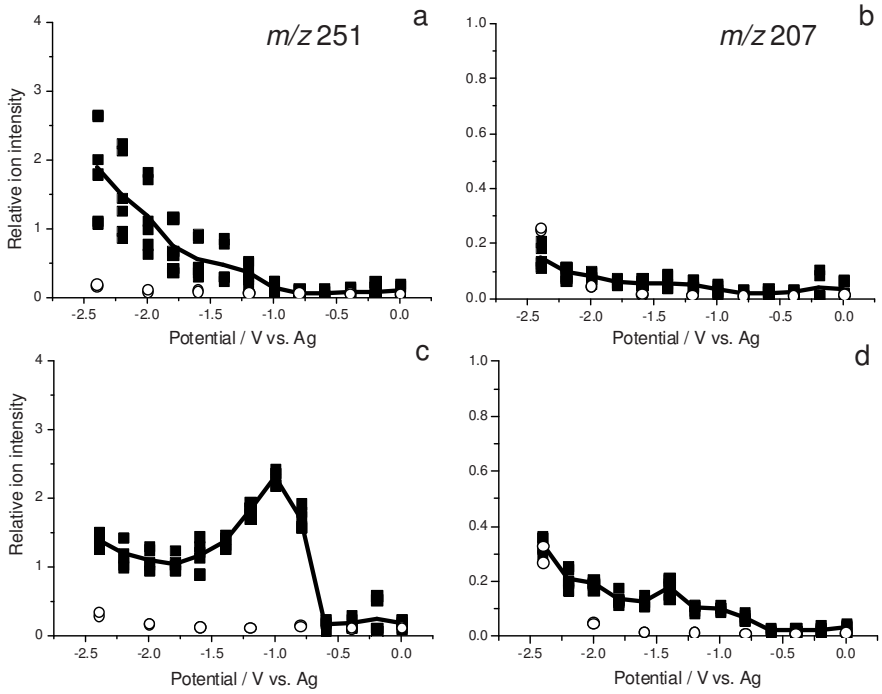

Figure 5. Ion intensities of the *m/z* 251 and 207 oxidation products of lidocaine, obtained on a gold electrode at different potentials, from a solution of 10 mM lidocaine under air (squares) and argon atmosphere (open circles) in 0.1 M tetrabutylammonium perchlorate (a) *m/z* 251 in acetonitrile, (b) *m/z* 207 in acetonitrile, (c) *m/z* 251 in acetonitrile/water 99/1 v/v, and (d) *m/z* 207 in acetonitrile/water 99/1 v/v. Ion intensities were normalized relative to the intensity of the signal for acetaminophen, which was added as internal standard to all LC-MS analyses. Batch oxidations of aerated solutions were performed in triplicate, and all LC-MS analyses in duplicate.

We separated the compartments at the working (cathodic half-cell) and auxiliary (anodic half-cell) electrodes with a porous Vycor frit, which allows passage of ions and small organic molecules, but prevents extensive mixing of the solutions in the two compartments. No significant difference was observed between the magnitude of currents passing through the electrodes in the presence and absence of the Vycor frit. The product distributions between the anodic and cathodic compartments are shown in **Figure 6**. The *m/z* 207 product was observed almost

exclusively in the anodic compartment, while the *m/z* 251 product was present in both parts, but mainly in the cathodic compartment. This shows that the N-dealkylation product of lidocaine (*m/z* 207) is produced by direct oxidation at the auxiliary electrode. The presence of the *m/z* 251 in both compartments indicates that a reactive (oxygen) species is involved, that can migrate or diffuse from the cathodic to the anodic half-cell.

2.3.4 LC-MS/MS analysis of oxidation products at m/z 207 and 251

The structures of the oxidation products at *m/z* 207 and 251 were characterized by LC-MS/MS. **Figure 7** shows product ion scans for lidocaine, *m/z* 235, and its two oxidation products. The product ion scan for the unmodified lidocaine peak (parent ion at *m/z* 235) showed an intense fragment ion at *m/z* 86 corresponding to the tertiary amine group (**Figure 7-a**). The corresponding fragments containing the aromatic ring did not give rise to detectable ions. The product ion scan for *m/z* 207 showed an intense signal at *m/z* 58 (**Figure 7-b**) corresponding to the absence of one ethyl chain from the original tertiary amine group, confirming that this is the N-dealkylation product. It has been demonstrated that anodic oxidation of amines proceeds via electron transfer and deprotonation, to give the iminium intermediate that, after hydrolysis and intramolecular rearrangement, leads to N-dealkylation (**Scheme 2**) [26].

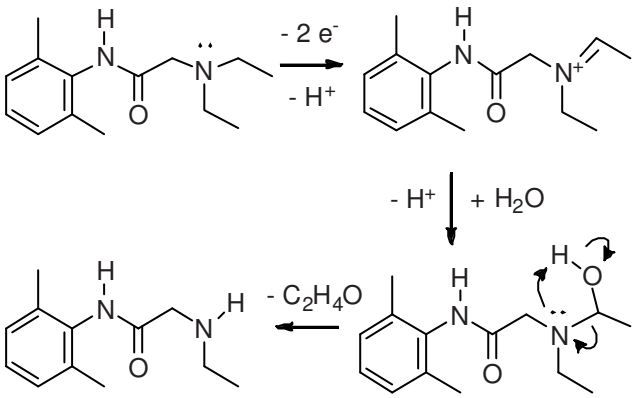

Scheme 2. Proposed reaction mechanisms for the electrochemical N-dealkylation initiated by single electron transfer (SET) on the auxiliary electrode.

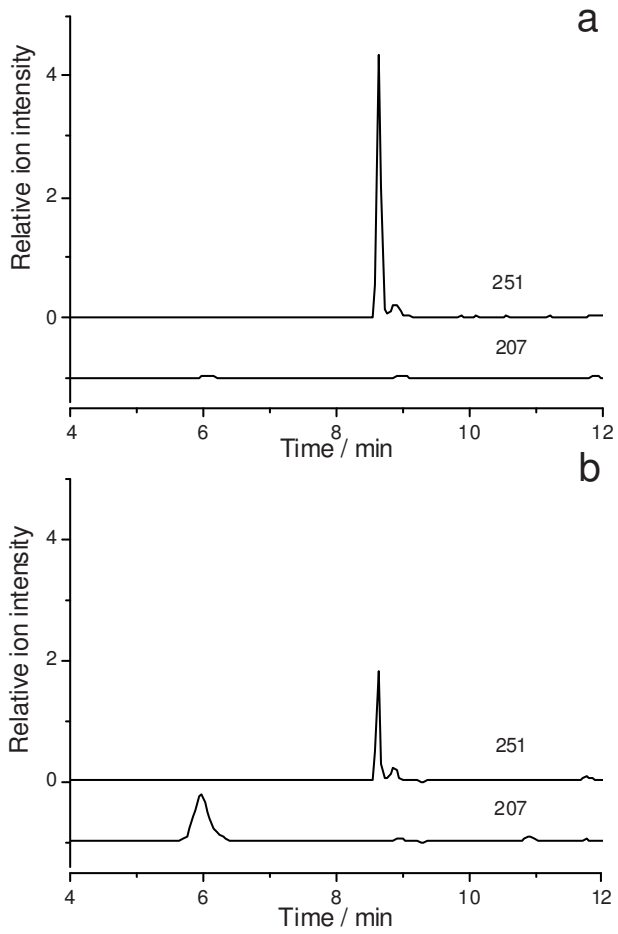

Figure 6. LC-MS analysis of oxidation products obtained from 10 mM lidocaine oxidized in an aerated solution of 0.1 M tetrabutylammonium perchlorate in acetonitrile/water 99/1 (v/v) on a gold electrode at -1.0 V for one hour in a two-compartment cell. (a) Cathodic compartment (working electrode), and (b) anodic compartment (auxiliary electrode).

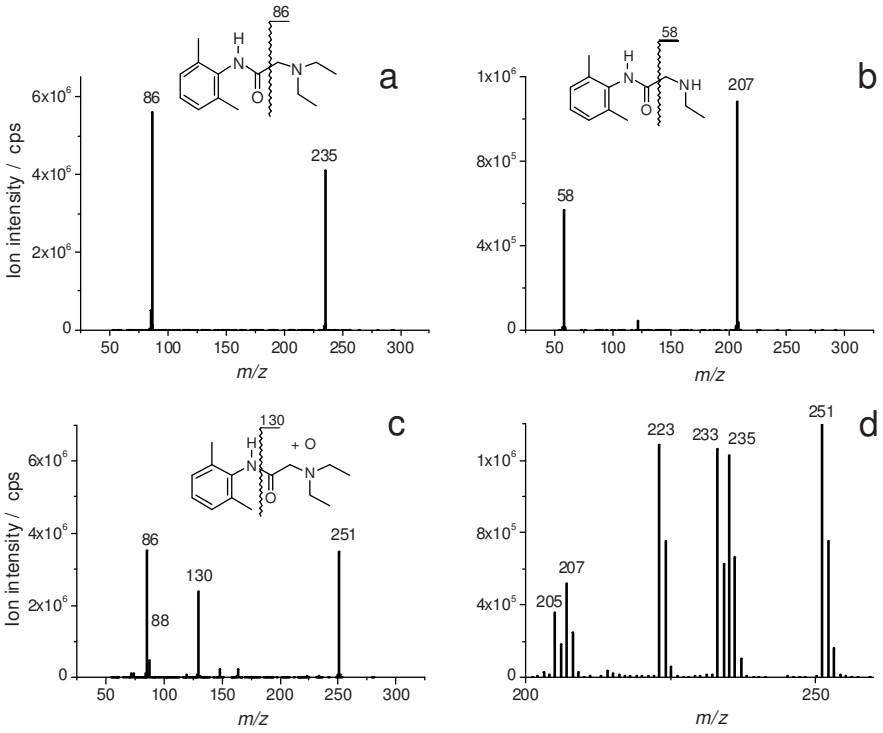

Figure 7. Positive product ion scans (LC-ESI-MS/MS) of (a) lidocaine (*m/z* 235), (b) its *m/z* 207 N-dealkylation product, and (c) its *m/z* 251 N-oxide product. (d) APCI-MS spectrum for the N-oxide, showing thermal degradation in the heated nebulizer.

The product ion scan for *m/z* 251 showed fragments at *m/z* 86, 88 and 130 (**Figure 7-c**). Incorporation of an oxygen atom in lidocaine can take place in the following positions: the aromatic ring (hydroxylation on carbon 3 or 4), one of the methyl groups (benzylic hydroxylation), and on the amino-nitrogen (N-oxide formation). Fragment ion *m/z* 130 points to incorporation of oxygen on the right hand side of the amide bond, which rules out hydroxylation in the ring or in the benzylic position. Fragment ion *m/z* 86 seems to exclude formation of the N-oxide. However, the fragment ion at *m/z* 88 supports the assumption of N-oxide formation (see **Scheme 3-a**). Formation of the fragment ion *m/z* 86 can be rationalized by OH group migration in the protonated N-oxide. Since the combination of electrospray ionization and CID does not provide a distinction between N-oxide

and some other oxidation product, the sample was subjected to atmospheric pressure chemical ionization (APCI). During APCI, N-oxides readily undergo thermal degradation prior to ionization, leading to diagnostic ions [27]. **Figure 7-d** shows the thermally-induced degradation of the MW=250 Da oxidation product, with peaks at *m/z* 235, 223 and 207 which correspond to oxygen atom loss, Cope elimination, and Meisenheimer rearrangement, respectively, as illustrated in **Scheme 3-b**, and described by Ma et al. [27]. This was confirmed in a control experiment, where the N-oxide was synthesized by reaction of lidocaine with m-chloroperbenzoic acid. LC retention time and MS/MS spectrum of the chemically synthesized N-oxide were identical to those obtained for the electrochemical reaction product.

2.3.5 N-oxide formation and hydroxylation

Since electrochemical reduction of molecular oxygen may generate radical species and hydrogen peroxide, we incubated lidocaine with hydrogen peroxide and subjected lidocaine to the Fenton reaction, which catalytically activates hydrogen peroxide to form hydroxyl radicals.

Incubation of lidocaine with 1 vol % hydrogen peroxide for one hour under the same solvent conditions as used for electrochemistry resulted in a significant amount of the *m/z* 251 product, with the same retention time and MS/MS spectrum as the electrochemically-generated N-oxide. No measurable amount of other oxidation products was detected. Apparently, the electrochemically generated ROS is hydrogen peroxide, produced as follows: superoxide anions generated at the working electrode at -1.0 V abstract a proton from water, or lidocaine itself in the absence of water, to generate perhydroxyl radicals (reaction 3), followed by formation of hydrogen peroxide in reactions 4 and 7. The reaction between hydrogen peroxide and tertiary amines has been documented to lead to the formation of N-oxides [28]. The relatively high amount of the N-oxide in the anodic compartment is explained by diffusion of hydrogen peroxide or migration of its anion from the cathodic to the anodic compartment.

The Fenton reaction in the presence of lidocaine leads to a number of products, including five LC peaks at *m/z* 251 (**Figure 8**). Co-injection with 3-hydroxylidocaine shows that this compound co-elutes with peak c (**Figure 8-a**), and that its MS/MS spectrum (**Figure 8-a**) is identical to that of 3-hydroxylidocaine. According to the MS/MS spectra (**Figure 8-b and c**), it is likely that the other two major *m/z* 251 peaks are 4-hydroxylidocaine (peak b) and lidocaine that is hydroxylated on the benzylic position (peak d). Benzylic hydroxylation leads to facile water loss as indicated by the fragment at *m/z* 233. The short retention times of peaks b, c, and d are consistent with benzylic and aromatic hydroxylation, which reduce the hydrophobicity of lidocaine. The small peak e has the same MS/MS spectrum as peak d, but cannot be easily assigned. Peak f has an identical MS/MS spectrum and retention time as the N-oxide generated by electrochemistry.

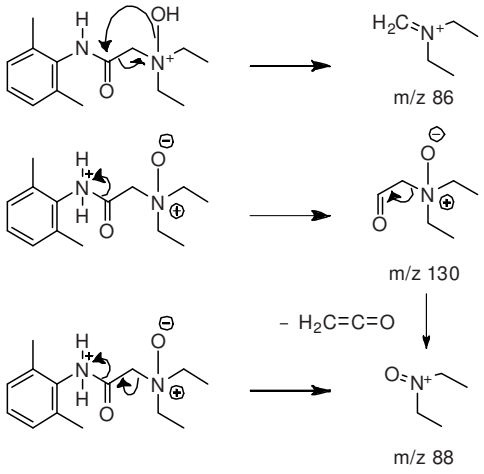

(a) Collision-induced fragmentation

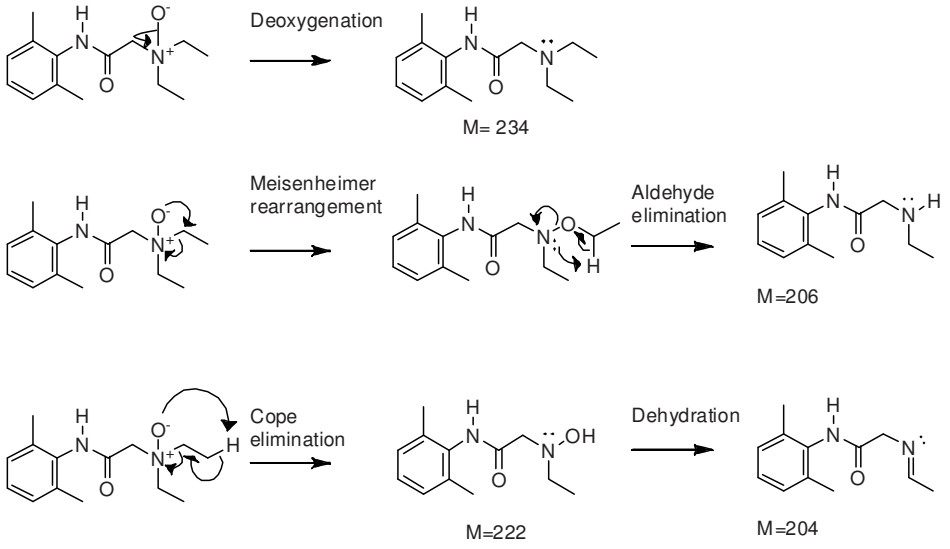

(b) Thermally-induced degradation

Scheme 3. (a) Proposed collision-induced fragmentation during MS/MS for the protonated N-oxide of lidocaine (see **Figure 7-c**); (b) Proposed thermally-induced degradation during APCI for the N-oxide of lidocaine (see **Figure 7-d**).

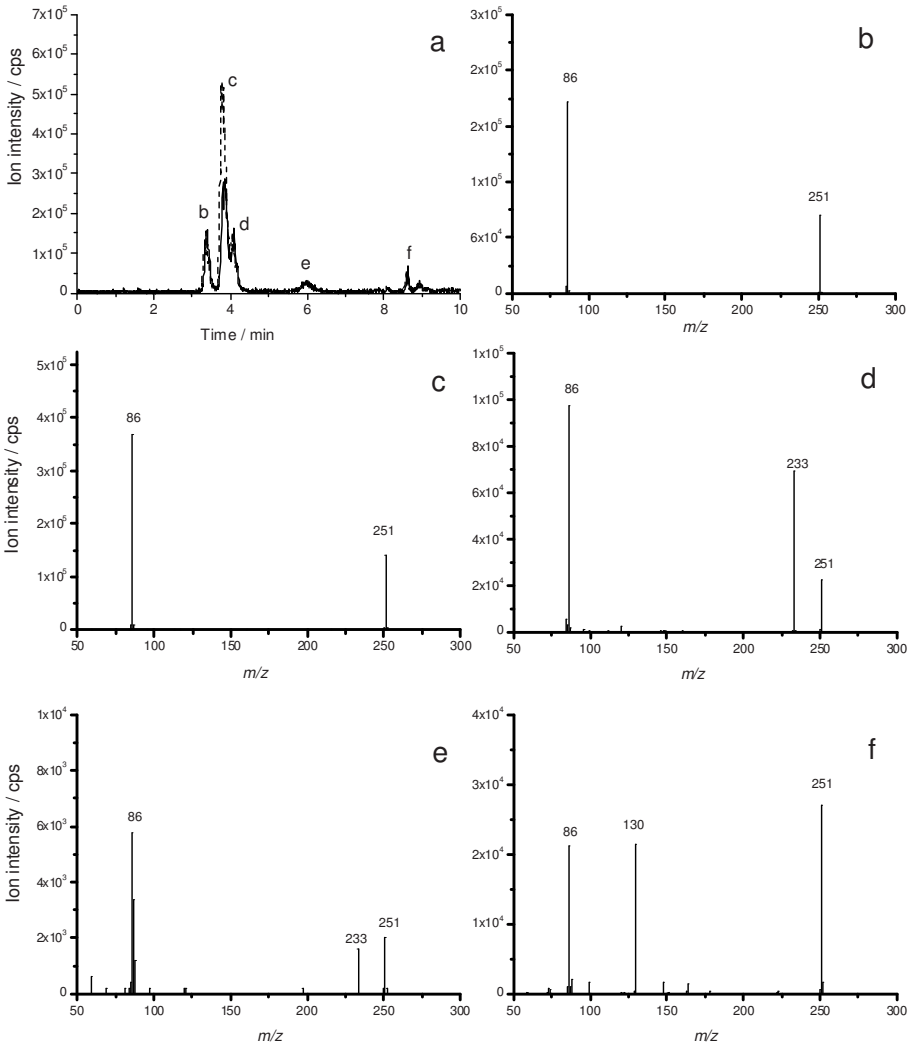

Figure 8. (a) Extracted ion chromatogram for *m/z* 251, obtained from the Fenton reaction in the presence of lidocaine (solid line), the same sample with co-injected 3-hydroxylidocaine (dashed line), and (b-f) the corresponding MS/MS spectra for *m/z* 251 peaks labeled b to f.

These results indicate that hydroxyl radicals, generated by the Fenton reaction, lead primarily to hydroxylation. These hydroxylation products were not observed in the EC cell. Therefore, reduction of molecular oxygen, under our conditions does not generate hydroxyl radicals in sufficient amounts to produce detectable hydroxylation of lidocaine.

2.4 Conclusions

Electrochemical reduction of molecular oxygen on a gold electrode led to ROS intermediates, as shown by CV. The major reactive species was hydrogen peroxide as indicated by formation of the N-oxide of lidocaine as main oxidation product. Addition of 1 % water resulted in well-controlled conditions with an optimum potential for product formation of -1.0 V. A standard single-compartment cell led to a mixture of the N-oxide and the N-dealkylation product due to H_2O_2-mediated and direct electrochemical oxidation, respectively. Separation of anodic and cathodic compartments shows that direct oxidation occurs at the auxiliary electrode at a positive potential of 1.1 V. Aromatic or benzylic hydroxylation products, both *in vivo* metabolites of lidocaine, are not formed in the electrochemical cell. These can be produced by reaction with hydroxyl radicals using the Fenton reaction.

2.5 References

[1] Lohmann, W.; Karst, U. Electrochemistry meets enzymes: instrumental on-line simulation of oxidative and conjugative metabolism reactions of toremifene. *Anal. Bioanal. Chem.* **2009**, *394*, 1341-1348.

[2] Lohmann, W.; Dötzer, R.; Gütter, G.; Van Leeuwen, S. M.; Karst, U. On-line electrochemistry/liquid chromatography/mass spectrometry for the simulation of pesticide metabolism. *J. Am. Soc. Mass Spectrom.* **2009**, *20*, 138-145.

[3] Lohmann, W.; Karst, U. Biomimetic modeling of oxidative drug metabolism: Strategies, advantages and limitations. *Anal. Bioanal. Chem.* **2008**, *391*, 79-96.

[4] Johansson, T.; Weidolf, L.; Jurva, U. Mimicry of phase I drug metabolism--novel methods for metabolite characterization and synthesis. *Rapid Commun. Mass Spectrom.* **2007**, *21*, 2323-2331.

[5] Jurva, U.; Wikström, H. V.; Bruins, A. P. In vitro mimicry of metabolic oxidation reactions by electrochemistry/mass spectrometry. *Rapid Commun. Mass Spectrom.* **2000**, *14*, 529-533.

[6] Jurva, U.; Bissel, P.; Isin, E. M.; Igarashi, K.; Kuttab, S.; Castagnoli, N., Jr. Model electrochemical-mass spectrometric studies of the cytochrome P450-catalyzed oxidations of cyclic tertiary allylamines. *J. Am. Chem. Soc.* **2005**, *127*, 12368-12377.

[7] Jurva, U.; Wikström, H. V.; Weidolf, L.; Bruins, A. P. Comparison between electrochemistry/mass spectrometry and cytochrome P450 catalyzed oxidation reactions. *Rapid Commun. Mass Spectrom.* **2003**, *17*, 800-810.

[8] Sawyer, D. T. *Oxygen Chemistry*; Oxford University Press, Inc., 1991.

[9] Oda, Y.; Imaoka, S.; Nakahira, Y.; Asada, A.; Fujimori, M.; Fujita, S.; Funae, Y. Metabolism of lidocaine by purified rat liver microsomal cytochrome P-450 isozymes. *Biochem. Pharmacol.* **1989**, *38*, 4439-4444.

[10] Meunier, B.; de Visser, S. P.; Shaik, S. Mechanism of Oxidation Reactions Catalyzed by Cytochrome P450 Enzymes. *Chem. Rev.* **2004**, *104*, 3947-3980.

[11] Newcomb, M.; Hollenberg, P. F.; Coon, M. J. Multiple mechanisms and multiple oxidants in P450-catalyzed hydroxylations. *Arch. Biochem. Biophys.* **2003**, *409*, 72-79.

[12] Sawyer, D. T.; Valentine, J. How super is superoxide? S. *Acc. Chem. Res.* **1981**, *14,* 393-400.

[13] Sawyer, D. T.; Chiericato, G.; Angelis, C. T.; Nanni, E. J.; Tsuchiya, T. Effects of media and electrode materials on the electrochemical reduction of dioxygen. *Anal. Chem.* **1982**, *54*, 1720-1724.

[14] Lorenzola, T. A.; Lopez, B. A.; Giordano, M. C. Molecular Oxygen Electroreduction at Pt and Au Electrodes in Acetonitrile Solutions. *J. Electrochem. Soc.* **1983**, *130*, 1359-1365.

[15] Lund, H.; Hammerich, O. *Organic Electrochemistry*, 4th ed.; Marcel Dekker, Inc., 2001.

[16] Kolthoff, I. M.; Jordan, J. Oxygen Induced Electroreduction of Hydrogen Peroxide and Reduction of Oxygen at the Rotated Gold Wire Electrode. *J. Am. Chem. Soc.* **1952**, *74*, 570-570.

[17] Barton, D.; Ollis, W. D. *Comprehensive Organic Chemistry: Chapter 6 Amines and related compounds*; Pergamon Press, 1979.

[18] Bard, A. J.; Faulkner, L. R. *Electrochemical methods fundamentals and applications*, 2nd ed.; John Wiley & Sons, Inc., 2001.

[19] Jovancicevic, V.; Bockris, J. O. M. The Mechanism of Oxygen Reduction on Iron in Neutral Solutions. *J. Electrochem. Soc.* **1986**, *133*, 1797-1807.

[20] Goolsby, A. D.; Sawyer, D. T. Electrochemical reduction of superoxide ion and oxidation of hydroxide ion in dimethyl sulfoxide. *Anal. Chem.* **1968**, *40*, 83-86.

[21] Barrette, W. C.; Sawyer, D. T. Determination of dissolved hydrogen and effects of media and electrode materials on the electrochemical oxidation of molecular hydrogen. *Anal. Chem.* **1984**, *56*, 653-657.

[22] Che, Y.; Tsushima, M.; Matsumoto, F.; Okajima, T.; Tokuda, K.; Ohsaka, T. Water-Induced Disproportionation of Superoxide Ion in Aprotic Solvents. *J. Phys. Chem.* **1996**, *100*, 20134-20137.

[23] Singh, P. S.; Evans, D. H. Study of the Electrochemical Reduction of Dioxygen in Acetonitrile in the Presence of Weak Acids. *J. Phys. Chem. B* **2006**, *110*, 637-644.

[24] Andrieux, C. P.; Hapiot, P.; Savéant, J. M. Mechanism of superoxide ion disproportionation in aprotic solvents. *J. Am. Chem. Soc.* **1987**, *109*, 3768-3775.

[25] Savéant, J.-M. Molecular Catalysis of Electrochemical Reactions. Mechanistic Aspects. *Chem. Rev.* **2008**, *108*, 2348-2378.

[26] Smith, P. J.; Mann, C. K. Electrochemical dealkylation of aliphatic amines. *J. Org. Chem.* **1969**, *34*, 1821-1826.

[27] Ma, S.; Chowdhury, S. K.; Alton, K. B. Thermally induced N-to-O rearrangement of tert-N-oxides in atmospheric pressure chemical ionization and atmospheric pressure photoionization mass spectrometry. *Anal. Chem.* **2005**, 3676-3682.

[28] Oswald, A.; Guertin, D. Nitrogen Compounds. I. Peroxide Intermediates of Tertiary Alkylamine Oxidation by H_2O_2. *J. Org. Chem.* **1963**, *28*, 651-657.

Chapter 3
Electrochemical Oxidation by Square-Wave Potential Pulses in the Imitation of Oxidative Drug Metabolism*

Electrochemistry combined with mass spectrometry (EC-MS) is an emerging analytical technique in the imitation of oxidative drug metabolism at the early stages of new drug development. Here, we present the benefits of electrochemical oxidation by square-wave potential pulses for the oxidation of lidocaine, a test drug compound, on a platinum electrode. Lidocaine was oxidized at constant potential and by square-wave potential pulses with different cycle times, and the reaction products were analyzed by LC-MS(/MS). Application of constant potentials of up to +5.0 V resulted in relatively low yields of N-dealkylation and 4-hydroxylation products, while oxidation by square-wave potential pulses generated up to 50 times more of the 4-hydroxylation product at cycle times between 0.2 and 12 s (estimated yield of 10%). The highest yield of the N-dealkylation product was obtained at cycle times shorter than 0.2 s. Tuning of the cycle time is thus an important parameter to modulate the selectivity of electrochemical oxidation reactions. The N-oxidation product was only obtained by electrochemical oxidation under air atmosphere due to reaction with electrogenerated hydrogen peroxide. Square-wave potential pulses may also be applicable to modulate the selectivity of electrochemical reactions with other drug compounds in order to generate oxidation products with greater selectivity and higher yield based on the optimization of cycle times and potentials. This considerably widens the scope of direct-electrochemistry based oxidation reactions for the imitation of in vivo oxidative drug metabolism.

* Published as: Nouri-Nigjeh, E.; Permentier, H.P.; Bischoff, R.; Bruins, A.P. Electrochemical oxidation by square-wave potential pulses in the imitation of oxidative drug metabolism, Analytical Chemistry, Vol. 83, 2011, 5519-5525.

3.1 INTRODUCTION

The imitation of oxidative drug metabolism by Cytochrome P450s (CYP) at the early stages of new drug development requires fast and accurate analytical techniques [1, 2]. Electrochemistry combined with mass spectrometry (EC-MS) is emerging as a versatile analytical technique capable of the generation and identification of many known *in vivo* metabolites [3-5]. Although different oxidation products may be generated at different potentials, constant potential oxidations often lack in selectivity when it comes to generation of defined metabolites. In addition, electrode fouling and/or passivation associated with constant potential oxidation of organic compounds may attenuate surface reactivity and thereby reduce product yield [6].

Platinum electrodes have been widely used for organic compound oxidation and detection due to their excellent conductivity and chemical stability even at high positive potentials [7]. Johnson and co-workers showed that electrochemical detection of various organic compounds on Pt electrodes can be significantly improved using square-wave potential pulses, as well as other potential waveforms, with cycle times between 0.2 and 2 s. Adsorbed molecules generated during oxidation are usually desorbed during the anodic formation of a surface oxide. Because the formation of surface oxide can attenuate surface reactivity, a subsequent negative potential step quickly allows the cathodic dissolution of the surface oxide to restore the reactivity of the fresh surface [6, 8].

A second function of square-wave potential pulses is claimed to involve the generation of intermediate reactive oxygen species during the oxidation of water on the Pt electrode. Production of OH radicals adsorbed on the Pt electrode may participate in O-transfer reactions to the preadsorbed organic molecules on the surface. Square-wave potential pulses have been applied successfully to achieve anodic detection of numerous polar aliphatic compounds [9].

The aim of pulsed potential electrochemical detection is sensitive and reproducible current measurement, but the reaction products are not characterized by spectrometric methods [10-14]. Synthetic organic electrochemistry on the other hand [15], aims at the production and characterization of specific molecules. In this field, there have been no reports thus far of the use of square-wave potential pulses.

The electrochemical production of drug metabolites by means of square-wave potential pulses might allow both higher yields through surface renewal and access to additional products through O-transfer reactions. In the present study, lidocaine, a local anesthetic drug, was used as a test compound. The *in vivo* metabolites of lidocaine result from N-dealkylation, N-oxidation, and aromatic and benzylic hydroxylation (**Scheme 1**) [5, 16, 17]. Direct electrochemical oxidation of lidocaine on a porous graphite electrode gave only the N-dealkylated product [18]. N-oxidation of lidocaine was observed in the presence of electrochemically generated

hydrogen peroxide [19]. Here, we show that square-wave potential pulses with different cycle times lead to a marked change in the distribution of lidocaine reaction products as analyzed and identified by LC-MS(/MS).

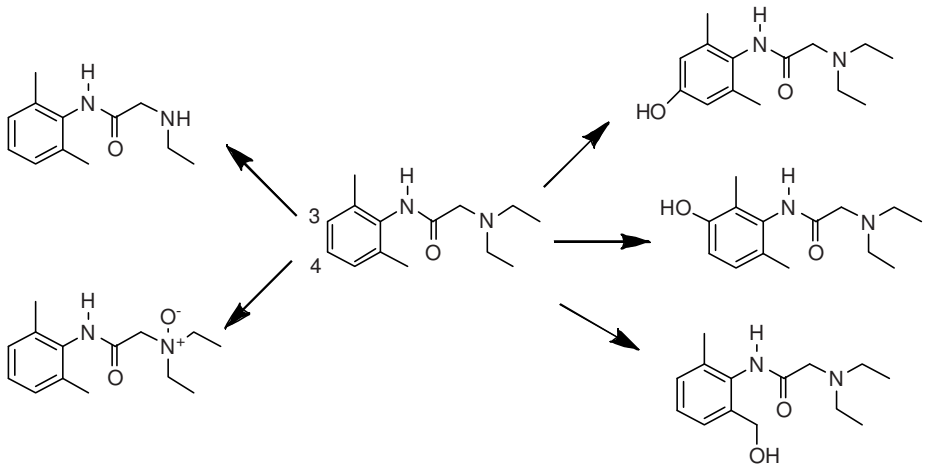

Scheme 1. *In vivo* metabolites of lidocaine due to oxidative metabolism by Cytochrome P450s [5, 16, 17].

3.2 EXPERIMENTAL PROCEDURES

Reagents. Tetrabutylammonium perchlorate (TBAP, 86893) and lidocaine (L7757) were purchased from Sigma-Aldrich. Water was purified by a Maxima Ultrapure water system (ELGA, High Wycombe, Bucks, UK). Ultra-pure HPLC grade acetonitrile (ACN) was purchased from Merck. $H_2{}^{18}O$ with 97 atom % ^{18}O ($H_2{}^{18}O$, 329878) was purchased from Sigma-Aldrich. 3-Hydroxylidocaine (CAS No. 34604-55-2) was purchased from Toronto Research Chemicals Inc.

Electrode preparation. The surface of the platinum disk working electrode was polished with a lapping sheet (Micromesh grade 3200) prior to each experiment. After mechanical polishing the surface was washed with ethanol and air-dried.

Electrochemical measurements. Electrochemical experiments were performed with a home-made potentiostat controlled by a MacLab system (ADInstruments, Castle Hill, NSW, Australia) and EChem v.1.52 software (eDAQ, Denistone East, NSW, Australia). A two-compartment electrochemical cell was constructed by using a porous Vycor tip with Teflon heat shrink (MF-2064, Bioanalytical Systems (BASi), West Lafayette, IN, USA) to separate working and auxiliary half-cells. The working electrode was a 2 mm diameter platinum disk (MF-2013, BASi) and the auxiliary

electrode was a platinum wire (MW-4130, BASi). Potentials were measured against a silver wire pseudo-reference electrode (MF-2017, BASi), to eliminate the possibility of chloride contamination of the working solution during prolonged electrolysis in the presence of conventional reference electrodes. The reference electrode was placed in the working compartment. All experiments were performed at ambient temperature. For deaeration and aeration, argon and synthetic air, respectively, were bubbled at 25 mL/min via a sparge tube (MW-4145, BASi) through the 1 mL solution during all experiments (4 mL solution was used for the experiments presented in **Figure 6**). The auxiliary compartment was always under argon purging. In the case of pulsed potential experiments, the upper and lower potential steps within one cycle were of equal duration (e.g. 1 s steps for 2 s cycle time).

Solutions containing 10 mM lidocaine and 0.1 M TBAP dissolved in ACN/H_2O 99/1 (v/v) (0.1 M TBAP used as electrolyte to provide sufficient conductivity for electrochemical experiments) were subjected to constant potential oxidation and to oxidation by square-wave potential pulses with continuous gas flow, for 30 min prior to LC-MS analysis. Samples were collected from the working compartment and diluted 100 times in water containing 10 µM acetaminophen, as an internal standard for LC-MS signal normalization, immediately after the batch oxidations and stored at room temperature until LC-MS analysis.

LC-MS analysis. LC-MS experiments were carried out on an LC-Packings Ultimate HPLC system (LC-Packings, Amsterdam, the Netherlands) coupled to an API 365 triple quadrupole mass spectrometer (MDS Sciex, Concord, ON, Canada) upgraded to EP10+ (Ionics, Bolton, ON, Canada) with electrospray ionization in the positive mode in the TurboIonSpray source. The MS spectra were acquired between *m/z* 100-600 (step size 1.0 amu, dwell time 1 ms).

A C_{18} reversed-phase column (GraceSmart RP 18 5 µm, 2.1×150 mm; Grace Davison, Lokeren, Belgium) was used at a flow rate of 200 µL/min. Solvent A: H_2O/ACN 95/5 (v/v) with 0.1 % formic acid; Solvent B: ACN/H_2O 95/5 (v/v) with 0.1 % formic acid. 5 µL of a diluted oxidation product mixture was injected and a linear gradient of 5-50 % B in 20 min was used for elution. Peak heights were normalized with respect to the peak height of the acetaminophen internal reference compound. In case the ion counting detector of the MH^+ ion was saturated, the $^{13}C_1$ isotope intensity was taken, and the corresponding monoisotopic ^{12}C ion intensity was calculated using the theoretical isotope distribution.

N-dealkylation, N-oxidation, aromatic and benzylic hydroxylation products were identified by LC-MS/MS analysis, and in the case of the aromatic hydroxylation at 4-position further evidence was obtained by co-injection with the 3-hydroxylidocaine as reference compound, as described before [19].

3.3 RESULTS AND DISCUSSION

3.3.1 Constant Potential Oxidation

In a previous study, N-dealkylation of lidocaine was achieved by on-line EC-MS in a porous graphite flow-through cell with a potential ramp from 0 to +1.8 V in a solution of ACN/H_2O 50/50 (v/v) [18, 20]. The amount of N-dealkylation product was shown to decrease above +0.8 V in a potential ramp experiment, although no other oxidation products were observed at higher potentials [18]. The oxidation conditions in our current batch cell with a Pt working electrode at potentials below +2.0 V resulted in N-dealkylation and N-oxidation. At potentials of +2.0 V and higher 4-hydroxylation, as well as small amounts of doubly oxidized products (mainly 3,4-dihydroxylation) were observed. **Figure 1** shows the distribution of oxidation products as a function of the applied potential on the Pt working electrode when purged with argon and air, respectively.

The N-dealkylation product was barely detected at potentials above +2.0 V, both under argon and under air atmosphere (**Figures 1-a and 1-b**). The N-dealkylation yield was not affected by the presence of air, which is consistent with the proposed reaction mechanism, which does not involve dissolved molecular oxygen, and proceeds via direct electron transfer from the tertiary amine to the electrode followed by deprotonation to give an iminium intermediate that, after hydrolysis and intramolecular rearrangement, leads to the N-dealkylation product [21].

Hydroxylation at the 4-position of the aromatic ring in lidocaine was observed at potentials of +2.0 V or more (**Figures 1-c and 1-d**), although overall yield was low. The 4-hydroxylation product is most likely generated through an anodic substitution reaction by water molecules, which is initiated by a two-electron transfer to the electrode simultaneously with the formation of a Wheland-type intermediate, resulting in the aromatic hydroxylation product after deprotonation (**Scheme 2**) [22, 23]. Although unsubstituted aromatic rings can be oxidized at higher positive potentials [20], the electron-donating amide and the two methyl substituents presumably decrease the oxidation potential of the aromatic ring in lidocaine and direct the hydroxylation reaction towards the 4-position through resonance stabilization of the charge of the radical cation intermediate. Whereas direct electrochemical oxidation is apparently unable to generate the 3-hydroxylation product, *in vivo* oxidative metabolism by CYP produces both the 3- and the 4-hydroxylation products (**Scheme 1**) indicating that *in vivo* aromatic hydroxylation does not involve a radical cation intermediate, but that it proceeds via an oxygen insertion mechanism as proposed for reaction of the oxo-ferryl radical cation [24]. The range of aromatic hydroxylation reactions by direct electrochemistry is thus restricted in comparison to CYP due to the different nature of the reaction mechanism.

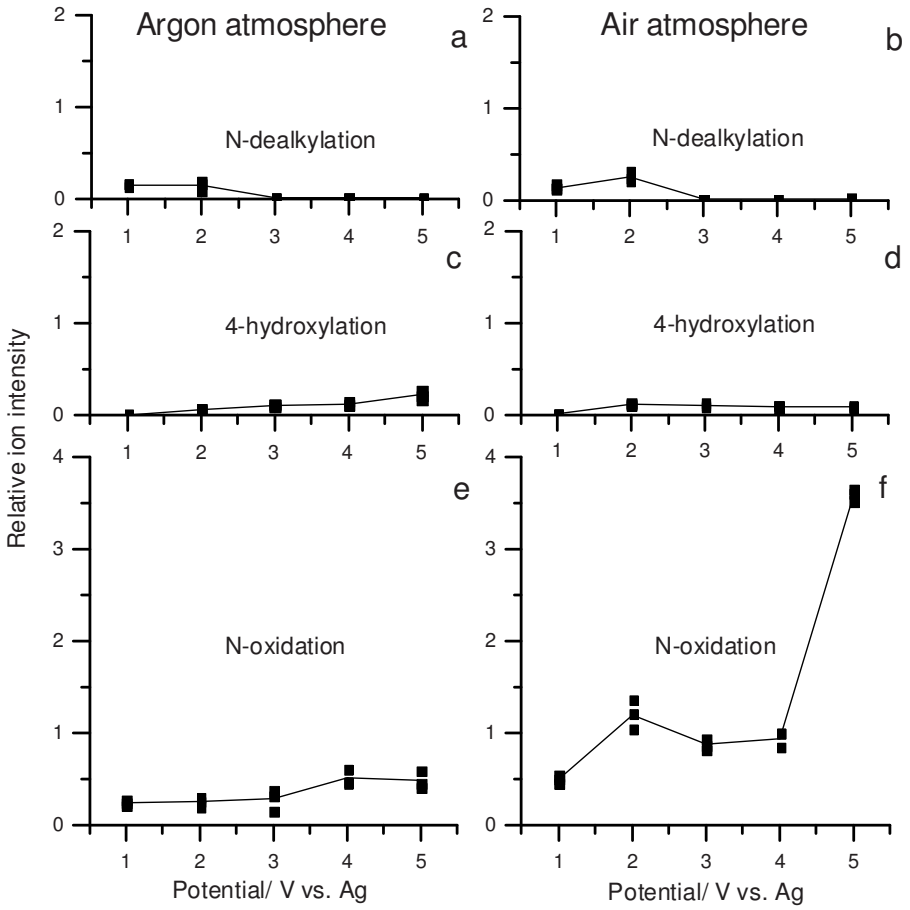

Figure 1. Relative MH^+ ion intensities of the N-dealkylation (a and b), the 4-hydroxylation (c and d), and the N-oxidation (e and f) products of lidocaine from a solution of 10 mM lidocaine in 0.1 M tetrabutylammonium perchlorate in acetonitrile/water 99/1 (v/v) at different oxidation potentials under argon and air atmosphere, respectively. Ion intensities were normalized relative to the intensity of the signal for acetaminophen, which was added as internal standard to all LC-MS analyses. Experiments were performed in triplicate.

In contrast to N-dealkylation and 4-hydroxylation, formation of the N-oxidation product is strongly dependent on the presence of dissolved molecular oxygen in the solution with a sharp increase in yield between +4.0 and +5.0 V (**Figures 1-e and 1-f**). N-oxidation has been reported to result from the reaction between lidocaine and electrochemically generated hydrogen peroxide [19], through peroxide intermediate formation and decomposition [25]. Hydrogen peroxide is generated in the cathodic compartment of the counter electrode and reaches the anodic compartment by diffusion through the porous frit membrane that separates both compartments, as previously reported [19].

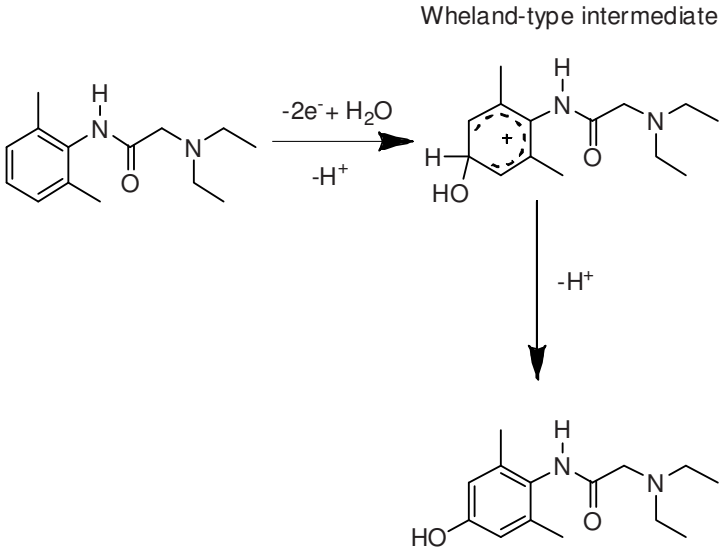

Scheme 2. Proposed anodic substitution mechanism initiated by the abstraction of two electrons from the aromatic ring followed by substitution with water proceeding through a Wheland-type intermediate [23].

Stable isotope labeling was used to reveal the source of the oxygen atom in the N-oxidation product. According to the proposed N-oxidation mechanism, hydrogen peroxide is generated by reduction of molecular oxygen and the oxygen atom should originate from dissolved molecular oxygen. Since the only oxygen sources in our experiment are molecular oxygen and water, we replaced $H_2{}^{16}O$ by $H_2{}^{18}O$, to test this hypothesis. LC-MS analysis showed that the N-oxidation product incorporated only ^{16}O confirming that the oxygen atom in the N-oxidation product originated from dissolved molecular oxygen. The low amount of N-oxidation product observed under argon atmosphere (**Figure 1-e**) may therefore be explained by incomplete removal of residual oxygen during argon purging.

3.3.2 Oxidation by Square-Wave Potential Pulses

The absolute yield of N-dealkylation and 4-hydroxylation products under constant potential conditions was below 1 %. Yields were estimated by comparison of the MH^+ ion intensities of the products with that of lidocaine under the assumption that the electrospray ionization efficiencies for lidocaine and its oxidation products are similar. In order to affect the kinetics of the oxidation reaction, we modified constant potential oxidation by adding a lower potential step to generate a square-wave potential pulse with variable cycle time.

In view of the results presented in **Figures 1-c and 1-d**, an upper oxidation potential of +3.0 V was selected for generation of the 4-hydroxylation product, while the lower potential step was varied between +3.0 and -2.0 V with a cycle time of 2 s. The yield of the 4-hydroxylation product at different lower potentials shows that alternating between +3.0 V and a lower potential of +0.5 V or less leads to a more than tenfold increase in 4-hydroxylation product, indicating that the surface properties of the electrode are significantly affected by potential steps below +0.5 V (**Figure 2-a**). It was suggested previously that although surface reactivity could be attenuated by formation of an inert platinum oxide layer during oxidation, a subsequent reduction step can restore the reactivity of the fresh surface [5, 8]. To test the oxide layer formation under our condition and its subsequent reduction, the surface was oxidized at +3.0 V with times ranging from 0, 0.01, 0.05, 0.1, 0.5, to 1.0 s in the absence of lidocaine followed by linear stripping voltammograms recorded from +1.0 to 0.0 V at a scan rate of 1 V/s (**Figure 2-b**). A fresh surface (0 s) did not show any reduction peak across the recorded potential region that implies the absence of oxide layer on the fresh surface. However, application of the oxidation potential even for 0.01 s led to a negative current peak at approximately +0.5 V indicating rapid formation of an oxide layer on the Pt surface at +3.0 V, and its subsequent reduction at potentials lower than +0.5 V. In addition, reduction of the presumed oxide layer at +0.5 V coincides with the potential at which we observe a dramatic increase in the yield of 4-hydroxylation product of lidocaine (**Figure 2-a**). This indicates strongly that reduction of the oxide layer on the Pt electrode surface at or below +0.5 V reactivates the electrode surface for the next pulse cycle leading to increased yields.

Based on the above results, we selected -1.0 V as the lower potential level and monitored product distribution as a function of cycle time ranging from 0.02 to 200 s by LC-MS (**Figure 3**). N-dealkylation was only detected at cycle times shorter than 0.2 s (**Figures 3-a and 3-b**). Since N-dealkylation was nearly absent upon constant potential oxidation at +3.0 V (**Figures 1-a and 1-b**), repeated and fast switching of the surface potential apparently facilitated electron transfer from the tertiary amine moiety of lidocaine to the electrode. The yield of the 4-hydroxylation product also showed a strong dependence on cycle time, with an optimum at cycle times around 1 s independent of an argon or air atmosphere (**Figures 3-c and 3-**

d). Whereas the yield of the 4-hydroxylation product was low at a constant potential of +3.0 V or at short cycle times, it increased about 50-fold (estimated total yield of 10%) at cycle times of 1 s (see **Figures 3-c and 1-c**). The selectivity of pulsed electrochemical oxidation of lidocaine can thus be directed at the N-dealkylation or at the 4-hydroxylation product by selection of the cycle time.

The cause of this change in selectivity is currently unclear. Orientation of lidocaine on the working electrode, the life time of different reactive intermediates of oxidized lidocaine, and recovery of a fresh Pt surface may all be controlled by the potential levels of the square-wave potential pulses, and may have their effect on the competition between N-dealkylation and 4-hydroxylation.

A change of atmosphere from argon to air did not affect the yield of the 4-hydroxylation product (**Figures 3-c and 3-d**), while a higher yield of the N-dealkylation product was observed under air atmosphere, possibly because oxygen reduction generates superoxide anions that may be sufficiently basic for proton abstraction to form the iminium intermediate, facilitating generation of the N-dealkylation product [21]. Generation of the N-oxidation product requires molecular oxygen (see **Figures 1-e and 1-f**), but it is also dependent on cycle time (**Figures 3-e and 3-f**). A lower yield of the N-oxidation product was observed at cycle times between 0.2 and 12 s. It is intriguing that a minimum in N-oxidation yield coincides with the optimum for the 4-hydroxylation reaction suggesting a competition between the electrochemical generation of hydrogen peroxide and oxidation of the aromatic ring for subsequent reaction with water.

The anodic substitution mechanism (see **Scheme 2**) implies that the oxygen atom in 4-hydroxylated lidocaine originates from water. To verify this we replaced $H_2{}^{16}O$ by $H_2{}^{18}O$ during oxidation of lidocaine using square-wave potential pulses. The extracted ion chromatograms (**Figure 4**) show that the major part of the 4-hydroxylation product contained ^{18}O, while about 15-20 % of ^{16}O incorporation was observed, which is likely due to a remaining 3 % of $H_2{}^{16}O$ in commercial $H_2{}^{18}O$ vial and to residual water from the atmosphere. This result is in agreement with the proposed mechanism. Producing the N-oxidation product using square-wave potential pulses in the presence of $H_2{}^{18}O$ resulted in approximately 30% incorporation of ^{18}O while the remainder contained ^{16}O in accordance with the proposed mechanism through which molecular oxygen is reduced to hydrogen peroxide. The 30% of ^{18}O incorporation in the N-oxidation product under pulsed potential conditions might be due to oxidation of $H_2{}^{18}O$ to $^{18}O_2$ followed by reduction to $H_2{}^{18}O_2$.

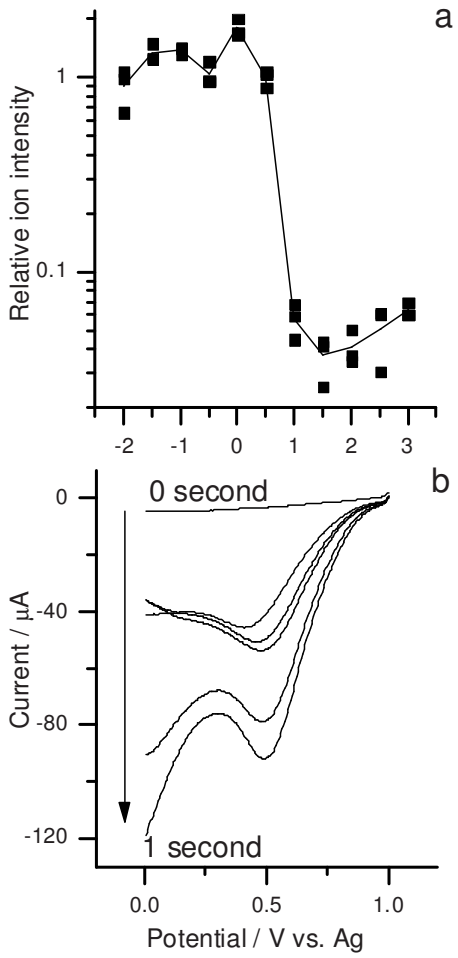

Figure 2. (a) Relative MH^+ ion intensities of the 4-hydroxylation product of lidocaine measured by LC-MS after electrochemical oxidation with square-wave potential pulses alternating between an upper potential of +3.0 V and lower potentials ranging from -2.0 to +3.0 V with a fixed cycle time of 2 s. Ion intensities were normalized relative to the intensity of the signal for acetaminophen, which was added as internal standard to all LC-MS analyses. Experiments were performed in triplicate. Ion intensities are plotted on a logarithmic scale. (b) Linear stripping voltammograms recorded at a scan rate of 1 V/s from +1.0 to 0.0 V after constant potential oxidation at +3.0 V (Pt electrode) for 0, 0.01, 0.05, 0.10, 0.5, and 1.0 s in the absence of lidocaine (the arrow shows the respective traces from top to bottom).

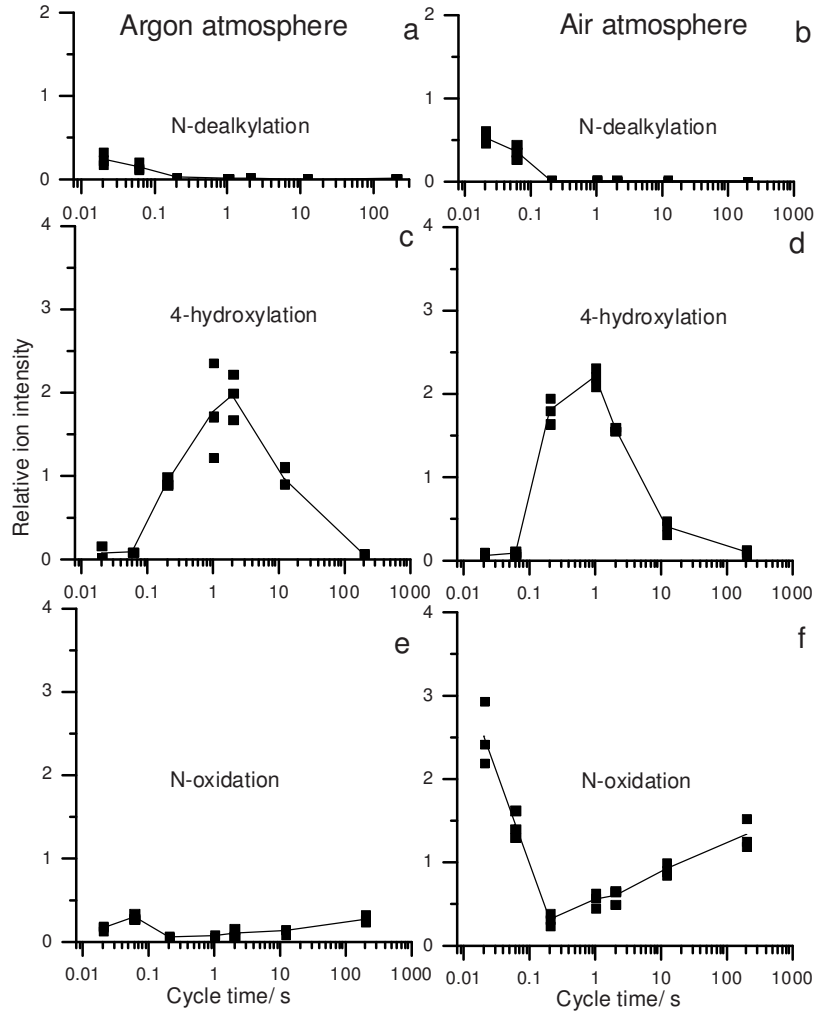

Figure 3. Relative MH^+ ion intensities of the N-dealkylation (a and b), 4-hydroxylation (c and d), and N-oxidation (e and f) products of lidocaine from a solution of 10 mM lidocaine in 0.1 M tetrabutylammonium perchlorate in acetonitrile/water 99/1 (v/v) at varying cycle times (plotted logarithmically) of square-wave potential pulses alternating between +3.0 V and -1.0 V under argon and air atmosphere, respectively. Ion intensities were normalized relative to the intensity of the signal for acetaminophen, which was added as internal standard to all LC-MS analyses. Experiments were performed in triplicate.

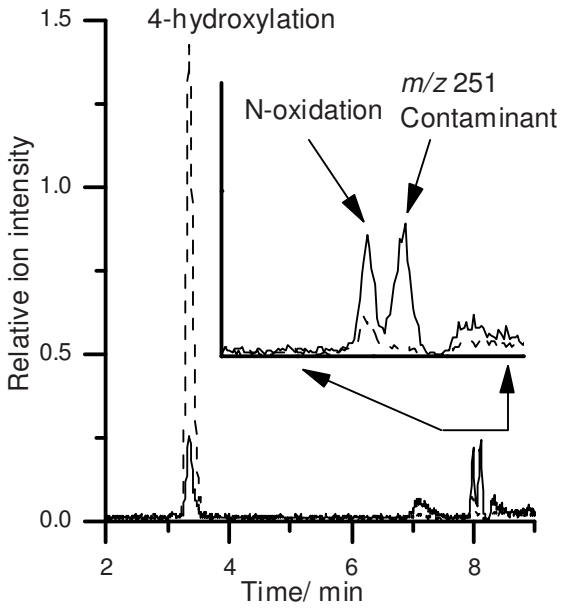

Figure 4. LC-MS analysis of lidocaine oxidation products in the presence $H_2{}^{18}O$ with square-wave potential pulses alternating between +3.0 V and -1.0 V and a cycle time of 2 s under air atmosphere. The extracted ion chromatograms correspond to the MH^+ ions of the 4-hydroxylation and the N-oxidation products at *m/z* 251 (solid line, ^{16}O) and 253 (dashed line, ^{18}O).

The only observed hydroxylation product of lidocaine upon pulsed potential oxidation was 4-hydroxylidocaine, whereas the Fenton reaction, which leads to generation of hydroxyl radicals, results additionally in 3-hydroxylation and benzylic hydroxylation [19]. The absence of the latter hydroxylation products indicates strongly that no adsorbed OH radicals are generated on the Pt electrode during water oxidation. Pulsed potential oxidation of lidocaine on a gold electrode showed the same response as on the Pt electrode, whereas the yield of the 4-hydroxylation product was much lower using a glassy carbon electrode. This supports further that this reaction requires a noble metal surface that can be reactivated through redox cycling (**Figure 5**). In addition, a linear increase in the generation of 4-hydroxylation product was observed under pulsed potential condition over a 30 minute period, suggesting that successful surface reactivation was achieved under pulse condition (**Figure 6**).

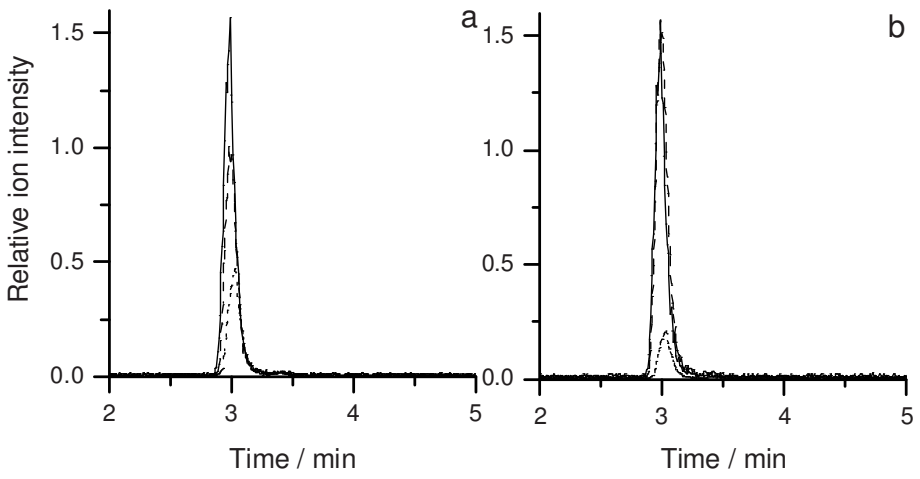

Figure 5. (a) LC-MS analysis of the 4-hydroxylation product of lidocaine obtained with square-wave potential pulses alternating between +3.0 V and -1.0 V at a cycle time of 2 s under air atmosphere on a platinum electrode (solid line, electrode diameter: 2.0 mm), a gold electrode (dashed line, electrode diameter: 1.6 mm), and a glassy carbon electrode (dotted line, electrode diameter: 3.0 mm); (b) the same data plotted after normalization according to the surface area of the platinum electrode.

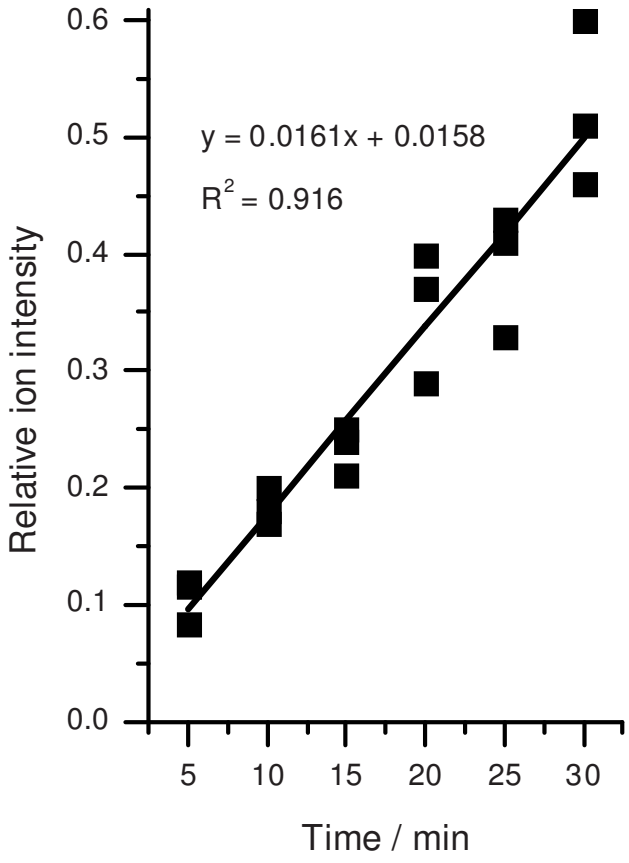

Figure 6. Relative MH^+ ion intensities of the 4-hydroxylation product of lidocaine measured by LC-MS after electrochemical oxidation with square-wave potential pulses alternating between +3.0 V and -1.0 V at a cycle time of 2 s under air atmosphere on a platinum electrode. Lidocaine was oxidized for different times of 5, 10, 15, 20, 25, and 30 minutes in a 4 mL solution of 10 mM lidocaine in 0.1 M tetrabutylammonium perchlorate in acetonitrile/water 99/1 (v/v). 10 µL samples were taken every five minutes for LC-MS analysis. Experiments were performed in triplicate.

3.4 CONCLUSIONS

Constant potential oxidation of lidocaine generates low yields of N-dealkylation and 4-hydroxylation products. By varying the cycle time of square-wave potential pulses and the voltage of the lower potential step, we increased the yield of 4-hydroxylidocaine by about 50-fold relative to constant potential conditions resulting in an overall yield of approximately 10% at a cycle time of 1 s, whereas N-dealkylation was favored at short cycle times below 0.2 s. Pulsed potentials are thus effective in modulating electrochemical oxidation reactions that are initiated by direct electron transfer. We show that the Pt electrode surface is rapidly passivated under oxidative conditions and that it is regenerated during the low potential step of the square-wave pulse. How cycle time affects the selectivity of the reaction (N-dealkylation at short pulse times versus 4-hydroxylation at longer pulse times) remains to be elucidated. It is conceivable that the lidocaine molecule reorients itself on the electrode during pulsing and that different parts of the molecule are in contact with the electron-transferring surface. Further experiments are needed to study this in greater detail. Square-wave potential pulses may be applicable to other drug compounds in order to generate oxidation products with greater selectively and higher yield based on optimization of cycle times and potentials. This could widen the scope of direct-electrochemistry based oxidation reactions for the imitation of *in vivo* drug metabolism.

3.5 REFERENCES

[1] Lohmann, W.; Karst, U. Electrochemistry meets enzymes: instrumental on-line simulation of oxidative and conjugative metabolism reactions of toremifene. *Anal. Bioanal. Chem.* **2009**, *394*, 1341–1348.

[2] Lohmann, W.; Dötzer, R.; Gütter, G.; Van Leeuwen, S. M.; Karst, U. On-line electrochemistry/liquid chromatography/mass spectrometry for the simulation of pesticide metabolism. *J. Am. Soc. Mass Spectrom.* **2009**, *20*, 138-145.

[3] Baumann, A.; Lohmann, W.; Schubert, B.; Oberacher, H.; Karst, U. Metabolic studies of tetrazepam based on electrochemical simulation in comparison to in vivo and in vitro methods. *J. Chromatogr. A* **2009**, *1216*, 3192-3198.

[4] Madsen, K. G.; Olsen, J.; Skonberg, C.; Hansen, S. H.; Jurva, U. Development and Evaluation of an Electrochemical Method for Studying Reactive Phase-I Metabolites: Correlation to in Vitro Drug Metabolism. *Chem. Res. Toxicol.* **2007**, *20*, 821-831.

[5] Johansson, T.; Weidolf, L.; Jurva, U. Mimicry of phase I drug metabolism--novel methods for metabolite characterization and synthesis. *Rapid Commun. Mass Spectrom.* **2007**, *21*, 2323-2331.

[6] Hoekstra, J. C.; Johnson, D. C. Waveform optimization for integrated square-wave detection of biogenic amines following their liquid chromatographic separation. *Anal. Chim. Acta.* **1999**, *390,* 45-54.

[7] Panizza, M.; Cerisola, G. Direct And Mediated Anodic Oxidation of Organic Pollutants. *Chem. Rev.* **2009**, *109,* 6541-6569.

[8] Johnson, D. C.; LaCourse, W. R. Liquid chromatography with pulsed electrochemical detection at gold and platinum electrodes. *Anal. Chem.* **1990**, *62,* 589-597.

[9] Johnson, D. C.; Dobberpuhl, D.; Roberts, R.; Vandeberg, P. Pulsed amperometric detection of carbohydrates, amines and sulfur species in ion chromatography --the current state of research. *J. Chromatogr. A* **1993**, *640,* 79-96.

[10] Williams, D. G.; Johnson, D. C. Pulsed voltammetric detection of arsenic(III) at platinum electrodes in acidic media. *Anal. Chem.* **1992**, *64,* 1785-1789.

[11] Angerstein-Kozlowska, H.; Conway, B. E.; Sharp, W. B. A. The real condition of electrochemically oxidized platinum surfaces: Part I. Resolution of component processes. *J. Electroanal. Chem.* **1973**, *43,* 9-36.

[12] Tilak, B. V.; Conway, B. E.; Angerstein-Kozlowska, H. The real condition of oxidized pt electrodes: Part III. Kinetic theory of formation and reduction of surface oxides. *J. Electroanal. Chem.* **1973**, *48,* 1-23.

[13] Austin, D. S.; Johnson, D. C.; Hines, T. G.; Berti, E. T. Square-wave hydrodynamically modulated voltammetry for study of anodic electrocatalysis. *Anal. Chem.* **1983**, *55,* 2222-2226.

[14] Johnson, D. C.; Feng, J.; Houk, L. L. Direct electrochemical degradation of organic wastes in aqueous media. *Electrochim. Acta.* **2000**, *46,* 323-330.

[15] Lund, H.; Hammerich, O. *Organic Electrochemistry*, 4th ed.; Marcel Dekker, Inc.: New York, 2001.

[16] Oda, Y.; Imaoka, S.; Nakahira, Y.; Asada, A.; Fujimori, M.; Fujita, S.; Funae, Y. Metabolism of lidocaine by purified rat liver microsomal cytochrome P-450 isozymes. *Biochem. Pharmacol.* **1989**, *38*, 4439-4444.

[17] Thomas, J.; Meffin, P. Aromatic hydroxylation of lidocaine and mepivacaine in rats and humans. *J. Med. Chem.* **1972**, *15*, 1046-1049.

[18] Jurva, U.; Wikström, H. V.; Bruins, A. P. In vitro mimicry of metabolic oxidation reactions by electrochemistry/mass spectrometry. *Rapid Commun. Mass Spectrom.* **2000**, *14*, 529-533.

[19] Nouri-Nigjeh, E.; Permentier, H. P.; Bischoff, R.; Bruins, A. P. Lidocaine Oxidation by Electrogenerated Reactive Oxygen Species in the Light of Oxidative Drug Metabolism. *Anal. Chem.* **2010**, *82*, 7625–7633.

[20] Jurva, U.; Wikström, H. V.; Weidolf, L.; Bruins, A. P. Comparison between electrochemistry/mass spectrometry and cytochrome P450 catalyzed oxidation reactions. *Rapid Commun. Mass Spectrom.* **2003**, *14,* 800-810.

[21] Smith, P. J.; Mann, C. K. Electrochemical dealkylation of aliphatic amines. *J. Org. Chem.* **1969**, *34*, 1821-1826.

[22] Eberson, L. Electrolytic substitution reactions. III. Isomer distributions and isotope effects in nuclear and side-chain anodic acetoxylation of aromatic compounds. *J. Am. Chem. Soc.* **1967**, *89*, 4669-4677.

[23] Eberson, L.; Nyberg, K. Anodic aromatic substitution. *Acc. Chem. Res.* **1973**, *6*, 106-112.

[24] Meunier, B.; de Visser, S. P.; Shaik, S. Mechanism of Oxidation Reactions Catalyzed by Cytochrome P450 Enzymes. *Chem. Rev.* **2004**, *104*, 3947-3980.

[25] Oswald, A. A.; Guertin, D. L. Organic Nitrogen Compounds. I. Peroxide Intermediates of Tertiary Alkylamine Oxidation by Hydrogen Peroxide. *J. Org. Chem.* **1963**, *28*, 651-657.

Chapter 4
Electrochemical Oxidation by Square-Wave Potential Pulses in the Imitation of Phenacetin to Acetaminophen Biotransformation*

Electrochemistry in combination with mass spectrometry is emerging as a versatile analytical technique in the imitation of oxidative drug metabolism during the early stages of drug discovery and development. Here, we present electrochemical O-dealkylation of phenacetin to acetaminophen by square-wave potential pulses consisting of consecutive sub-second oxidation and reduction steps. This O-dealkylation could not be achieved by oxidation at constant potential or longer potential pulses because of the fast hydrolysis of the reactive intermediates. Electrochemical conversion by square-wave potential pulses can thus widen the scope of electrochemical synthesis of metabolites and imitation of in vivo drug metabolism.

* Submitted as: Nouri-Nigjeh, E.; Bischoff, R.; Bruins, A.P.; Permentier, H.P. Electrochemical oxidation by square-wave potential pulses in the imitation of phenacetin to acetaminophen biotransformation, Analyst, Submitted.

4.1 Introduction

New analytical techniques capable of imitating various *in vivo* oxidation reactions are required to study oxidative drug metabolism during the early stages of drug discovery and development [1, 2]. Direct electrochemical oxidation in combination with mass spectrometry has been shown to be a versatile analytical technique in the imitation of *in vivo* oxidation reactions that are initiated by single electron transfer (SET), such as N-dealkylations, whereas it proved to be difficult to promote oxidation reactions that are initiated by oxygen insertion or hydrogen atom transfer (HAT), such as O-dealkylations [3, 4]. Biotransformation of phenacetin to the therapeutically active acetaminophen, a known O-dealkylation reaction catalyzed by CYP1A2, a member of Cytochrome P450 family, is considered to be initiated by HAT from the alpha carbon of the ethoxy group [5, 6]. We have recently shown that the use of square-wave potential pulses could imitate the oxidation reactions initiated by SET, by higher yields and selectivity based on the applied cycle time [7]. In this study we show that though the transformation of phenacetin to acetaminophen by direct electrochemical oxidation is not possible, the electrochemical oxidation by sub-second square-wave potential pulses promotes the transformation of phenacetin to acetaminophen. The reaction mechanism will be studied by isitope labelling and stabilization and characterization of the intermediates.

As proposed by Kissinger and colleagues, the electrochemical oxidation of phenacetin involves formation of a quinone-imine cation intermediate, where the oxygen remains substituted (**Scheme 1**, compound **1**) [8]. Water or hydroxide anions attack rapidly, liberating ethanol and producing N-acetyl-p-benzo-quinone imine (NAPQI) [8]. Similarly, the peroxidase-catalyzed O-demethylation of 9-methoxyellipticine was shown to proceed through the formation of a quinone-imine derivative intermediate followed by demethoxylation [9]. In aqueous solutions a rate constant of 2500 s^{-1} for the decomposition of **1** to NAPQI at pH 6.7 was measured by double potential step chronoamperometry [8]. NAPQI is the major *in vivo* and *in vitro* oxidation product of acetaminophen, but electrochemical oxidation of acetaminophen in water results in dimerization between pH 5 and 7, aromatic hydroxylation at basic pH, and oxidation to p-quinone at acidic pH [10]. NAPQI reacts *in vivo* with nucleophilic antioxidants such as glutathione (GSH) during phase II drug metabolism.

4.2 Experimental Procedure

Reagents. All reagents were from electrochemical and analytical grade and purchased from Sigma-Aldrich. Water was purified by a Maxima Ultrapure water system (ELGA, High Wycombe, Bucks, UK).

Electrode preparation. The surface of a platinum disk electrode with 2.0 mm diameter (MF-2071, Bioanalytical Systems (BASi), West Lafayette, IN, USA) was polished with a lapping sheet (Micromesh grade 3200) prior to each experiment. After mechanical polishing the surface was washed with ethanol and air-dried.

Electrochemical set up. Electrochemical experiments were performed with a home-made potentiostat controlled by a MacLab system (ADInstruments, Castle Hill, NSW, Australia) and EChem v.1.52 software (eDAQ, Denistone East, NSW, Australia). The electrochemical cell was a three electrode cell in which the working electrode was a platinum disk and the auxiliary electrode a platinum wire (MW-4130, BASi). It was constructed as a two-compartment cell by using a porous Vycor tip with Teflon heat shrink (MF-2064, BASi) to separate working and auxiliary half-cells. The reference electrode was placed in the working compartment. The auxiliary compartment was always under continuous argon atmosphere. Potentials were measured against a silver wire pseudo-reference electrode (MF-2017, BASi), instead of conventional reference electrodes, to eliminate the possibility of chloride contamination of the working solution during prolonged electrolysis. All experiments were performed at ambient temperature.

Solutions containing 10 mM phenacetin and 0.1 M tetrabutylammonium perchlorate (TBAP) dissolved in acetonitrile/water 99/1 (v/v) (0.1 M TBAP used as electrolyte to provide sufficient conductivity for electrochemical experiments) were subjected to constant potential and potential pulse oxidation, for 30 minutes prior to LC-MS and LC-MS/MS analysis. Samples were collected and diluted 100 times in water containing 0.5 μM lidocaine, as an internal standard for LC-MS signal normalization, immediately after the batch oxidations and stored at room temperature until LC-MS analysis.

LC-MS analysis. LC-MS experiments on 100-times diluted samples were carried out on an LC-Packings Ultimate HPLC system (LC-Packings, Amsterdam, the Netherlands) coupled to an API 365 triple quadrupole mass spectrometer (MDS Sciex, Concord, ON, Canada) upgraded to EP10+ (Ionics, Bolton, ON, Canada) with electrospray ionization in the positive mode. The MS parameters were as follows: ion spray voltage 4800 V, OR 40 V, and RNG 120 V, with scans between *m/z* 100-600 (step size 1.0 amu, dwell time 1 ms). MS/MS parameters were as follows: ion spray voltage 5000 V, OR 40 V, RNG 170 V, and collision energy 20-30 eV, with product ion scans between *m/z* 50-500 (step size 1.0 amu, dwell time 1 ms). Heated turbo gas (nitrogen) with a flow rate of 1.0 L/min was used at 450 °C for LC-MS and LC-MS/MS experiments. Negative ion Atmospheric Pressure Chemical Ionization (APCI) experiments were done with OR -5 V, and RNG -30 V, with scans between *m/z* 50-500 (step size 1.0 amu, dwell time 1 ms); the discharge current of the APCI source was 3 μA, and the heated nebulizer temperature was 250 °C. APCI generated the molecular anion of p-quinone at *m/z* 108.

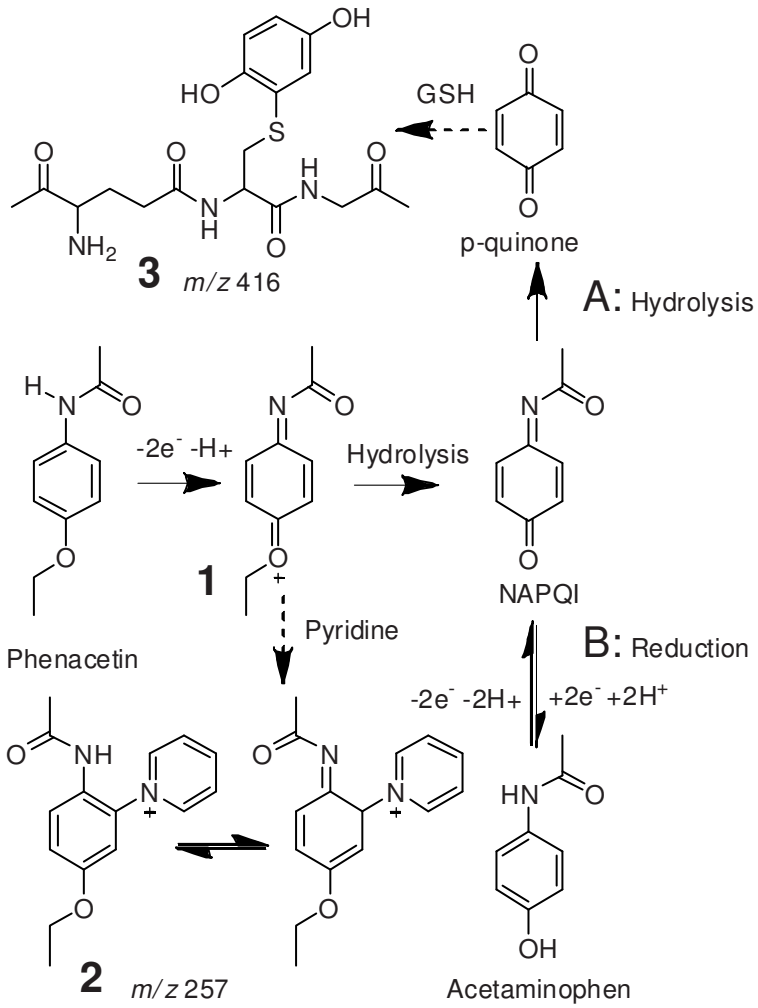

Scheme 1. Electrochemical oxidation of phenacetin to p-quinone (path **A**) and to acetaminophen (path B) in a solution of 0.1 M tetrabutylammonium perchlorate in acetonitrile/water 99/1 (v/v). After initial oxidation, the quinone-imine intermediate **1**, is hydrolyzed to NAPQI. In the presence of pyridine, **1** reacts instead to generate **2**. Under constant potential oxidation, NAPQI is hydrolyzed further to p-quinone (path A), and reaction of p-quinone after addition of glutathione (GSH) generates **3**. Under square-wave potential pulses, generation of NAPQI was followed by reduction to acetaminophen (path **B**) during the reduction step of the potential pulse.

A C18 reversed-phase column (GraceSmart RP 18 5µm, 2.1×150 mm; Grace Davison, Lokeren, Belgium) was used at a flow rate of 200 µL/min. Solvent A: H2O/ACN 95/5 (v/v) with 0.1 % formic acid; Solvent B: ACN/H2O 95/5 (v/v) with 0.1 % formic acid. 5 µL of a diluted oxidation product mixture was injected and a linear gradient of 5-50 % B in 20 minutes was used for elution.

4.3 Results and discussion

The products of electrochemical oxidation of phenacetin at a constant potential of +3.0 V in 0.1 M tetrabutylammonium (TBA) perchlorate in acetonitrile/water 99/1 (v/v) were analyzed by liquid chromatography-tandem mass spectrometry (LC-MS/MS). No oxidation product of phenacetin was observed by positive ion electrospray ionization (ESI). However, p-quinone was detected by negative ion atmospheric pressure chemical ionization (APCI). The absence of detectable amounts of p-quinone in the LC-(ESI)-MS analysis is due to its very low electrospray ionization efficiency. In order to verify the formation of **1**, constant potential oxidation in the presence of 1 vol % pyridine was performed, which produced a compound with *m/z* 257 resulting from nucleophilic attack of pyridine on **1** to generate **2** (see **Scheme 1**). The structure of **2** was in agreement with MS/MS analysis (**Figure 1**). As shown in **Figure 1**, the oxidation product (*m/z* 257) loses pyridine (a), ketene (b), and ethene (c). This confirms that nucleophilic attack of pyridine on 1 makes it detectable by LC-MS(/MS).

Compound **1** is expected to be hydrolyzed rapidly to NAPQI and NAPQI can be further hydrolyzed to p-quinone with a half-life of a few seconds (path A in **Scheme 1**) [11]. In order to reveal the presence of NAPQI as an intermediate and confirm p-quinone as the final oxidation product, reaction mixture was diluted in an aqueous solution of 1 mM GSH to capture them in analogy to phase II drug metabolism. LC-MS(/MS) confirmed generation of the reaction product of GSH with p-quinone (compound **3** in **Scheme 1** and **Figure 2**). As shown in **Figure 2**, in order to reveal the generation of p-quinone during constant potential oxidation, an experiment was performed to capture p-quinone by using glutathione (a reaction that occurs also *in vivo*). LC-MS analysis showed a reaction product at *m/z* 416 after dilution of the reaction mixture in an aqueous solution of 1 mM glutathione. Collision induced dissociation (CID) of this reaction product showed the y_2, b_2, and z_2 fragments. The reaction of p-quinone standard with glutathione, as a control experiment, showed the same product at *m/z* 416 with the same CID fragmentation pattern. There was no detectable amount of the reaction product of GSH with NAPQI.

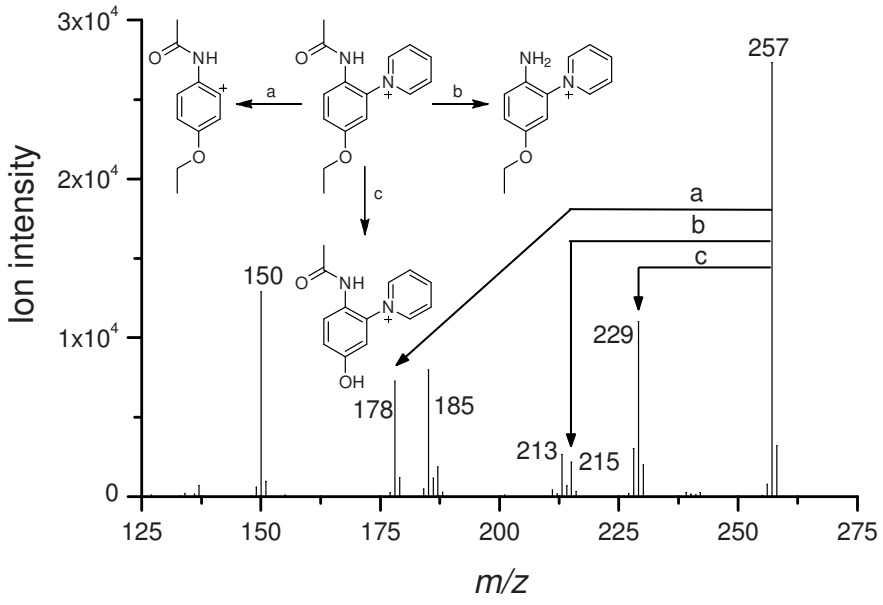

Figure 1. Collision induced dissociation (CID) at a collision energy of 30 eV of the oxidation product at *m/z* 257, **2** in **Scheme 1**, generated during electrochemical oxidation at constant potential of +3.0 V from a solution of 10 mM phenacetin in 0.1 M tetrabutylammonium perchlorate dissolved in acetonitrile/water 99/1 (v/v) in the presence of 1 vol % pyridine.

We reasoned that after hydrolysis of **1,** the short-lived NAPQI intermediate could be reduced to acetaminophen by an immediate reduction step in a square-wave potential pulse. Oxidation at +3.0 V was thus followed by reduction at -1.0 V with a cycle time that was varied between 20 ms and 200 s. **Figure 3** shows that acetaminophen was produced with increasing yield when cycle times are shorter than 1 s. One hour electrochemical oxidation with potential pulses of 200 ms cycle time resulted in 6-7% conversion of phenacetin to acetaminophen based on LC-MS analyses of the reaction products and standard addition of acetaminophen. We expect that this yield can be further augmented by using longer reaction times and electrodes with a larger surface area.

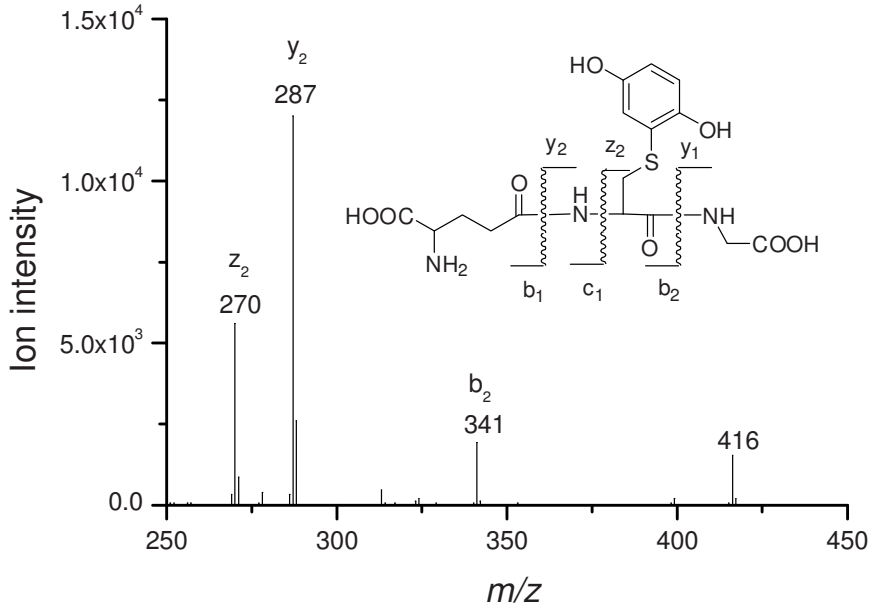

Figure 2. Collision induced dissociation (CID) at a collision energy of 25 eV of the reaction product at *m/z* 416, **3** in **Scheme 1.**

We hypothesize that the oxidation of phenacetin under square-wave potential pulses begins with formation of **1**, which reacts with water to generate NAPQI. By rapidly changing the potential on the surface, NAPQI is reduced to acetaminophen (path B in **Scheme 1**). When phenacetin was subjected to square-wave potential pulses of 200 ms in the presence of pyridine, **2** was generated, while no acetaminophen was observed. Therefore, scavenging **1** with pyridine blocks the generation of acetaminophen during square-wave potential pulses in agreement with the proposed reaction mechanism.

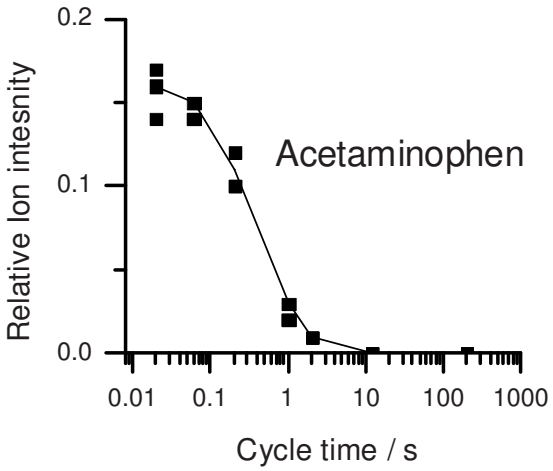

Figure 3. MH+ ion intensities of acetaminophen (relative to a lidocaine standard) extracted from LC-MS analyses of a solution of 10 mM phenacetin in 0.1 M tetrabutylammonium perchlorate in acetonitrile/water 99/1 (v/v) that was subjected to square-wave potential pulses alternating between +3.0 V and -1.0 V of varying cycle times for 30 min (individual results of triplicate reactions are shown).

Compound **1** may convert to NAPQI by reaction with water either on the alpha carbon of the ethoxy group leading to O-deethylation, or on the aromatic ring leading to O-deethoxylation through nucleophilic addition and intramolecular rearrangement (see **Scheme 2**). The latter is the proposed mechanism in O-dealkylations catalyzed by peroxidases [9]. To study the hydrolysis mechanism, $H_2{}^{16}O$ was substituted by $H_2{}^{18}O$ followed by mass spectrometric analysis of the reaction products. Both ^{18}O- and ^{16}O-labeled acetaminophen were found under pulse conditions indicating that hydrolysis proceeds via either of the two reaction pathways.

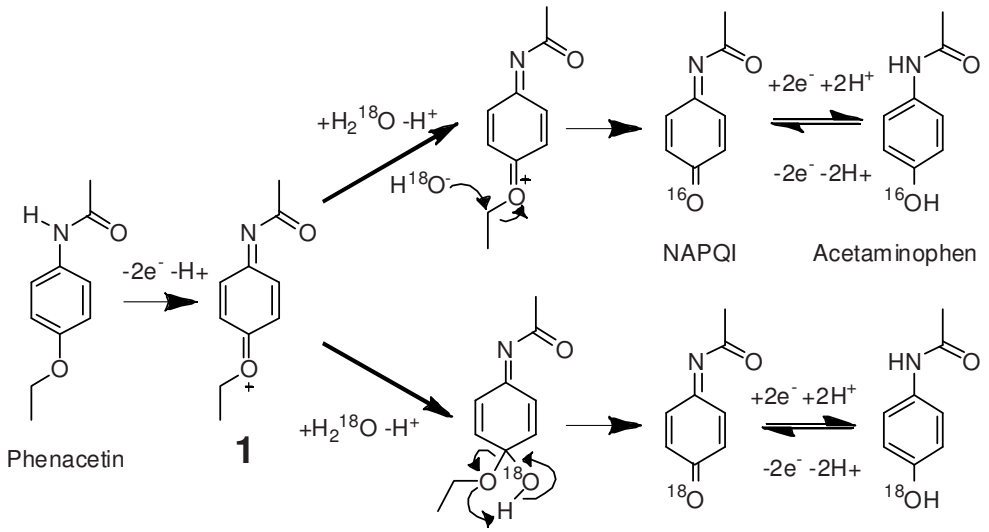

Scheme 2. Electrochemical oxidation of phenacetin under square-wave potential pulses proceeds via the quinone-imine intermediate **1.** Hydrolysis to NAPQI may occur through two parallel reaction pathways which can be verified by performing the reaction in the presence of $H_2{}^{18}O$. Hydrolysis on the ethoxy alpha carbon leads to O-deethylation (top reaction) without incorporation of ^{18}O in NAPQI. Hydrolysis on the aromatic ring leads to O-deethoxylation through nucleophilic addition and intramolecular rearrangement (bottom reaction) with incorporation of ^{18}O in NAPQI. In both cases the hydrolysis is followed by the reduction of NAPQI to acetaminophen during the reduction step.

4.4 Conclusions

In conclusion, the electrochemical approach using square-wave potential pulses is capable of converting phenacetin to acetaminophen, a dealkylation reaction that is not accessible by electrochemical oxidation at constant potential. Pulse time played a crucial role: only short, sub-second pulse times promoted the O-dealkylation reaction. The combination of electrochemical oxidation with a reduction step in the form of a square-wave potential pulse, thus widens the scope of electrochemistry in the imitation of oxidative drug metabolism, as well as the synthesis of drug metabolites.

4.5 REFERENCES:

[1] Oritz de Montellano, P. R., Cytochrome P450: Structure, Mechanism, and Biochemistry. third ed.; Kluwer Academic/Plenum Publishers: New York, 2005.

[2] Karst, U. Electrochemistry/Mass Spectrometry (EC/MS)—A New Tool To Study Drug Metabolism and Reaction Mechanisms. *Angew. Chem. Int. Ed.* **2004**, *43,* 2476-2478.

[3] Jurva, U.; Wikstrom, H. V.; Weidolf, L.; Bruins, A. P. Comparison between electrochemistry/mass spectrometry and cytochrome P450 catalyzed oxidation reactions. *Rapid Commun. Mass Spectrom.* **2003**, *17*, 800-10.

[4] Jurva, U.; Bissel, P.; Isin, E. M.; Igarashi, K.; Kuttab, S.; Castagnoli Jr., N. Model electrochemical-mass spectrometric studies of the cytochrome P450-catalyzed oxidations of cyclic tertiary allylamines. *J. Am. Chem. Soc.* **2005**, *127*, 12368-77.

[5] Walsky, R. L.; Obach, R. S. Validated assays for human Cytochrome P450 activities. *Drug Metab. Dispos.* **2004**, *32*, 647-660.

[6] Meunier, B.; de Visser, S. P.; Shaik, S. Mechanism of Oxidation Reactions Catalyzed by Cytochrome P450 Enzymes. *Chem. Rev.* **2004**, *104*, 3947-3980.

[7] Nouri-Nigjeh, E.; Permentier, H. P.; Bischoff, R. P. H.; Bruins, A. P. *Anal. Chem.* **2011**, *83*, 5519-5525.

[8] Miner, D. J.; Rice, J. R.; Riggin, R. M.; Kissinger, P. T. Voltammetry of acetaminophen and its metabolites. *Anal. Chem.* **1981**, *53*, 2258-2263.

[9] Meunier, G.; Meunier, B. Peroxidase-catalyzed O-demethylation reactions. Quinone-imine formation from 9-methoxyellipticine derivatives. *J. Biol. Chem.* **1985**, *260*, 10576-10582.

[10] Nematollahi, D.; Shayani-Jam, H.; Alimoradi, M.; Niroomand, S. Electrochemical oxidation of acetaminophen in aqueous solutions: Kinetic evaluation of hydrolysis, hydroxylation and dimerization processes. *Electrochim. Acta* **2009**, *54*, 7407-7415.

[11] Miner, D. J.; Kissinger, P. T. Evidence for the involvement of N-ACETYL-p-quinoneimine in acetaminophen metabolism. *Biochem. Pharma.* **1979**, *28*, 3285-3290.

Chapter 5
Electrocatalytic Activation of Hydrogen Peroxide on a Platinum Electrode in the Imitation of Oxidative Drug Metabolism by Cytochrome P450s*

Electrochemistry in combination with mass spectrometry has shown promise as a versatile technique not only in the analytical assessment of oxidative drug metabolism, but also for small-scale synthesis of drug metabolites. However, electrochemistry is generally limited to reactions initiated by direct electron transfer. In the case of substituted-aromatic compounds, oxidation proceeds through a Wheland-type intermediate where resonance stabilization of the positive charge determines the regioselectivity of the anodic substitution reaction, and hence limits the extent of generating drug metabolites in comparison with in vivo oxygen insertion reactions. In this study, we show that the electrocatalytic oxidation of hydrogen peroxide on a platinum electrode generates reactive oxygen species, presumably surface-bound platinum-oxo species, which are capable of oxygen insertion reactions in analogy to oxo-ferryl radical cations in the active site of Cytochrome P450. Electrochemical oxidation of lidocaine at constant potential in the presence of hydrogen peroxide produces both 3- and 4-hydroxylidocaine, suggesting reaction via an arene rather than a Wheland-type intermediate. No benzylic hydroxylation was observed, excluding the presence of freely diffusing radicals. The results of the present study extend the possibilities of electrochemical imitation of oxidative drug metabolism to oxygen insertion reactions.

* Submitted as: Nouri-Nigjeh, E.; Bischoff, R.; Bruins, A.P.; Permentier, H.P. Electrocatalytic activation of hydrogen peroxide on a platinum electrode in the mimicry of oxidative drug metabolism by Cytochrome P450s, Chemical Research in Toxicology, Submitted.

5.1 INTRODUCTION

Drug metabolism and toxicological studies are shifting toward the earlier stages of drug discovery and development. This makes it indispensable to develop fast and accurate analytical techniques capable of detecting and characterizing drug metabolites. Electrochemistry in combination with mass spectrometry has shown promise as a versatile technique not only in the analytical assessment of oxidative drug metabolism, but also for small-scale synthesis of drug metabolites [1-4]. However, electrochemistry is mainly restricted to reactions initiated by single electron transfer (SET), such as N-dealkylation, or hydroxylation of substituted aromatic ring systems [5, 6]. Further research is thus required to extend the range of electrochemical techniques to cover the full range of *in vivo* drug metabolism by imitating reactions initiated by hydrogen atom transfer (HAT) or oxygen insertion.

Lidocaine, a local anesthetic drug with a variety of *in vivo* metabolites, has been used as a test compound in the evaluation of new electrochemical techniques [7, 8]. The *in vivo* oxidative drug metabolism of lidocaine by Cytochrome P450s (CYP) encompasses N-dealkylation, N-oxidation, and aromatic and benzylic hydroxylation reactions [9-11]. An early study showed that electrochemistry can imitate the N-dealkylation reaction by application of a constant positive potential of less than 1.5 V vs. Pd/H_2 in an on-line electrochemical cell coupled to a mass spectrometer [12], where the reaction proceeds through initial electron transfer from the tertiary amine moiety to the electrode to generate an imine intermediate followed by hydrolysis and cleavage after intramolecular rearrangement [13]. N-oxidation of lidocaine was achieved through electrochemical reduction of molecular oxygen and generation of hydrogen peroxide in a two-compartment electrochemical cell under air atmosphere [7]. This reaction proceeds most likely through a peroxide intermediate [14].

Whereas the only oxidation product at potentials below 1.5 V is N-dealkylation [10], we have recently shown that oxidation at more positive potentials (optimum at 3.0 V) using 99/1 (v/v) acetonitrile/water and tetrabutylammonium perchlorate (TBAP) as supporting electrolyte results in 4-hydroxylation [8]. Four-hydroxylation is probably initiated by electron transfer from the aromatic ring moiety to generate a Wheland-type intermediate, that leads to the hydroxylation product through deprotonation and an anodic substitution reaction (**Scheme 1A**) [15, 16]. The presence of an amide substituent on the aromatic ring decreases the oxidation potential compared with an unsubstituted benzene ring and directs the anodic substitution reaction toward the 4-position by resonance-stabilization. Since the anodic substitution reaction proceeds through the Wheland-type intermediate, the regioselectivity of the reaction excludes the formation of the 3-hydroxylidocaine. In contrast, *in vivo* aromatic hydroxylation is believed to follow a concerted oxygen insertion mechanism by oxo-ferryl radical cations (Compound I) in CYP and

formation of an arene intermediate and does not involve the Wheland-type intermediate (**Scheme 1B**) [17]. Therefore, for electrochemistry to imitate *in vivo* oxidative drug metabolism more closely, the generation of reactive oxygen species (ROS) that mimic the generated ROS during catalytic activation of molecular oxygen by CYP is required.

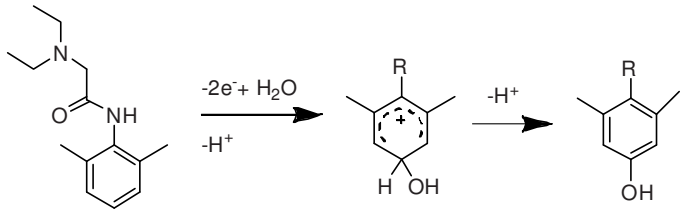

Wheland-type intermediate

Electrochemistry-mediated aromatic hydroxylation

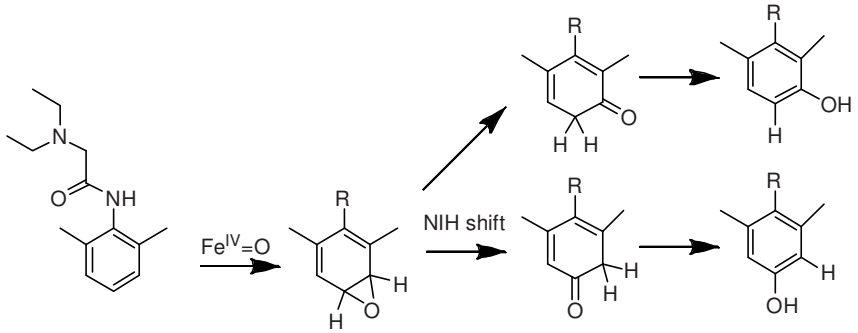

Arene intermediate

Cytochrome P450-mediated aromatic hydroxylation

Scheme 1. (a) Electrochemistry-mediated aromatic hydroxylation of lidocaine through an anodic substitution mechanism proceeding via a Wheland-type intermediate, which after deprotonation results only in 4-hydroxylation. (b) Aromatic hydroxylation of lidocaine by the oxo-ferryl radical cation in the reactive state of Cytochrome P450 through an oxygen insertion mechanism and an NIH shift reaction, which gives rise to both 3- and 4-hydroxylation products.

Platinum electrodes are widely used for the oxidation of organic compounds as they are stable even at high positive potentials. They are also used for electrocatalytic oxidation of hydrogen peroxide to generate molecular oxygen [18, 19]. This reaction supposedly begins by binding of H_2O_2 to electrochemically generated Pt(II) sites on the electrode surface, and it is overall a two-electron and two-proton transfer process, i.e. $H_2O_2 \rightarrow 2H^+ + O_2 + 2e^-$, depending strongly on the pH, electrode surface condition as well as the O_2, and H_2O_2 concentrations [18-20].

However, the generation of ROS during the electrocatalytic oxidation of H_2O_2 on the Pt electrodes has not been studied yet. Here we report that electrocatalytic oxidation of H_2O_2 on a Pt electrode leads to aromatic hydroxylation of lidocaine in the 3-position thus extending the electrochemistry-based imitation of P450-mediated, oxidative metabolism of lidocaine.

5.2 EXPERIMENTAL PROCEDURES

Reagents. Tetrabutylammonium perchlorate (TBAP, 86893), hydrogen peroxide (30 vol % in water (31642)), $H_2{}^{18}O$ with 97 atom % ^{18}O ($H_2{}^{18}O$, 329878), and lidocaine (L7757) were purchased from Sigma-Aldrich. Throughout this article, H_2O_2 denotes 30% H_2O_2 in water. Water was purified by a Maxima Ultrapure water system (ELGA, High Wycombe, Bucks, UK). Ultra-pure HPLC grade acetonitrile (ACN) was purchased from Merck. 3-Hydroxylidocaine (CAS No. 34604-55-2) was purchased from Toronto Research Chemicals Inc.

Electrode preparation. The surface of the working electrode was polished with a lapping sheet (Micromesh grade 3200) prior to each experiment. After mechanical polishing the surface was washed with ethanol and air-dried.

Electrochemical experiments. Electrochemical oxidations were performed with a home-made potentiostat controlled by a MacLab system (ADInstruments, Castle Hill, NSW, Australia) and EChem v.1.52 software (eDAQ, Denistone East, NSW, Australia). A two-compartment electrochemical cell was constructed by using a porous Vycor tip with Teflon heat shrink (MF-2064, Bioanalytical Systems (BASi), West Lafayette, IN, USA) to separate compartments of the working and auxiliary electrodes. The working electrodes were platinum (MF-2013, BASi) or glassy carbon (MF-2012, BASi) disks, respectively, and the auxiliary electrode was a platinum wire (MW-4130, BASi). Potentials were measured against a silver wire pseudo-reference electrode (MF-2017, BASi), which was placed in the working electrode compartment. All experiments were performed at ambient temperature, while the auxiliary electrode and working electrode compartments were constantly purged with argon and synthetic air, respectively. Solutions containing 10 mM lidocaine and 0.1 M TBAP dissolved in ACN/H_2O_2 99/1 (v/v) were subjected to constant potential oxidation for 30 min prior to LC-MS analysis. Samples were collected from the working electrode compartment and diluted 100 times in water containing 10 µM acetaminophen as internal standard for LC-MS signal normalization, immediately after the batch oxidations and stored at room temperature until LC-MS analysis.

LC-MS(/MS) analysis. LC-MS experiments on 100-times diluted samples were carried out on an LC-Packings Ultimate HPLC system (LC-Packings, Amsterdam, the Netherlands) coupled to an API 365 triple quadrupole mass spectrometer (MDS Sciex, Concord, ON, Canada) upgraded to EP10+ (Ionics, Bolton, ON,

Canada) with electrospray ionization in the positive mode using the TurboIonSpray source. The MS parameters were as follows: ion spray voltage 4800 V, OR 40 V, and RNG 120 V, with scans between *m/z* 100-600 (step size 1.0 amu, dwell time 1 ms). MS/MS parameters were as follows: ion spray voltage 5000 V, OR 40 V, RNG 170 V, and collision energy 20 eV (step size 1.0amu, dwell time 1 ms). Heated turbo gas (nitrogen) with a flow rate of 1.0 L/min was used at 450 °C for LC-MS(/MS) analysis.

A C_{18} reversed-phase column (GraceSmart RP 18 5µm, 2.1×150 mm; Grace Davison, Lokeren, Belgium) was used at a flow rate of 200 µL/min. Solvent A: H_2O/ACN 95/5 (v/v) with 0.1 % formic acid; Solvent B: ACN/H_2O 95/5 (v/v) with 0.1 % formic acid. Five and 50 µL of a diluted oxidation product mixture where subjected to LC-MS and MS/MS analysis, respectively, using a linear gradient of 5-50 % B in 20 min. Peak heights were normalized with respect to the peak height of acetaminophen as internal reference compound.

5.3 RESULTS AND DISCUSSION

Electrochemical oxidation of lidocaine at +3.0 V from a solution of ACN/H_2O 99/1 (v/v) has been reported to result in 4-hydroxylation. The N-oxide was formed in a chemical reaction with electrochemically generated hydrogen peroxide.(*8*) In the present study, oxidation at +3.0 V in a solution of ACN/H_2O_2 99/1 (v/v), yielded two oxidation products with *m/z* 251 and one with *m/z* 267 (**Figure 1-a)**. LC-MS/MS analysis of the two *m/z* 251 products (**Figures 1-b and 1-c**) suggests that both are aromatic hydroxylation products. Benzylic hydroxylation was ruled out since it is expected to give water loss upon fragmentation by collision induced dissociation (CID) [7]. Peak II co-eluted with 3-hydroxylidocaine which lead us to the conclusion that peak I corresponds to 4-hydroxylidocaine.

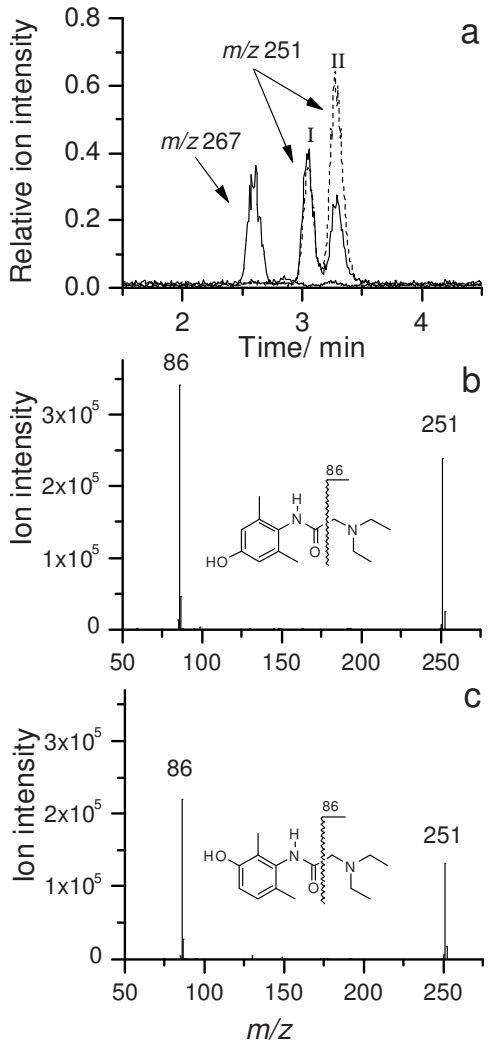

Figure 1. (a) LC-MS analysis of lidocaine oxidation products from a solution of acetonitrile/hydrogen peroxide 99/1 (v/v) with 0.1 M tetrabutylammonium perchlorate at +3.0 V on a platinum electrode. Extracted ion chromatograms are shown of the MH^+ ions at m/z 267, and *m/z* 251 before (solid line), and after (dashed line) addition of 0.25 µM 3-hydroxylidocaine as a standard. (b and c) Collision induced dissociation fragmentation spectra of peaks I and II (c) measured with a collision energy of 20 eV.

MS/MS analysis of the *m/z* 267 oxidation product, showed a fragment at *m/z* 249, corresponding to loss of a water molecule, in addition to the *m/z* 86 fragment, from the tertiary amine part of lidocaine. In order to elucidate the structure of this oxidation product, we synthesized 3,4-dihydroxylidocaine by pulsed electrochemical oxidation of 3-hydroxylidocaine as described before [8]. 3,4-dihydroxylidocaine co-eluted with the *m/z* 267 oxidation product and had the same CID fragment at *m/z* 249 (**Figure 2-a**). For further confirmation, 3,4-dihydroxylidocaine was synthesized from 3-hydroxylidocaine in the presence of $H_2{}^{18}O$ resulting in an oxidation product with *m/z* 269. CID produced two fragments at *m/z* 249 and 251, which are attributed to the loss of $H_2{}^{18}O$ or $H_2{}^{16}O$, respectively (**Figure 2-b**). Taken together this confirms the identity of the *m/z* 267 oxidation product as 3,4-dihydroxylidocaine. As expected, production of 3,4-dihydroxylidocaine from 3-hydroxylidocaine was easer than hydroxylation of lidocaine due to the presence of two electron-donating substituents. Further oxidation to 3,4-benzoquinone lidocaine was not observed under our conditions.

The yield for the 3- and 4-hydroxylation products, and the 3,4-dihydroxylation products of lidocaine at constant potentials ranging from +1 to +5 V on a platinum electrode are shown in **Figures 3-a** and **3-b**, respectively. All hydroxylation products showed a maximum yield at +3.0 V.

To study the effect of the electrode material, constant potential oxidations were repeated on a glassy carbon electrode in the presence of H_2O_2. Only very small amounts of hydroxylation and dihydroxylation products were detected on this type of electrode. Moreover, aromatic hydroxylation products were completely absent at potentials above +2.0 V (see **Figures 3-c** and **3-d)**. The surface properties of the platinum electrode are therefore critical in the electrocatalytic oxidation of H_2O_2 to allow aromatic hydroxylation of lidocaine.

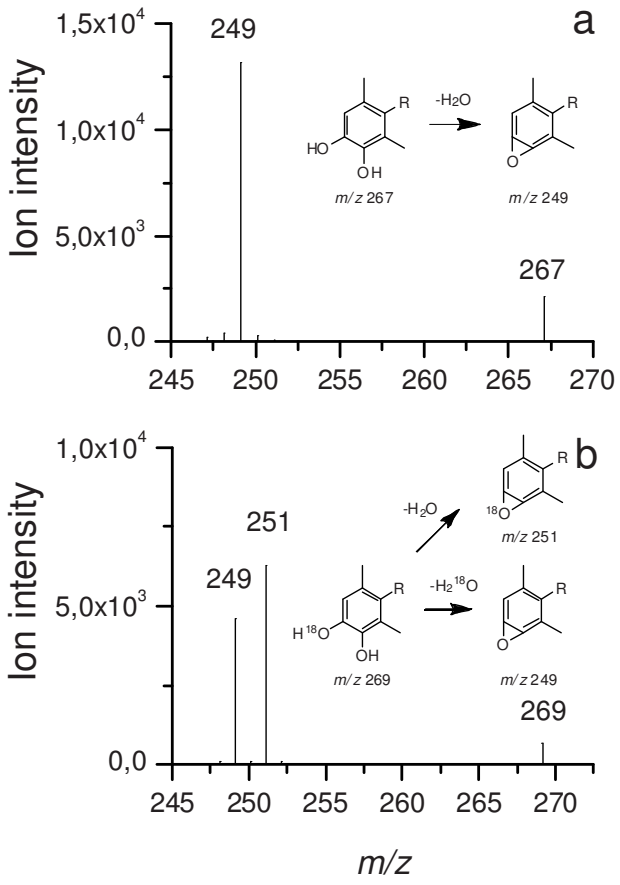

Figure 2. Collision induced fragmentation spectra of 3,4-dihydroxylidocaine. Synthesized by square-wave pulses from lidocaine in the presence of $H_2{}^{16}O$ (a) or from 3-hydroxylidocaine in the presence of $H_2{}^{18}O$ (b). (R represents the rest of lidocaine molecule)

If hydroxylation of lidocaine were initiated by HAT, we should have observed extensive benzylic hydroxylation, as shown previously for the Fenton reaction [7]. Since no benzylic hydroxylation was observed in the present study, a hydroxylation reaction based on a HAT mechanism by freely diffusing radicals, e.g. hydroxyl radicals, is unlikely. Accordingly, generation of the 3-hydroxylation product on a Pt

electrode in the presence of H_2O_2 appears to follow an oxidation mechanism that is neither initiated by direct electron transfer nor by a HAT mechanism due to freely diffusing radicals. We hypothesize that electrocatalytic oxidation of H_2O_2 on a Pt electrode might involve surface-bound platinum-oxo species capable of promoting oxygen insertion in a mechanism reminiscent of the reaction of oxo-ferryl radical cations during the aromatic hydroxylation of substrates by CYP. Oxygen insertion by the putative platinum-oxo species might proceed through an arene oxide intermediate that results in both 3- and 4- hydroxylation products after tautomerization, as shown in **Scheme 2**.

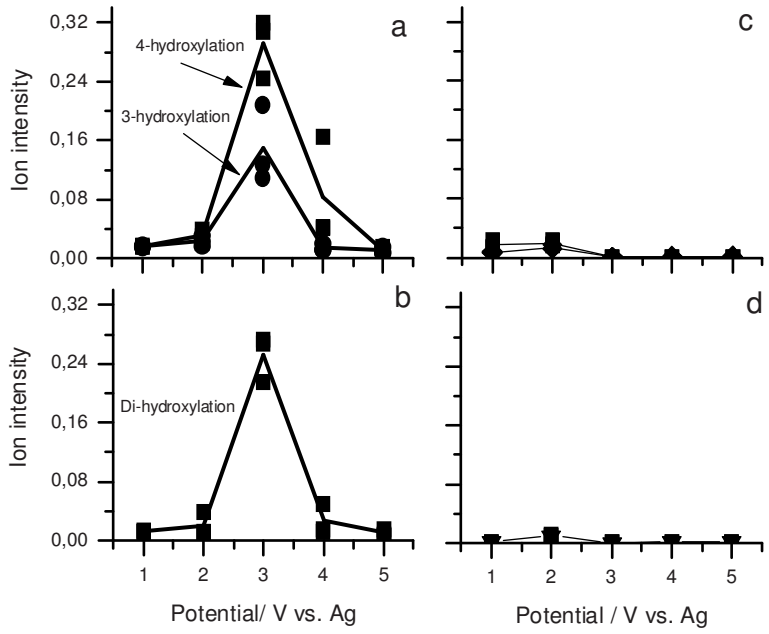

Figure 3. Relative product ion distribution for the 3- and 4-hydroxylation products of lidocaine and the 3,4-dihydroxylation product versus the applied potential from a solution of 10 mM lidocaine in acetonitrile/hydrogen peroxide 99/1 (v/v) with 0.1 M tetrabutylammonium perchlorate on a platinum electrode (a, b), and a glassy carbon electrode (c, d).

The role of the putative platinum-oxo species that were generated during electrocatalytic oxidation of H_2O_2 in the hydroxylation of lidocaine were further studied by adding 1 vol % pyridine. Pyridine may react either with reactive intermediates of lidocaine, notably the arene intermediate, or with reactive platinum-oxo species directly, as illustrated in **Scheme 2**. In fact, oxidation of lidocaine in the presence of pyridine only led to 4-hydroxylidocaine and a pyridine-oxide product at *m/z* 96. This indicates that reaction between pyridine and the putative platinum-oxo species competes with the formation of 3-hydroxylidocaine but not with that of 4-hydroxylidocaine. This is consistent with the mechanism in **Scheme 1A** where 4-hydrxylation occurs through direct oxidation. Therefore, pyridine addition supports the generation of the putative platinum-oxo species and their selective reaction toward the more abundant substrate, i.e. pyridine, during the electrocatalytic oxidation of H_2O_2. Further study of the Pt electrode surface and reactive intermediates should provide more insight into nature of the putative platinum-oxo species and the reaction mechanism.

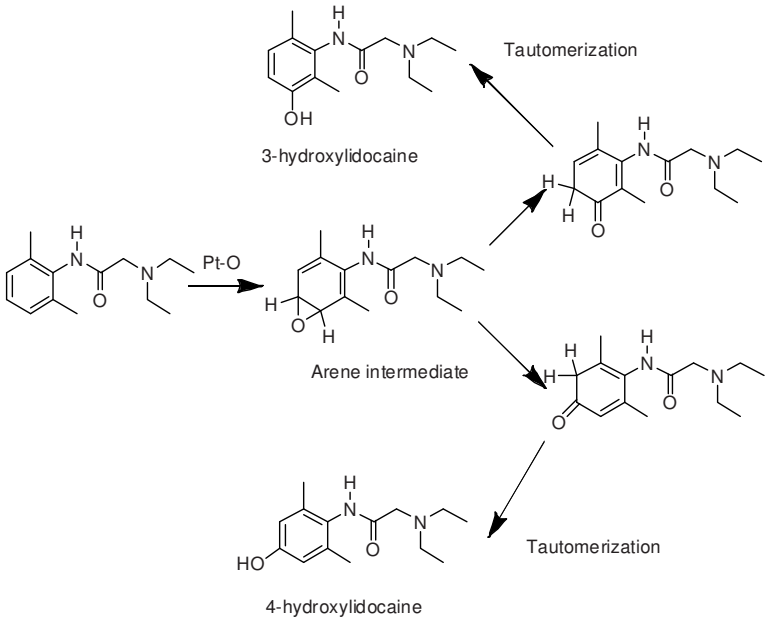

Scheme 2. Oxygen transfer mechanism by surface-bound platinum-oxo species based on a concerted oxygen insertion mechanism, proceeding via an arene oxide intermediate.

5.4 CONCLUSIONS

Lidocaine is metabolized *in vivo* to aromatic hydroxylation products at the 3- and 4-position as well as to the benzylic hydroxylation product, through the action of P450 enzymes. Direct electron transfer oxidation by electrochemistry leads only to 4-hydroxylidocaine, whereas freely diffusing hydroxyl radicals from the Fenton reaction generate all three products. Electrocatalytic oxidation of hydrogen peroxide on a platinum electrode in the presence of lidocaine produces both 3- and 4-hydroxylidocaine without concomitant benzylic hydroxylation. We suggest that this selectivity is due to generation of reactive surface-bound platinum-oxo species that are capable of oxygen insertion in analogy to oxo-ferryl radical cations, which are the main reactive species in the catalytic cycle of P450. The results of this study thus extend the application of electrochemistry in the imitation of oxidative drug metabolism by P450 in that it mimics oxygen insertion reactions.

5.5 REFERENCES

[1] Nouri-Nigjeh, E., Bischoff, R., Bruins, A. P. and Permentier, H. P. Electrochemistry in the mimicry of oxidative drug metabolism by Cytochrome P450s. *Curr. Drug Metab.* **2011**, *12*, 359-371.

(2) Baumann, A. and Karst, U. Online electrochemistry/mass spectrometry in drug metabolism studies: principles and applications. *Expert Opin. Drug Metab. Toxicol.* **2010**, *6*, 715-731.

[3] Lohmann, W. and Karst, U. Electrochemistry meets enzymes: instrumental on-line simulation of oxidative and conjugative metabolism reactions of toremifene. *Anal. Bioanal. Chem*. **2009**, *5*, 1341-1348.

[4] Karst, U. Electrochemistry/Mass Spectrometry (EC/MS)—A New Tool To Study Drug Metabolism and Reaction Mechanisms. *Angew. Chem. Int. Ed. Engl.* **2004**, *43*, 2476-2478.

[5] Jurva, U., Bissel, P., Isin, E. M., Igarashi, K., Kuttab, S. and Castagnoli Jr., N., Model electrochemical-mass spectrometric studies of the cytochrome P450-catalyzed oxidations of cyclic tertiary allylamines. *J. Am. Chem. Soc.* **2005**, *127*, 12368-12377.

[6] Jurva, U., Wikström, H. V., Weidolf, L. and Bruins, A. P. Comparison between electrochemistry/mass spectrometry and cytochrome P450 catalyzed oxidation reactions. *Rapid Commun. Mass Spectrom.* **2003**, *17*, 800-810.

[7] Nouri-Nigjeh, E., Permentier, H. P., Bischoff, R. and Bruins, A. P. Lidocaine Oxidation by Electrogenerated Reactive Oxygen Species in the Light of Oxidative Drug Metabolism. *Anal. Chem.* **2010**, *82*, 7625–7633.

[8] Nouri-Nigjeh, E., Permentier, H. P., Bischoff, R. and Bruins, A. P. Electrochemical oxidation by square-wave potential pulses in the imitation of oxidative drug metabolism. *Anal. Chem*. **2011**, *83*, 5519-5525.

[9] Johansson, T., Weidolf, L. and Jurva, U. Mimicry of phase I drug metabolism--novel methods for metabolite characterization and synthesis. *Rapid Commun. Mass Spectrom.* **2007**, *21*, 2323-2331.

[10] Oda, Y., Imaoka, S., Nakahira, Y., Asada, A., Fujimori, M., Fujita, S. and Funae, Y. Metabolism of lidocaine by purified rat liver microsomal cytochrome P-450 isozymes. *Biochem. Pharmacol.* **1989**, *38*, 4439-4444.

[11] Thomas, J. and Meffin, P. Aromatic hydroxylation of lidocaine and mepivacaine in rats and humans. *J. Med. Chem.* **1972**. *15*, 1046-1049.

[12] Jurva, U., Wikström, H. V. and Bruins, A. P. In vitro mimicry of metabolic oxidation reactions by electrochemistry/mass spectrometry. *Rapid Commun. Mass Spectrom.* **2000**, *14*, 529-533.

[13] Smith, P. J. and Mann, C. K. Electrochemical dealkylation of aliphatic amines. *J. Org. Chem.* **1969**, *34*, 1821-1826.

[14] Oswald, A. A. and Guertin, D. L. Organic Nitrogen Compounds. I. Peroxide Intermediates of Tertiary Alkylamine Oxidation by Hydrogen Peroxide. *J. Org. Chem.* **1963**, *28*, 651-657.

[15] Eberson, L. Electrolytic substitution reactions. III. Isomer distributions and isotope effects in nuclear and side-chain anodic acetoxylation of aromatic compounds. *J. Am. Chem. Soc.* **1967**, *89*, 4669-4677.

[16] Eberson, L. and Nyberg, K. Anodic aromatic substitution. *Acc. Chem. Res.* **1973**, *6*, 106-112.

[17] Meunier, B., de Visser, S. P. and Shaik, S. Mechanism of Oxidation Reactions Catalyzed by Cytochrome P450 Enzymes. *Chem. Rev.* **2004**, *104*, 3947-3980.

[18] Hall, S. B., Khudaish, E. A. and Hart, A. L. Electrochemical oxidation of hydrogen peroxide at platinum electrodes. Part I. An adsorption-controlled mechanism. *Electrochim. Acta* **1997**, *43*, 579-588.

[19] Hall, S. B., Khudaish, E. A. and Hart, A. L. Electrochemical oxidation of hydrogen peroxide at platinum electrodes. Part II: effect of potential. *Electrochim. Acta* **1998**, *43*, 2015-2024.

[20] Zhang, Y. and Wilson, G. S. Electrochemical oxidation of H_2O_2 on Pt and Pt + Ir electrodes in physiological buffer and its applicability to H_2O_2-based biosensors. *J. Electroanal. Chem.* **1993**, *345*, 253-271.

Chapter 6
Summary and Future Perspective

6.1 Summary

The thesis commences in **Chapter 1** with reviewing known electrochemical techniques and their advantages and limitations in the context of oxidative drug metabolism. The thesis continues with development of new electrochemical techniques to cover certain *in vivo* oxidative drug metabolism reactions which were not possible by constant potential oxidation. Electrochemically generated reactive oxygen species (ROS) in **Chapter 2**, electrochemical oxidation by square-wave potential pulses in **Chapters 3 and 4**, as well as electrocatalytic activation of hydrogen peroxide on a platinum electrode in **Chapter 5** are among the electrochemical techniques developed throughout my research.

Chapter 1 presents Cytochrome P450s (CYP), their discovery, structure, and role in *in vivo* oxidative drug metabolism by catalytic activation of molecular oxygen and the generation of ROS, mainly oxo-ferryl radical cations. **Chapter 1** further reviews different electrochemical techniques that have been developed so far, including direct electrochemical oxidation (in combination with mass spectrometry), oxidation by electrochemically generated ROS, and oxidation with modified electrodes containing metalloporphyrines and enzymes.

Direct electrochemical oxidation in combination with mass spectrometry, introduced in **Chapter 1**, has been used widely to imitate *in vivo* oxidative drug metabolism. The oxidation mechanisms were discussed in relation to *in vivo* oxidative drug metabolism. Direct electrochemical oxidation, accordingly, is capable of imitating oxidative reactions that are initiated by electron transfer, such as N-dealkylation and hydroxylation of substituted aromatic rings, whereas oxidation reactions which are initiated by hydrogen atom transfer (HAT) or oxygen atom insertion are difficult to imitate. Another major obstacle in imitation emerges when the oxidation products are oxidized more easily than the drug substrates, which prevents isolation of the latter. Finally the regioselectivity of direct electrochemical oxidation leading to charged intermediates, which presumably are

not present during *in vivo* oxidation by CYP, can limit the extent of imitation by favoring specific reaction pathways.

Electrochemically generated ROS may be able to imitate the oxidation reactions initiated by HAT. Electrochemically assisted Fenton, and Gif reactions activating hydrogen peroxide through homolytic and heterolytic bond cleavage to generate hydroxyl radicals and high valency iron species, respectively, are reviewed in **Chapter 1**. A wide range of oxidation reactions, in particular hydroxylations of non-activated aromatic rings, were achieved by these methods.

Metalloporphyrines, as surrogates for the active site of CYP, can be immobilized on the electrode surface to imitate oxidative drug metabolism by generation of reactive intermediates resembling those generated by CYP. Selection of metalloporphyrines with different substituents and metallic centers could determine the chemo- and stereoselectivity of the oxidation reactions.

Chapter 1 also addresses my work on the immobilization of metalloporphyrines via self-assembled monolayers (SAM) of alkanethiols, and their corresponding surface analysis using Surface Enhanced Resonance Raman Spectroscopy (SERRS). These might open a new road in the application of modified surfaces on-line with mass spectrometry that can be controlled by electrochemistry. Finally, chemoselective and stereoselective oxidation reactions can be mimicked by using electrodes that have been modified with immobilized enzymes, especially CYP itself.

Chapter 2 illustrates the use of electrochemically generated ROS, generated by electrochemical reduction of molecular oxygen and further radical reactions through the Haber-Weiss reaction, for oxidation of the test compound lidocaine. A two-compartment electrochemical cell was successfully constructed to isolate the reaction products from working and auxiliary compartments. N-oxidation occurred in the working compartment. I suggest that electrochemical reduction of molecular oxygen to hydrogen peroxide followed by reaction with the tertiary amine part of lidocaine to a peroxide intermediate and its subsequent decomposition resulted in the N-oxidation product. N-dealkylation was observed in the auxiliary compartment and occurs through direct electrochemical oxidation of lidocaine to an iminium intermediate followed by hydrolysis and intramolecular rearrangement. The use of electrochemically generated ROS can therefore extend the application of electrochemistry in the selective imitation of oxidative drug metabolism.

The N-oxidation product was identified using Atmospheric Pressure Chemical Ionization (APCI) through thermally-induced degradation reactions. This emphasizes the importance of using various ionization techniques in the identification of drug metabolites.

Chapter 3 explores square-wave potential pulses for the selective generation of metabolites of lidocaine with increased yield. This study shows that using square-wave potential pulses instead of constant potential oxidation increases the

yield of 4-hydroxylation up to fifty times depending on the cycle time. Whereas 4-hydroxylation of lidocaine was observed at cycle times of around one second, N-dealkylation was favored at shorter pulse times. The oxidation mechanism under square-wave potential pulses was studied by stripping linear voltammograms, which suggested the regeneration of the electrode surface under square-wave potential pulse conditions as the main reason behind the high yield oxidation. Isotope studies revealed the source of the oxygen atom in the N-oxidation and 4-hydroxylation: the oxygen atom in the N-oxide was derived from dissolved molecular oxygen and in the 4-hydroxylation product it originated from water. The exact mechanism leading to selectivity of oxidation during long and short pulses remains, however, unclear.

The use of square-wave potential pulses is not limited to high yield and selective oxidation reactions. Square-wave potential pulses may also be used to promote reactions that are not possible by constant potential oxidation. **Chapter 4** shows how to promote O-dealkylation of phenacetin to acetaminophen, a reaction that is not possible by direct electrochemical oxidation. Oxidation intermediates were successfully stabilized by scavenging them with nucleophiles and analyzed using LC-MS(/MS). Stable isotope labeling allowed studying the mechanism of hydrolysis and bond cleavage under square-wave potential pulses. While constant potential oxidation resulted in the p-quinone as the end product, fast-pulsed conditions transformed phenacetin to acetaminophen. Taken together **Chapters 3 and 4** show that square-wave potential pulses with different cycle times are a novel way to the high-yield and selective oxidation of drug compounds, as well as in promoting oxidation reactions that are not possible by constant potential oxidation.

Oxygen insertion by oxo-ferryl radical cations, in the *in vivo* oxidative drug metabolism by CYP, is the main mechanism behind aromatic hydroxylation. In **Chapter 5**, we present a novel approach based on the electrocatalytic activation of hydrogen peroxide on a platinum electrode that is thought to generate platinum-oxo species capable of promoting oxygen insertion reactions. The putative platinum-oxo species allows the generation of 3-hydroxylidocaine, which cannot be obtained through direct electrochemical oxidation. We suggest that oxygen insertion by the putative platinum-oxo species and formation of an arene intermediate is the reason behind this hydroxylation reaction. The absence of benzylic hydroxylation excludes the generation of freely diffusing radicals. The nature of the putative platinum-oxo species on the surface was studied further using an excess of pyridine as a competitive substrate. Pyridine quenched the reaction towards 3-hydroxylidocaine rather leading to the oxidation of pyridine. Catalytic activation of hydrogen peroxide on a platinum electrode surface, hence, further extends the application of electrochemistry in the mimicry of oxidative drug metabolism.

In conclusion, whereas direct electrochemical oxidation is merely capable of imitation of oxidative metabolisms which are initiated by electron tranfer, I extended the application of electrochemistry for the oxidation of drug compounds by adding

new methods to the electrochemical toolbox. **Scheme 1** illustrates all the electrochemical techniques that have been developed throughout this research in the oxidation of lidocaine as a test drug compound.

6.2 Future Perspective

The most promising research areas for continued development of electrochemistry in the mimicry of oxidative drug metabolism are the development of modified electrode surfaces, extending the application of square-wave potential pulses, and further studying the electrocatalytic activation of hydrogen peroxide.

Our study of the modification of electrode surfaces should be continued as it intrinsically represents a better mimicry model for CYP than bare electrodes. Electrochemical cells with modified surfaces that can be coupled to mass spectrometry are of great interest, but several technical problems were encountered which need to be overcome. First, axial coordination was used to anchor metalloporphyrines on the surface through SAM, which may lead to direct reduction of oxidative intermediates by the electrode, rather than oxidation of drug substrates. As a possible solution, square-wave potential pulses can be used to generate the reactive species in one step, and to allow the oxidation reaction to happen in the next step. Naturally, direct reduction of molecular oxygen to hydrogen peroxide on the electrode followed by chemical activation by adjacent metalloporphyrines would be a simpler solution. Chemoselectivity may be obtained by using different metalloporphyrines, with various metallic centers and substituents, based on preliminary results screening several drug substrates.

This thesis has added oxidation by square-wave potential pulses to the toolbox of techniques and of course the oxidation conditions can be further optimized, especially by using different potential wave forms. In the case of electrocatalytic activation of hydrogen peroxide on a platinum electrode, hydrogen peroxide can be generated by electrochemical reduction of molecular oxygen. This can be done through square-wave potential pulses in which a reduction step to reduce molecular oxygen to hydrogen peroxide is followed by the electrocatalytic activation of hydrogen peroxide in the subsequent oxidation step.

In our studies we have focused mainly on lidocaine as a test drug compound to compare different approaches, as well as to overcome issues with the identification of metabolites. A major hindrance in these studies is the requirement for careful identification of oxidation products which are often isomeric. A combination of detailed MS analyses, using ionization, fragmentation (MS^n) and isotope labeling studies, and NMR should be employed for their definitive identification in the common case where no reference compounds are available. Misidentification of the location of a hydroxyl group in a metabolite can otherwise lead to errors in the interpretation of the reaction mechanism.

Scheme 1. Various electrochemical techniques in the oxidation of lidocaine as a test drug compound in the light of oxidative drug metabolism. Electrochemical oxidation of lidocaine at the tertiary amine moiety under direct electrochemical oxidation leading to N-dealkylation through formation of an iminium intermediate (path **A**), direct electrochemical oxidation of lidocaine at the aromatic moiety to generate a Wheland-type intermediate which after deprotonation results in 4-hydroxylation (path **B**), electrochemical reduction of molecular oxygen to hydrogen peroxide followed by reaction with the tertiary amine moiety of lidocaine to generate a peroxide intermediate, which after decomposition results in N-oxidation (path **C**), and electrochemical activation of hydrogen peroxide on a platinum electrode to generate putative platinum-oxo species that react in an oxygen atom insertion manner to generate an arene intermediate that after tautomerization leads to 3-hydroxylation (path **D**).

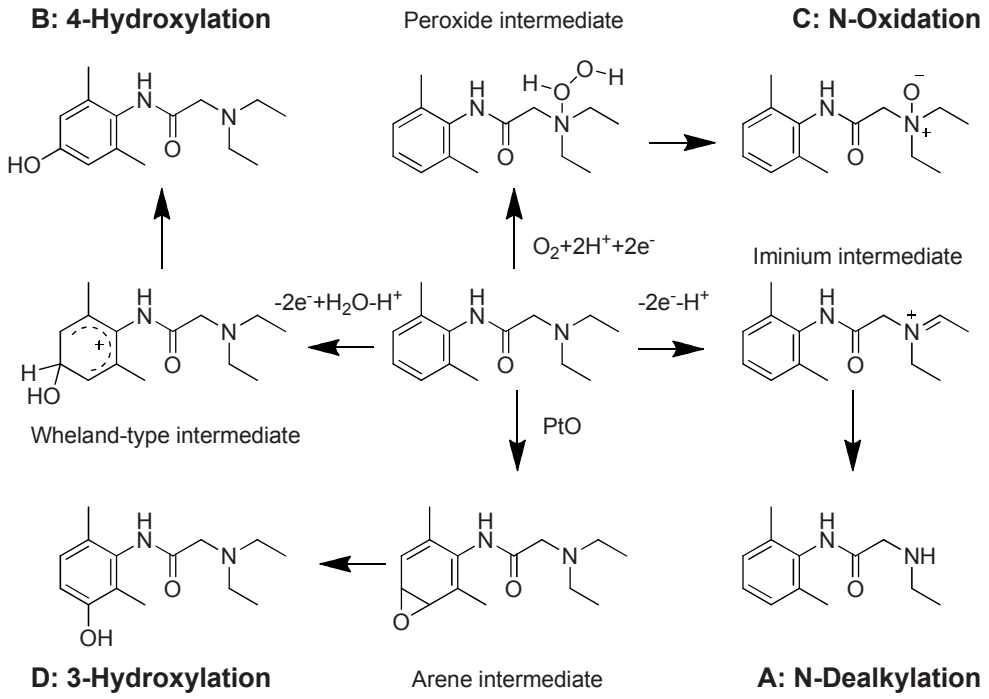

We have already checked the oxidation of various drug compounds under square-wave potential pulses, yet the other methods including electrocatalytically activated hydrogen peroxide can be applied to different substrates. A range of drug compounds with various functional groups and known metabolism by CYP should be tested both to verify the reaction mechanisms and to assess the specificity of the new oxidation techniques. It will remain to be investigated whether extensive optimization of reaction conditions is required for each new compound and desired metabolite, or whether more general guidelines for method development can be outlined.

Microfluidics where parallel channels can be operated separatly by electrochemistry is an attractive format for optimization of conditions or simultaneous generation of different metabolites. Electrodes operated under various pulsed conditions or differently modified electrodes with a range of metalloporphyrines can be employed in such a microchannel array.

Finally, next to down-scaling, upscaling of specific reactions to increase the absolute yield should be a major focus for future work. Toxicity testing of potential metabolites of new drug compounds depends on the availability of a sufficient amount of material. The studies described in this thesis have not focused on maximizing product yield, although in several cases, much higher yields were obtained than with previous (direct) electrochemical oxidation techniques. Yields of up to 10% were observed in some cases in a batch cell. Improvements in cell and electrode dimensions and the switch to flow-through instead of batch cells is expected to increase both yield and product purity. The conversion yield in flow-through cells can reach almost 100% but selectivity of product formation will depend on the careful control of reaction conditions. Upscaling of absolute amounts without loss in relative yield is thus a challenge.

Samenvatting

Het proefschrift geeft in **Hoofdstuk 1** een overzicht van elektrochemische technieken en hun voordelen en beperkingen binnen de context van het oxidatieve metabolisme van geneesmiddelen. In de volgende hoofdstukken wordt de ontwikkeling beschreven van nieuwe elektrochemische technieken, gericht op bepaalde *in vivo* oxidatiereacties die niet uitgevoerd kunnen worden met elektrochemische oxidatie bij constante potentiaal. Electrochemisch gevormde reactieve zuurstof deeltjes (reactive oxygen species, ROS) in **Hoofdstuk 2**, elektrochemische oxidatie door middel van een potentiaal, gepulst in een vierkantsgolfvorm in **Hoofdstukken 3** en **4**, en elektrolytische activering van waterstof peroxide op een platina electrode in **Hoofdstuk 5** behoren tot de elektrochemische technieken die ik tijdens mijn promotieonderzoek heb ontwikkeld.

Hoofdstuk 1 beschrijft de Cytochrome P450 enzymen (CYP), hun ontdekking, structuur en hun rol bij het oxidatieve *in vivo* metabolisme, dat plaats heeft door katalytische activering van moleculaire zuurstof en de vorming van ROS, voornamelijk oxo-ferryl radicaal kationen. Verder wordt een overzicht gegeven van diverse elektrochemische technieken die in de loop der tijd zijn ontwikkeld, met inbegrip van directe elektrochemische oxidatie (gecombineerd met massaspectrometrie), oxidatie door middel van elektrochemische gevormde ROS, en oxidatie met elektrodes die zijn gemodificeerd met metalloporphyrines en enzymen.

Directe electrochemische oxidatie gecombineerd met massaspectrometrie, genoemd in **Hoofdstuk 1**, is veel gebruikt voor de imitatie van *in vivo* metabolisme. De relatie tussen electrochemische oxidatiemechanismen en het metabolisme *in vivo* is al eerder onderzocht. Directe electrochemische oxidatie kan metabole reacties imiteren die worden gestart door overdracht van een electron, zoals N-dealkylering, en de hydroxylering van aromatische ringen met substituenten. Daarentegen zijn metabole oxidaties die beginnen met de overdracht van een waterstofatoom (hydrogen atom transfer, HAT) moeilijk na te bootsen. Verder is het een groot probleem bij electrochemische imitatie wanneer het product van een oxidatiereactie nog gemakkelijker wordt geoxideerd dan het substraat, zodat het product niet kan worden geïsoleerd. Tenslotte kunnen tijdens de directe electrochemische oxidatie geladen tussenprodukten worden gevormd, die niet

aanwezig zijn tijdens de *in vivo* oxidatie door CYP, en die specifieke reactiewegen kunnen bevorderen die ongewenst zijn vanuit het oogpunt van imitatie van CYP.

Electrochemisch gevormde ROS kunnen de oxidatiereacties imiteren die worden gestart door overdracht van een waterstofatoom (HAT). De elektrochemisch ondersteunde Fenton en Gif reacties, die waterstofperoxide activeren via homolytische en heterolytische breuk van de O-O binding met vorming van hydroxyl radicalen, worden besproken in **Hoofdstuk 1**. Een groot bereik aan oxidatiereacties, met name hydroxyleringen van niet-geactiveerde aromatische ringen, wordt bestreken met deze methoden.

Metalloporphyrinen die kunnen dienen als surrogaat voor het actieve centrum van CYP, kunnen worden vastgezet op de elektrochemische werkelectrode om metabolisme te imiteren door middel van reactieve intermediairen die lijken op de intermediairen die worden gevormd door CYP. Door keuze van metalloporphyrines met verschillende substituenten en centrale metaal-ionen kan de chemische- en stereo-selectiviteit van een oxidatiereactie worden bepaald.

Hoofdstuk 1 gaat ook in op mijn werk aan de immobilisatie van metalloporphyrines via self-assembled monolayers (SAM) van alkaanthiolen, en de analyse van deze gemodificeerde oppervlakken met Surface Enhanced Resonance Raman Spectroscopy (SERRS). Dit zou nieuwe wegen kunnen openen voor de toepassing van gemodificeerde electroden in cellen die rechtstreeks gekoppeld zijn met een massaspectrometer. Tenslotte kunnen chemisch-selectieve en stereoselectieve oxidatiereacties worden nagebootst door gebruik te maken van electroden waarop enzymen in het algemeen en CYP in het bijzonder, zijn vastgezet.

Hoofdstuk 2 beschrijft het gebruik van elektrochemisch gevormde ROS, gegenereerd door elektrochemische reductie van moleculaire zuurstof, en daaropvolgende radicaalreacties (Haber-Weiss) bij de oxidatie van lidocaine als test-substraat. Door toepassing van een electrochemische cel met gescheiden compartimenten voor de werkelectrode en de hulpelectrode, konden de producten die aan beide electroden worden gevormd, afzonderlijk worden geïsoleerd en gedetecteerd. N-oxidatie had plaats aan de werkelectrode. Mijn suggestie is dat electrochemische reductie van zuurstof leidt tot waterstofperoxide, dat vervolgens reageert met de tertiaire aminogroep van lidocaine. Het peroxide dat als tussenproduct ontstaat valt uiteen tot het N-oxide van lidocaine. N-dealkylering werd waargenomen in het compartiment van de hulpelectrode. Electrochemische oxidatie van lidocaine aan de positieve hulpelectrode geeft een iminium-tussenproduct, dat verder reageert door hydrolyse en intramoleculaire omlegging. Het gebruik van electrochemisch gevormde ROS biedt dus een uitbreiding van de mogelijkheden van electrochemie in de selectieve nabootsing van metabolisme.

Het N-oxide werd geïdentificeerd door middel van Atmospheric Pressure Chemical Ionization, waarbij specifieke thermisch-geïnduceerde fragmentaties

plaats hebben. Dit benadrukt hoe belangrijk het is diverse ionisatietechnieken te gebruiken bij de massaspectrometrische identificatie van metabolieten.

In **Hoofdstuk 3** wordt onderzocht of de modulatie van de celpotentiaal met vierkantsgolven de selectiviteit en opbrengst van de oxidatieproducten van lidocaine kan verhogen. De studie toont aan dat een pulsvormige potentiaal de opbrengst van de 4-hydroxylering met een factor 50 kan verhogen, als wordt gewerkt met de juiste cyclustijd van de vierkantsgolf. 4-Hydroxylering wordt bevorderd bij een cyclustijd van ongeveer 1 seconde, terwijl N-dealkylering wordt begunstigd als de pulstijd korter is. Het mechanisme van oxidatie met gepulste potentiaal werd onderzocht met "linear stripping voltammograms", hetgeen aanwijzing gaf voor het belang van regeneratie van het oppervlak van de werkelectrode, die plaats heeft door de potentiaal te pulsen. Het gebruik van de stabiele isotoop ^{18}O toonde aan dat het O-atoom in het N-oxide afkomstig is van de gebruikte moleculaire zuurstof, maar in het 4-hydroxyleringsprodukt wordt geleverd door water. Het precieze mechanisme dat verantwoordelijk is voor de selectiviteit tijdens korte en lange pulsen is voorlopig nog onduidelijk.

Het gebruik van gepulste potentialen is niet beperkt tot oxidatiereacties met hoge opbrengst en selectiviteit. Vierkantsgolfpulsen kunnen ook reacties bevorderen die niet optreden bij constante potentiaal. **Hoofdstuk 4** laat zien dat O-dealkylering van phenacetine kan leiden tot acetaminophen, hetgeen onmogelijk is bij constante oxidatiepotentiaal. Tussenproducten van de oxidatie konden worden gestabiliseerd door ze af te vangen met nucleofielen. Daarna werden ze geïdentificeerd met LC-MS(/MS). Stabiele isotopen werden gebruikt voor de studie van het mechanisme van hydrolyse en het breken van bindingen wanneer de cel-potentiaal wordt gepulst. Terwijl een constante cel-potentiaal leidt tot vorming van p-chinon als eindprodukt, kon phenacetine worden omgezet in acetaminophen bij gebruik van een gepulste potentiaal, die alterneert tussen oxidatie en reductie aan de werkelectrode. Aldus tonen de **Hoofdstukken 3** en **4** aan dat vierkantsgolfpulsen met variatie in cyclustijden een nieuwe weg openen tot hoge opbrengst en selectiviteit van de electrochemische oxidatie van xenobiotica, en bovendien reacties bevorderen die niet plaats hebben bij constante potentiaal.

Het invoegen van zuurstof door oxo-ferryl radicaal kationen is het voornaamste mechanisme dat de basis is van oxidatief metabolisme *in vivo*. In **Hoofdstuk 5** presenteren we een nieuwe benadering die is gebaseerd op de electrokatalytische activering van waterstofperoxide op een platina-electrode. We nemen aan dat een platina-oxo deeltje wordt gevormd dat het invoegen van zuurstof in een organisch molecule kan bevorderen. Het veronderstelde platina-oxo deeltje leidt tot vorming van 3-hydroxylidocaine, een produkt dat niet kan worden verkregen door directe electrochemische oxidatie. We suggereren dat het platina-oxo deeltje essentieel is voor het invoeren van zuurstof op de 3- positie. Omdat hydroxylering op de benzylische positie niet plaatshad, spelen radicalen die vrij bewegen in de oplossing geen rol. De aard van het veronderstelde platina-oxo deeltje op het platina oppervlak werd verder bestudeerd door toevoeging van pyridine, dat de

competitie tijdens de oxidatie kan aangaan met lidocaine. Pyridine blokkeerde de vorming van 3-hydroxylidocaine, en werd zelf geoxideerd. Aldus kan de katalytische activering van waterstofperoxide op een platina electrode de toepasbaarheid van electrochemie vergroten in het kader van de nabootsing van oxidatief metabolisme van geneesmiddelen en andere xenobiotica.

Als conclusie kan ik formuleren dat, terwijl directe electrochemische oxidatie beperkt is tot metabolisme dat begint met electronenoverdracht, de toepassing van electrochemie binnen de imitatie van oxidatief metabolisme een groter bereik heeft gekregen door nieuwe methoden toe te voegen aan het gereedschap van de synthetische electrochemie. **Schema 1** illustreert de electrochemische technieken die tijdens mijn promotieonderzoek zijn ontwikkeld, met lidocaine als teststof.

Een blik in de toekomst

De meestbelovende gebieden voor verder onderzoek aan electrochemie in het kader van oxidatief metabolisme zijn: de ontwikkeling van gemodificeerde electrodenoppervlakken, de uitbreiding van de toepassing van gepulste potentialen, en de nadere studie van de katalytische activering van waterstof peroxide.

Ons werk aan de modificatie van electrodenoppervlakken zou moeten worden voortgezet, omdat het een inherent beter model voor nabootsing van metabolisme door CYP biedt dan kale electroden. Een cel met een gemodificeerde electrode die wordt gekoppeld aan een massaspectrometer is van groot belang, maar tot nu toe zijn ernstige technische problemen ondervonden, die eerst moeten worden overwonnen. Ten eerste werd axiale coördinatie gebruikt voor de verankering van metalloporphyrines op het oppervlak door middel van een geordende monolaag van moleculen (self assembled monolayer, SAM). Dit kan leiden tot oxidatie van de tussenliggende monolaag, in plaats van oxidatie van een geneesmiddel. Als een mogelijke oplossing kan een vierkantsgolf-gepulste potentiaal worden gerbuikt om eerst een reactief deeltje te vormen in een eerste stap, en de eigenlijke oxidatie te laten plaatshebben in de tweede stap. Natuurlijk zou een directe reductie van moleculaire zuurstof op de electrode, gevolgd door een chemische activering door naburige metalloporphyrines een eenvoudiger methode zijn. Selectiviteit zou kunnen worden verkregen door gebruik te maken van verschillende metalloporphyrines, met diverse metaalcentra en substituenten, gebaseerd op voorlopige resultaten uit de screening van diverse substraten.

In dit proefschrift is de oxidatie met gepulste potentialen toegevoegd aan de gereedschappen van de synthetische electrochemie. Vanzelfsprekend is een nadere verbetering mogelijk, in het bijzonder door het gebruik van andere golfvormen van de pulsen. In het geval van de electrokatalytische activering van waterstofperoxide kan eerst waterstofperoxide worden gevormd door reductie van

zuurstof bij de ene potentiaal van de puls, waarna het zojuist gegenereerde waterstofperoxide wordt geactiveerd bij de tweede, oxiderende potentiaal.

Tijdens onze studie hebben we ons geconcentreerd op lidocaine als teststof, om een aantal opties te kunnen vergelijken, en om de metabolieten gemakkelijker te kunnen identificeren. Een belangrijke eis is de zorgvuldige identificatie van isomere oxidatieproducten. Een combinatie van gedetailleerde MS analyses, met gebruik van verschillende ionisatie methoden, fragmentatie, en stabiele isotopen en ook NMR, is nodig voor een eenduidige vaststelling van de structuur in het algemene geval dat referentiestoffen niet beschikbaar zijn. Verkeerde toekenning van de plaats van een hydroxy-groep in een metaboliet leidt tot fouten in de interpretatie van het mechanisme van de oxidatiereactie.

De methoden die hierboven zij toegepast op lidocaine en phenacetine moeten worden getest op andere substraten. Een reeks geneesmiddelen met diverse functionele groepen, waarvan het *in vivo* metabolisme door CYP bekend is, zou moeten worden onderzocht, om de reikwijdte en specificiteit van de nieuwe methoden vast te kunnen stellen. Bovendien moet duidelijk worden of een nadere fijnafstemming van de reactiecondities nodig is voor elk nieuw substraat, of dat algemene richtlijnen kunnen worden geformuleerd.

Geminiaturiseerde systemen met microreactoren in parallelle kanalen kunnen een aantrekkelijke mogelijkheid worden voor de gelijktijdige uitvoering van diverse electrochemische reacties, met diverse pulstechnieken en metalloporphyrines, om twee voorbeelden te noemen.

Tenslotte is naast de schaalverkleining ook de schaalvergroting een belangrijke vraag uit de praktijk, die in de toekomst moet worden beantwoord. Er is grote behoefte aan een voldoende hoeveelheid van een metaboliet die toxisch zou kunnen zijn. Electrochemische synthese vanuit het geneesmiddel zelf, in het bijzonder wanneer dit in een vroeg stadium van de ontwikkeling nodig is, verdient de voorkeur boven een volledig organisch chemische synthese, die in het algemeen bewerkelijk is. In dit proefschrift is nog geen aandacht besteed aan een optimale opbrengst. Een opbrengst van maximaal 10 % is in sommige gevallen waargenomen met onze methoden. Variatie van de afmetingen van de cel en de electroden, en het gebruik van doorstroomcellen kan een betere opbrengst en zuiverheid van de producten geven. De omzetting in doorstroomcellen kan 100 % benaderen, maar selectiviteit voor een bepaald product zal afhangen van zorgvuldige regeling van de reactieomstandigheden. Schaalvergroting zonder verlies van specificiteit is een grote uitdaging.

Schema 1. Diverse technieken voor de electrochemische oxidatie van lidocaine als modelstof voor het oxidatieve metabolisme. Directe electrochemische oxidatie van de tertiaire aminogroep leidt tot dealkylering via een iminium intermediair (route **A**), Directe electrochemische oxidatie van de aromaatring geeft een Wheland intermediair, dat wordt gedeprotoneerd en resulteert in 4-hydroxylering (route **B**). Electrochemische reductie van moleculaire zuurstof tot waterstofperoxide, dat met lidocaine reageert tot het N-oxide (route **C**). Electrochemische activering van waterstofperoxide op de Pt electrode geeft een geoxideerd platina deeltje dat met de aromaatring reageert tot een areen-zuurstof verbinding die tautomeriseert tot 3-hydroxylidocaine (route **D**).

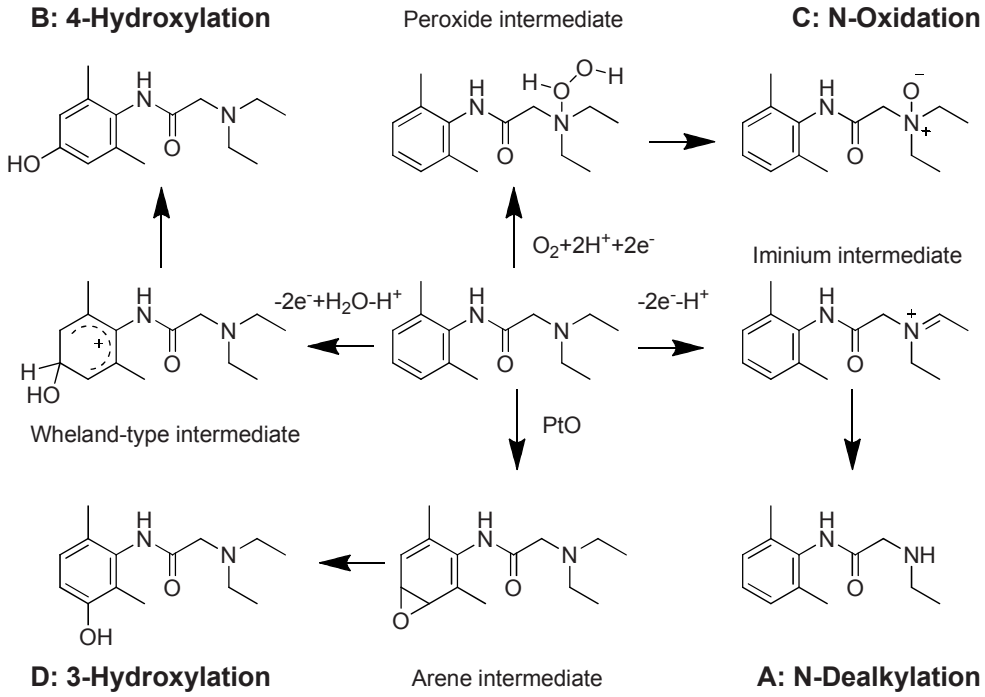

Acknowledgement

I thank Professor Rainer Bischoff because of giving me a great opportunity to join his department, and I thank my supervisors, Dr. Hjalmar Permentier and Dr. Andries Bruins, for their precious and consistent support to complete this thesis.

I am indeed honored by learning Mass Spectrometry from one of the best. Thanks a lot Andries. Your help, teaching, and the time you spend during your retirement had a great impact on my project. Thanks Hjalmar, for helping me to solve technical problems and reading my manuscripts. You are a talented scientist.

Julien, merci beaucoup. I thank you, my officemate. I enjoyed accompanying you for several years. Thanks for all the good time we have had together.

Margot, heel erg bedankt voor de goede tijd, en vooral jullie tuinfeest was erg leuk. Annie, hartelijk bedankt voor de gezellige tijden. Waarschijnlijk wordt de nieuwe dans een succes. Karin, ik kan zeggen thee met chocolade smaakt heerlijk! Marcel, bedankt voor de hulp met mijn technische problemen, jij bent heel deskundig op het gebied van massaspectrometrie. Ala, bedankt voor het heerlijke Indonesische eten, en ook de jaarlijkse bbq. Niels, bedankt voor de leuke gesprekken en de biertjes die we hebben gehad. Lisa, jij hebt een mooie zoon (Joshua), ik hoop dat alles goed gaat nu hij tandjes krijgt.

I also would like to thank the colleagues from Analytical Biochemistry group for the wonderful moments and their support: Berend, Vikram, Ishtiaq, Tess, Hanna, Laurette, and Lorenza. Ulrik and Lars, thanks for the great dinner in Sweden, I should take your advice more serious about the freezing weather in Gothenburg, to bring warm clothes and not to stay the whole trip shivering in a hotel.

Əziz xanivadəm uçun, anam uçun, bacim uçun, hayat nə gozəl bir şeymiş; sizlərlə yaşamak, sizlərlə paylaşmak, butun sevinclərimi, gozəl anlarimi, xatirələrimi. Sizləri dərin urəkdən sevirəm, və sizlərə həmişe xöşlüq arziliyiram.

Heydər Baba, kəndin günü batanda, Uşaqların şamın yeyib yatanda,
Ay buluddan çıxıb qaş-göz atanda, Bizdən də bir sən onlara qissə de,
Qissəmizdə çoxlu qəmü-qüssə de.

List of Publications

1. **Nouri-Nigjeh, E.**; de Vries, M.P.; Bischoff, R.; Bruins, A.P.; Permentier, H.P. Electrochemical oxidation of quaternary ammonium electrolytes, Analytical Chemistry, Ready for submission.

2. **Nouri-Nigjeh, E.**; Bischoff, R.; Bruins, A.P.; Permentier, H.P. Electrocatalytic activation of hydrogen peroxide on a platinum electrode in the mimicry of oxidative drug metabolism by Cytochrome P450s, Chemical Research in Toxicology, Submitted.

3. **Nouri-Nigjeh, E.**; Bischoff, R.; Bruins, A.P.; Permentier, H.P. Electrochemical oxidation by square-wave potential pulses in the imitation of phenacetin to acetaminophen biotransformation, Analyst, Submitted.

4. **Nouri-Nigjeh, E.**; Permentier, H.P.; Bischoff, R.; Bruins, A.P. Electrochemical oxidation by square-wave potential pulses in the imitation of oxidative drug metabolism, Analytical Chemistry, Vol. 83, 2011, 5519-5525.

5. **Nouri-Nigjeh, E.**; Bischoff, R.; Bruins, A.P.; Permentier, H.P. Electrochemistry in the mimicry of oxidative drug metabolism by Cytochrome P450s, Current Drug Metabolism, Special issue: Analytical techniques in Drug metabolism, Vol. 12, 2011, 359-371.

6. **Nouri-Nigjeh, E.**; Permentier, H.P.; Bischoff, R.; Bruins, A.P. Lidocaine oxidation by electrogenerated reactive oxygen species in the light of oxidative drug metabolism, Analytical Chemistry, Vol. 82, 2010, 7625-7633.

Oral and Poster Presentations:

1. **Nouri-Nigjeh, E.**; Permentier, H.P.; Bischoff, R.; Bruins, A.P. New electrochemical techniques in the imitation of oxidative drug metabolism by EC/MS, Oral Presentation First EC/MS workshop Münster, Germany, September 15, 2011.

2. **Nouri-Nigjeh, E.**; Permentier, H.P.; Bischoff, R.; Bruins, A.P. Electrochemically generated reactive oxygen species for in vitro drug metabolism, Oral Presentation AstraZeneca (Webcasted), Mölndal, Sweden, November 24, 2010.

3. **Nouri-Nigjeh, E.**; Permentier, H.P.; Bischoff, R.; Bruins, A.P. Electrochemistry in the mimicry of oxidative drug metabolism by Cytochrome P450s, Oral presentation Analytical Challenge 2010, NWO-Section Analytical Chemistry/KNCV, Lunteren, The Netherlands, November 1-2, 2010.

4. **Nouri-Nigjeh, E**.; Permentier, H.P.; Bischoff, R.; Bruins, A.P. Electrogenerated reactive oxygen species in the mimicry of oxidative species in the mimicry of oxidative metabolism of drug compounds by Cytochrome P450s, Poster presentation Annual meeting of the NWO/CW Study Group Analytical Chemistry, Lunteren, The Netherlands, November 2-3, 2009.

5. **Nouri-Nigjeh, E.**; Permentier, H.P.; Bischoff, R.; Bruins, A.P. Electrogenerated reactive oxygen species in the mimicry of oxidative metabolism of drug compounds by Cytochrome P450s, Poster presentation 18th International Mass Spectrometry Conference, Bremen, Germany, August 30-September 04, 2009.

6. **Nouri-Nigjeh, E.**; Permentier, H.P.; Bischoff, R.; Bruins, A.P. Adsorbed hemin as a suitable electrocatalyst in the mimicry of Cytochrome P450s, Poster presentation Annual meeting of the NWO/CW Study Group Analytical Chemistry, Lunteren, The Netherlands, November 3-4, 2008.

7. **Nouri-Nigjeh, E.**; Permentier, H.P.; Bischoff, R.; Bruins, A.P. Electrodes covered with hemin to mimic oxidative metabolism pathways mediated by Cytochrome P450s, Poster Presentation 58th Annual ISE Meeting, Seville, Spain, September 7-12, 2008.

8. **Nouri-Nigjeh, E.**; Permentier, H.P.; Bischoff, R.; Bruins, A.P. Immobilized Hemin as a suitable electrocatalyst in the mimicry of Cytochrome P450, Poster Presentation GUIDE Early Summer Meeting, Groningen, The Netherlands, June 5, 2008.

9. **Nouri-Nigjeh, E.**; Permentier, H.P.; Bischoff, R.; Bruins, A.P. Electrodes modified with immobilized hemin via SAMs to mimic difficult oxidation pathways mediated by Cytochrome P450 in EC/MS, Poster presentation Annual meeting of the NWO/CW Study Group Analytical Chemistry, Lunteren, The Netherlands, November 5-6, 2007.